SAND2009-4116C

Lasers and Microsystems: Predicting and Avoiding Laser Damage

Leslie M. Phinney

Microscale Sciences and Technology

Sandia National Laboratories

Albuquerque, New Mexico

(505) 845-8484, *lmphinn@sandia.gov*

July 19, 2009

Sandia is a multiprogram laboratory operated by Sandia Corporation, a Lockheed Martin Company, for the United States Department of Energy's National Nuclear Security Administration under contract DE-AC04-94AL85000.

Acknowledgements

Sandia National Laboratories, Albuquerque, New Mexico

Mike Baker
Carlton Brooks
Jaime Castaneda
Katie Francis
Allen Gorby
Tom Grasser
Sean Kearney
Kelly Klody
Ed Piekos
Alex Pimentel
Rosemarie Renn
Mike Rightley
John Sackos
Justin Serrano
Olga Blum Spahn
Wayne Trott
Jeremy Walraven
Channy Wong
MDL Staff

Funding and Facilities

Sandia National Laboratories, Engineering Sciences Research Foundation and Laboratory Directed Research and Development

National Science Foundation, Grant CTS-9984979

UIUC Materials Research Laboratory

Laser, Microfabrication, and CMM Facilities, DOE grant

Collaborator

Sai Koppaka, ZS Associates

Thomas Mackin, California Polytechnic, San Luis Obispo

James Rogers, Murray State University, Kentucky

Xiaojie Xue, Analog Devices

Sandia National Laboratories

Engineering Sciences Center at Sandia National Laboratories

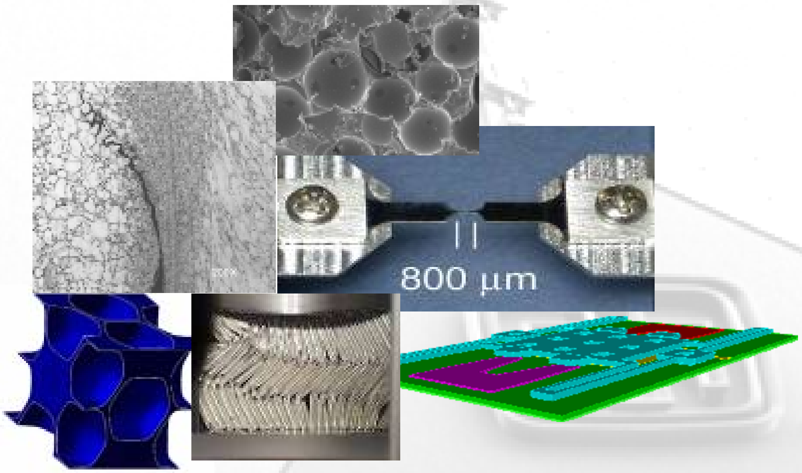

Solid/Material Mechanics & Structural Dynamics

Discipline areas:

- Solid Mechanics
- Structural Dynamics
- Material Mechanics

Thermal, Fluids & Aero-sciences

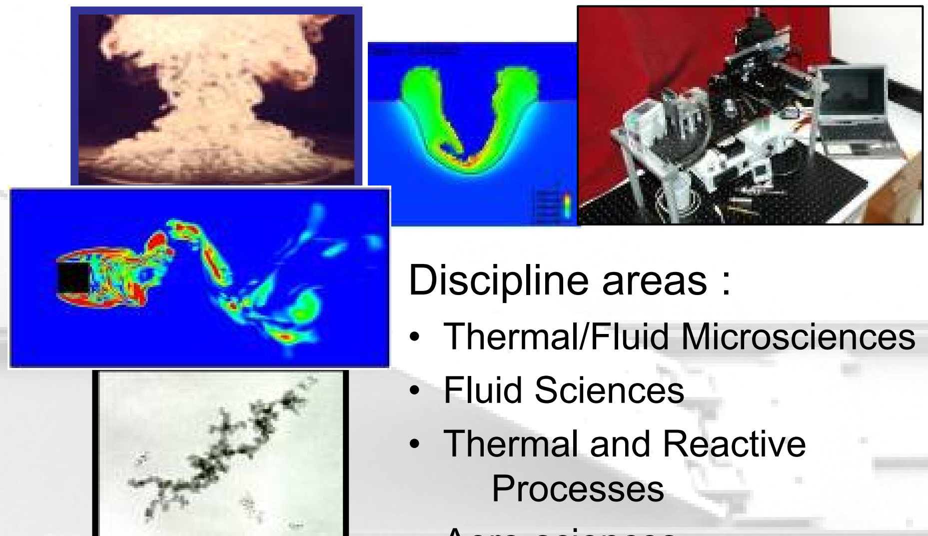

Discipline areas :

- Thermal/Fluid Microsciences
- Fluid Sciences
- Thermal and Reactive Processes
- Aero-sciences

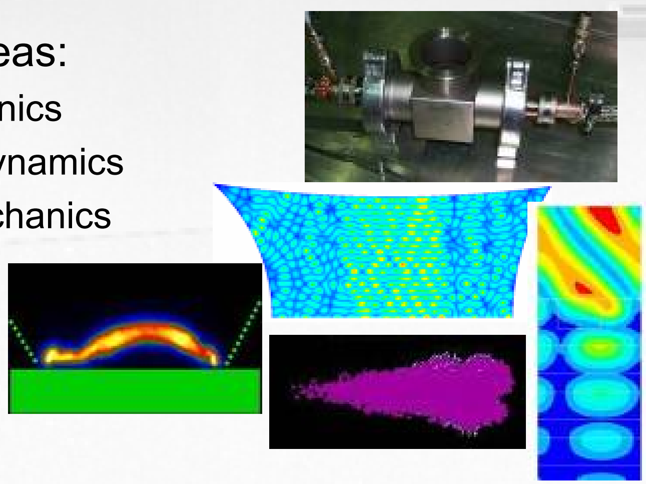

Electrical Sciences

Discipline areas:

- Electromagnetics and Plasma Physics
- Electrical Processes

Sandia National Laboratories

Lasers and Microsystems: Predicting and Avoiding Laser Damage

1. Applications
2. Thermal Test Structures and Devices
   – Surface Micromachining
   – Optical Thermal Microactuators
3. Laser Damage Experiments
   – Target Design: layers, posts
   – Underlying substrate
4. Temperature Measurements
   – Raman Thermometry
   – Variation of Peak Temperature with Power
5. Optical and Thermal Simulations
6. Diagnostics
7. Conclusions

Sandia National Laboratories

Optical MEMS or MicroOptoElectroMechanical Systems (MOEMS)

- Allows integration of increased system functionality for a given volume
- Includes optical mirrors, switches, cross connects, optical bench on a chip, etc.
- At high input powers, thermal management is a challenge

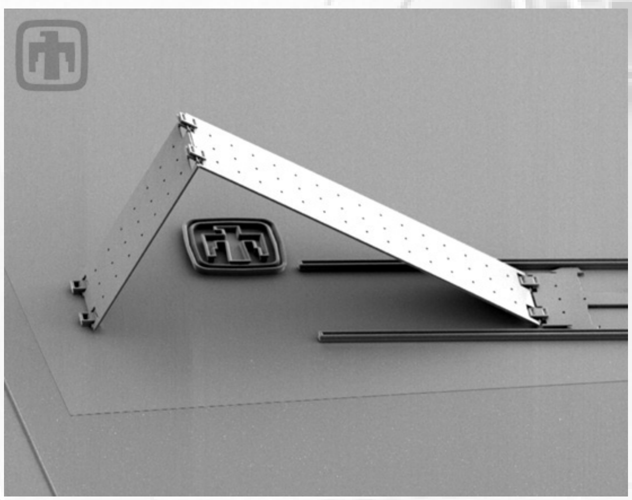

Micromirror
Sandia National Laboratories

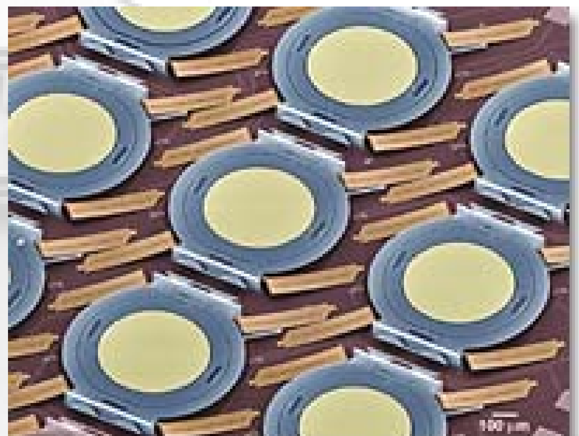

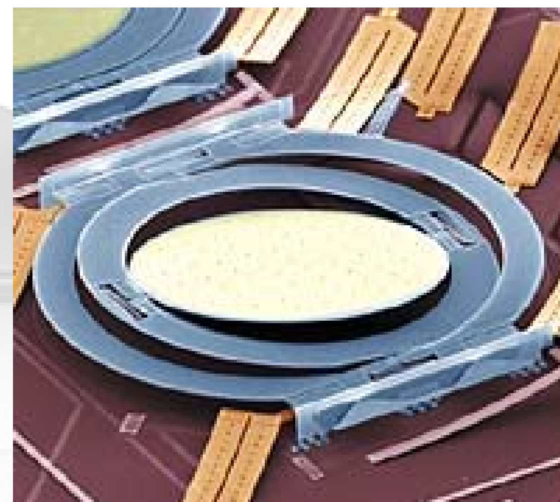

Optical Cross Connect
WaveStar™ Lambda Router, Lucent Technologies array of micromirrors route information to and from any of 256 input/output optical fibers

Texas Instruments Digital Light Processing^{TM}

http://www.dlp.com/

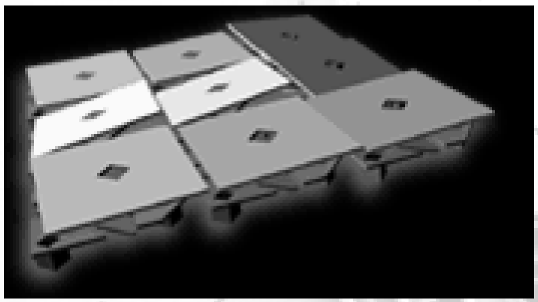

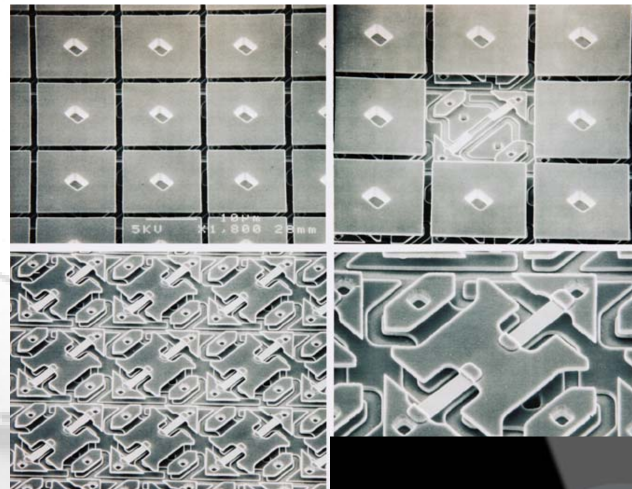

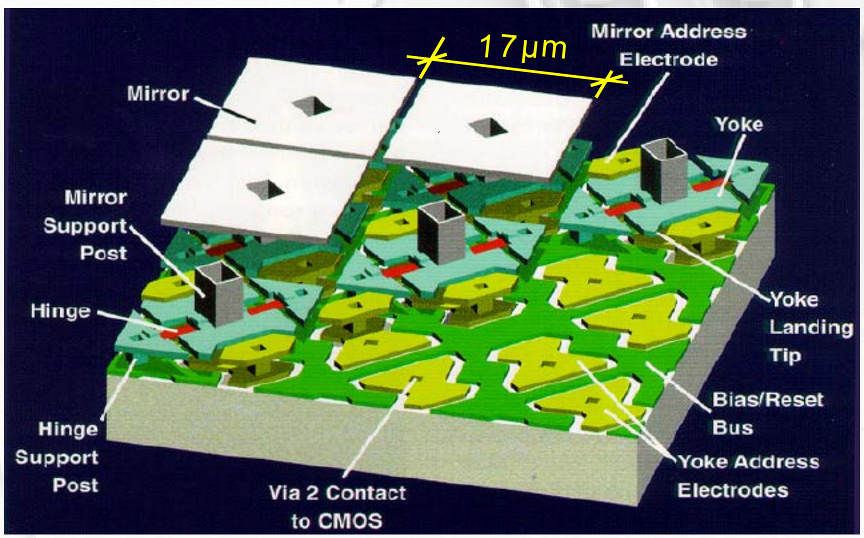

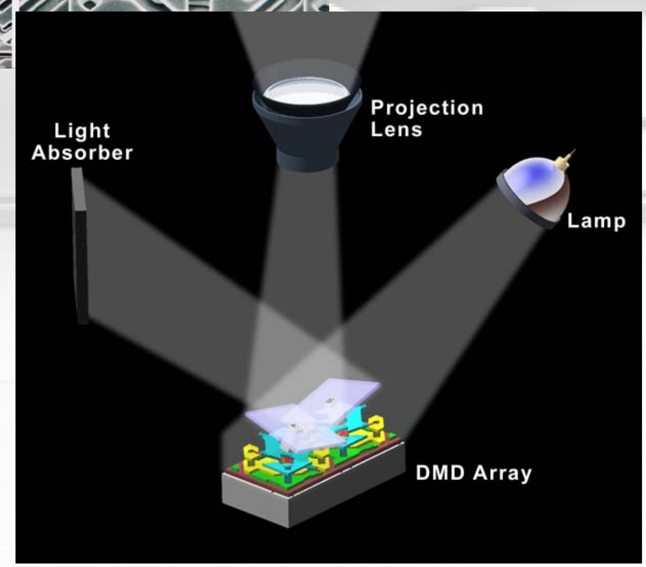

Digital Micromirror Device, Texas Instruments,
Larry J. Hornbeck, SPIE Conference, Oct. 23-34, 1995.

MEMS Based IR Imaging

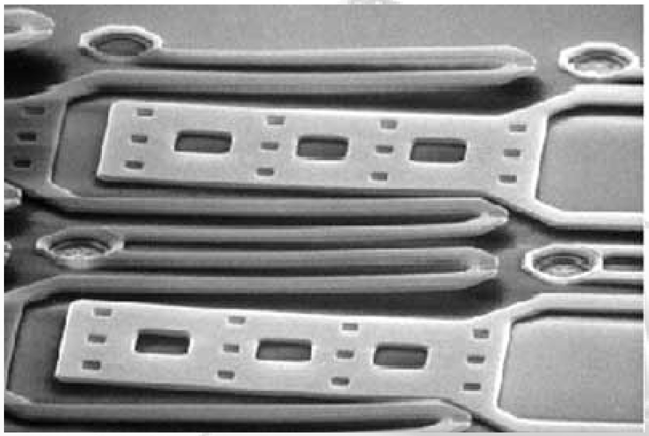

50 μm long MEMS cantilevers in IR imaging system

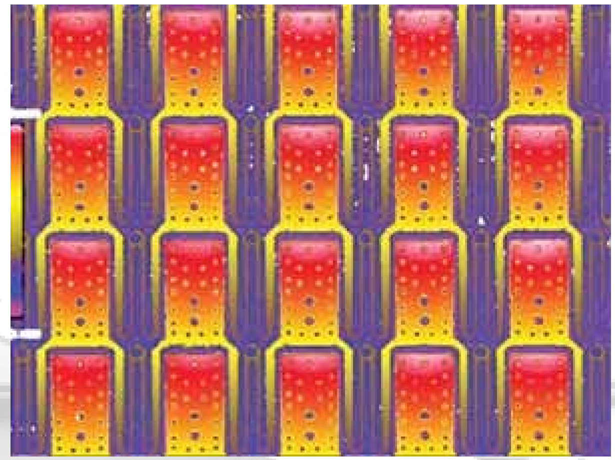

Array of MEMS cantilevers

Each MEMS cantilever corresponds to a pixel.

The bimetal cantilevers are heated by incident infrared radiation causing them to bend, changing the capacitance between the cantilever and an electrode on the substrate. The capacitance change is converted into an electrical signal that is proportional to the amount of absorbed IR light.

Hunter, S. R., et al., *Proc. of SPIE*, 5074, pp. 469-480, 2003.

Sarcon Microsystems, Knoxville, TN and Sarnoff Corporation, Princeton, NJ

Opto & Laser Europe, June 2003.

Optical Shutter

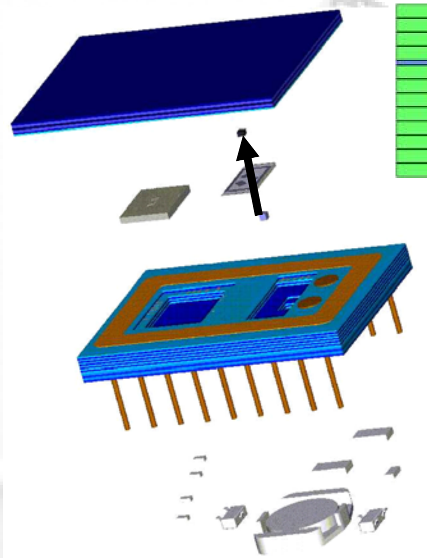

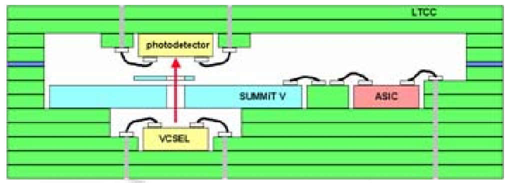

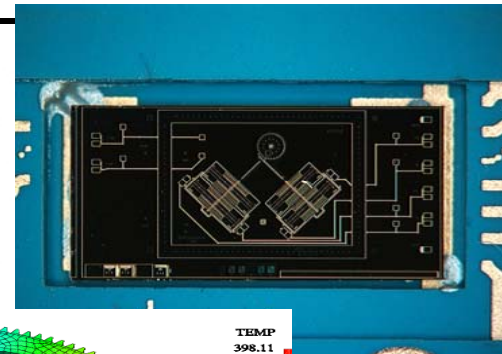

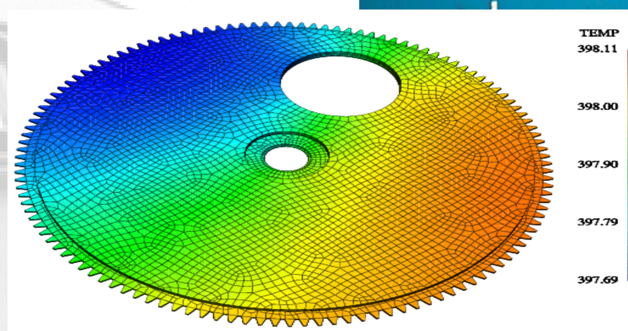

Picture of Product Emulator 1

- As components are reduced in size and packaged in a small confined space, the challenges of thermal management increase.
- The packaging, thermal management, and reliability solutions must be compatible with the transmission of force or motion, electrons, and photons into and out of the device.

Photonics and VCSELs
(Vertical Cavity Surface Emitting Lasers)

- Heat Transfer across a super-lattice.

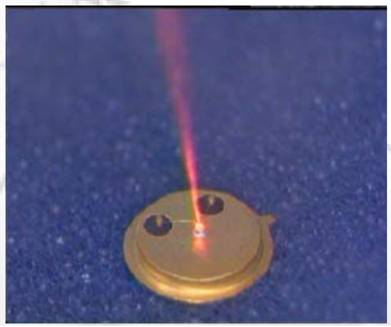

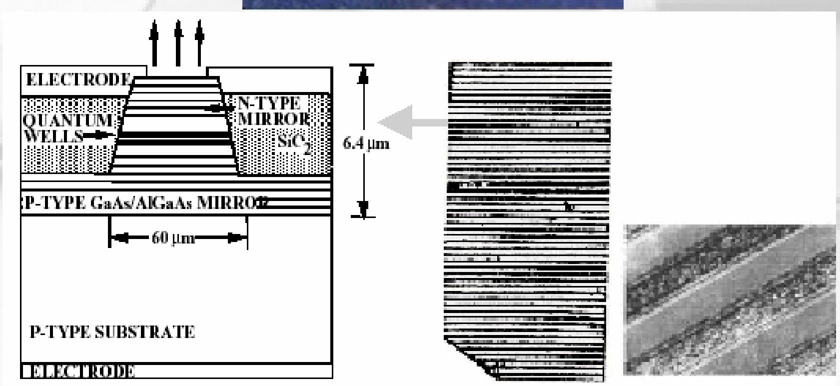

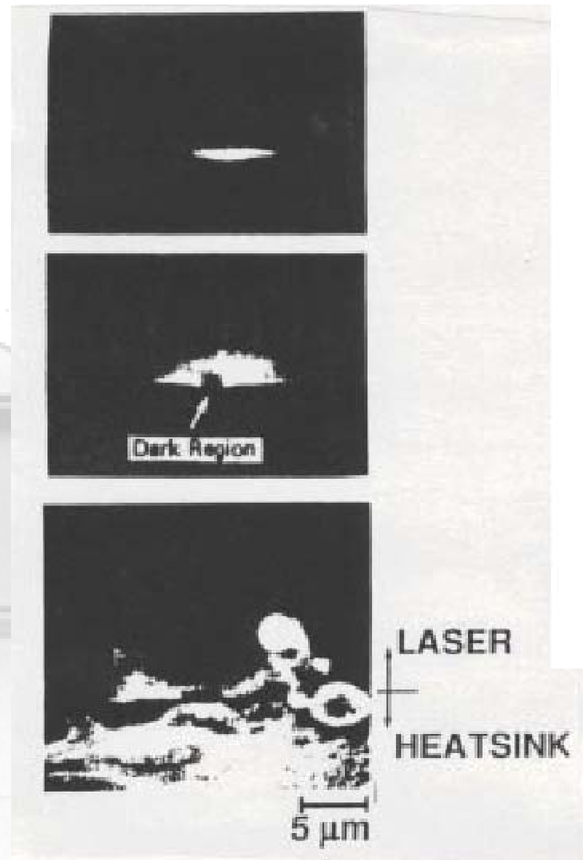

CATASTROPHIC DAMAGE

Laser Processing of Microsystems

Laser Processing of MEMS includes:

- direct etching for rapid prototyping
  (Müllenborn, Heschel, Larsen, Dirac, and Bouwstra, *J. Micromechanics and Microengineering*, **6**, pp. 49-51, 1996)
- bonding
  (Lin, *Microelectronics Journal*, **34**, pp. 179-185, 2003)
- cleaning
  (Lin and Cetinkaya, *J. Adhesion Science and Technology*, **17**, pp. 91-113, 2003)
- laser repair of adhered MEMS structures
  (Phinney and Rogers, *J. Adhesion Science and Technology*, **17**, pp. 603-622, 2003)

Laser Processing of MEMS Parts: Example Laser Repair of Adhered Cantilevers

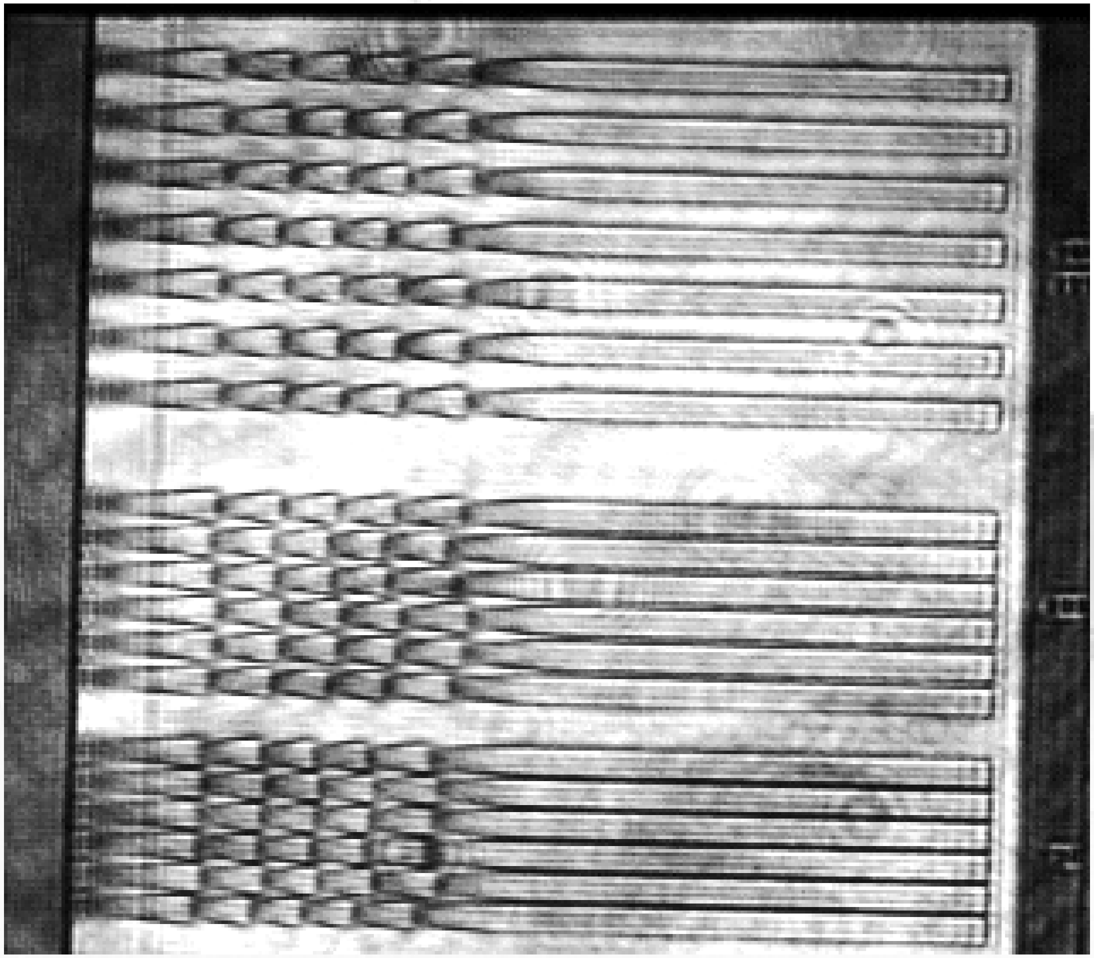

500 fps
polysilicon
L = 1000 μm
w = 30 μm
t = 2.6 μm
h = 1.9 μm
Nd:YAG
532 nm
4 ns, 20 Hz
J = 25 mJ/cm^2
ΔT = 37°C

—— 100 μm

Rogers and Phinney, *Microscale Thermophysical Engineering*, **8**, pp. 43-59, 2004.

Sandia National Laboratories

MEMS Thermal Actuators

Comtois actuators, J. H. Comtois et al., *Sensors and Actuators A*, 70, pp. 23-31, 1998.

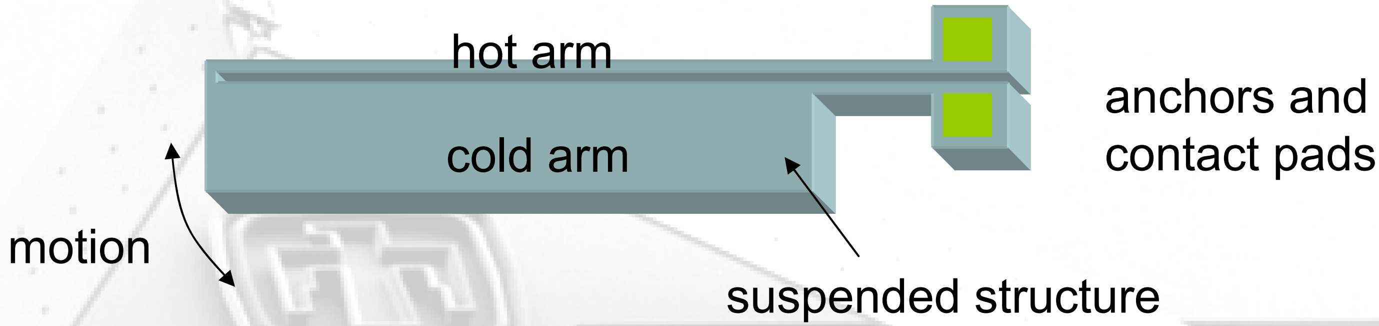

Bent-beam actuators, Que et al., *J. MEMS*, 10, pp. 247-254, 2001.

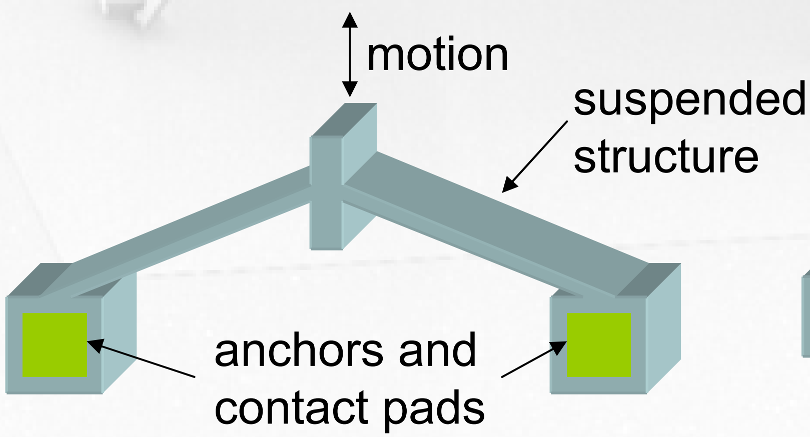

Multiple material actuators, Ataka et al., *J. MEMS*, 2, pp. 146-150, 1993.

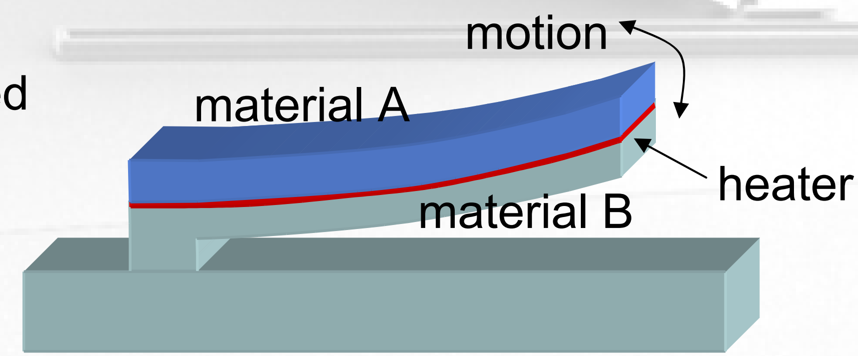

Sandia National Laboratories

Why Optical Actuation?

- Requires no electrical connections → intrinsic electrical isolation
- Compatible with harsh environments (radiation, high temperature, etc.)
- Enabling technology for all-optical MEMS devices
- Does not electrostatically attract particles
- Different actuation schemes possible, including radiation pressure, use of photostrictive materials and photothermal processes

Sandia National Laboratories

MEMS Optical Bent-beam Microthermal Actuator

- Leverage knowledge of electrically powered MEMS actuators for optimizing design
- Two designs:
  - ➢ Bent-beam
  - – Flexure

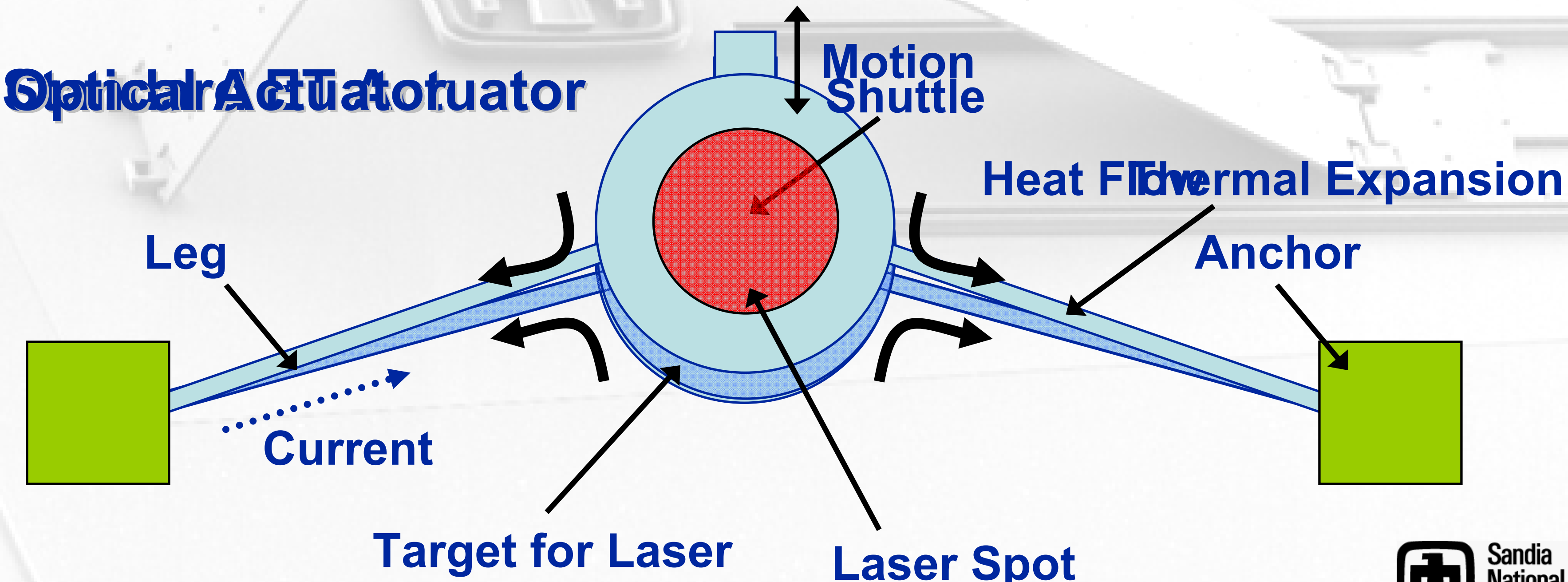

Sandia National Laboratories

MEMS Optical Flexure Microthermal Actuator

- Leverage knowledge of electrically powered MEMS actuators for optimizing design
- Two designs possible:
  - – Bent-beam
  - ➢ Flexure

Optical Actuator

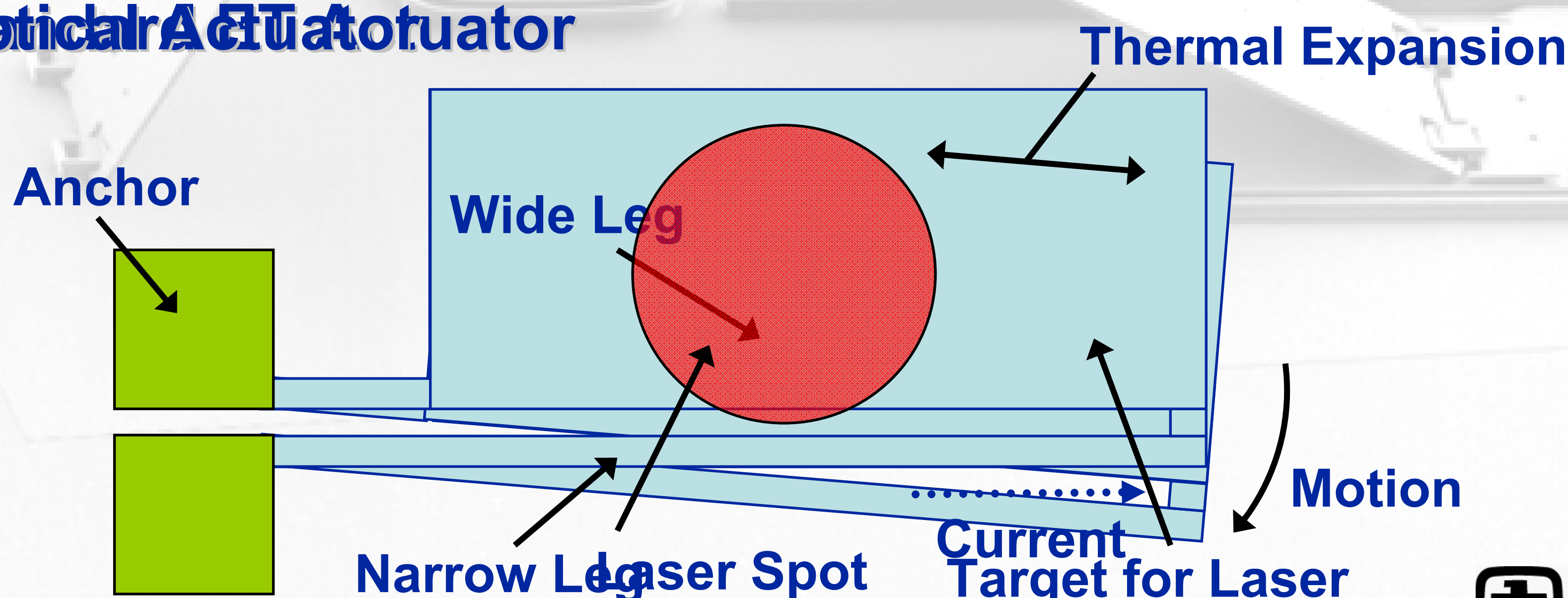

Sandia National Laboratories

Surface Micromachined MEMS Devices

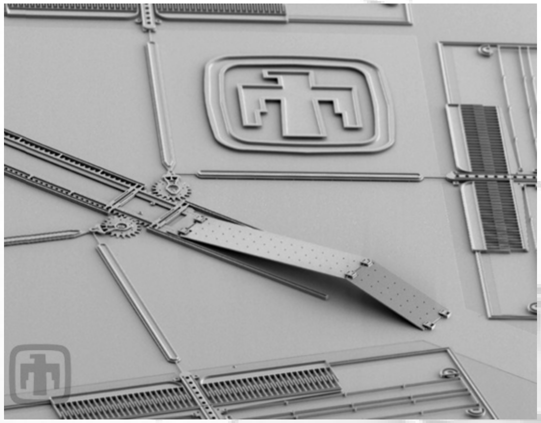

Hinged Silicon Mirror and Drive Motors

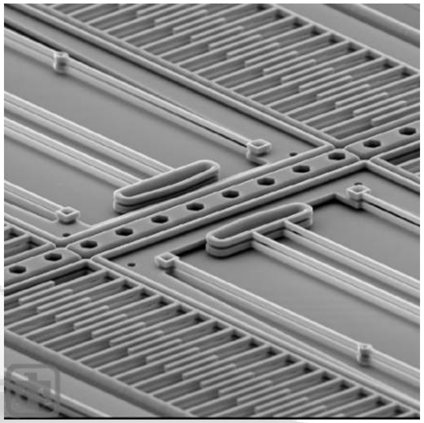

Comb Drive Detail

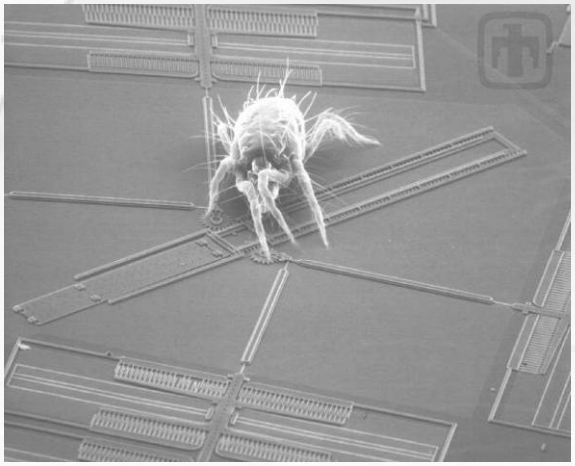

Spider Mite on a Mirror Assembly

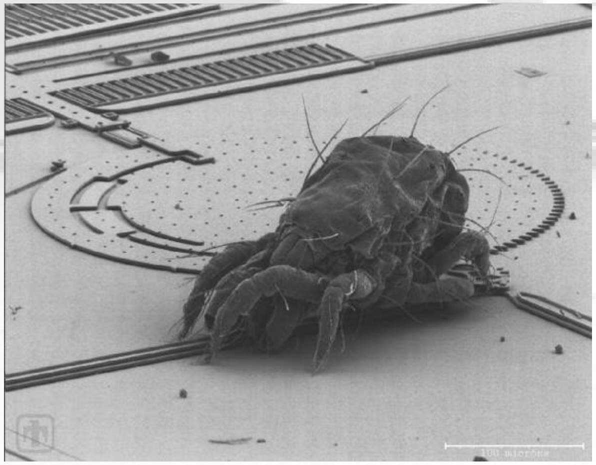

Spider Mite on a Microlock Mechanism

http://mems.sandia.gov

Sandia National Laboratories

SUMMiT™ V

Sandia's Ultra-planar Multi-level MEMS Technology

SUMMiT™ Layers

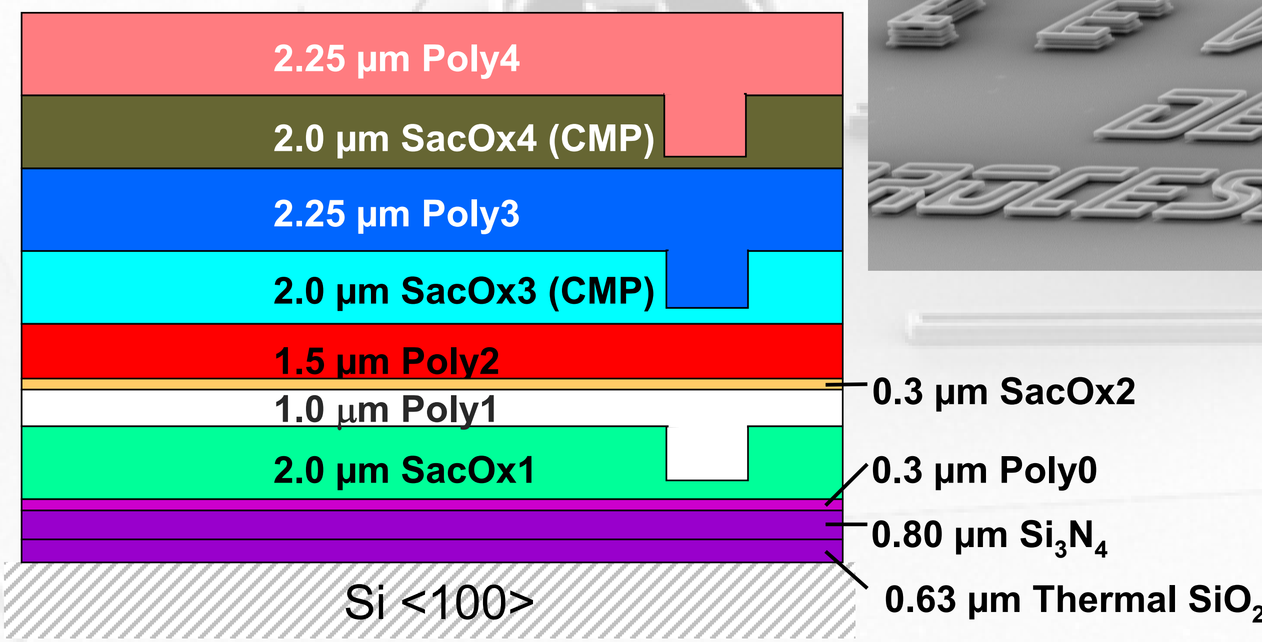

All Polycrystalline Si (Poly) is doped with Phosphorus.

Micromachined Actuators and Structures

Laser Powered Thermal Actuators

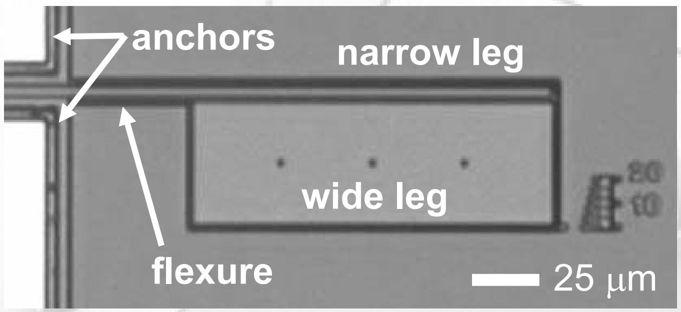

Flexure style actuator

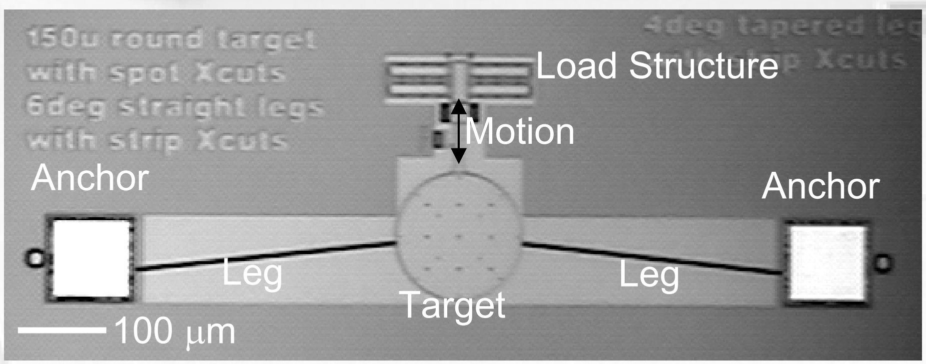

Bent-beam actuator

Test Structures

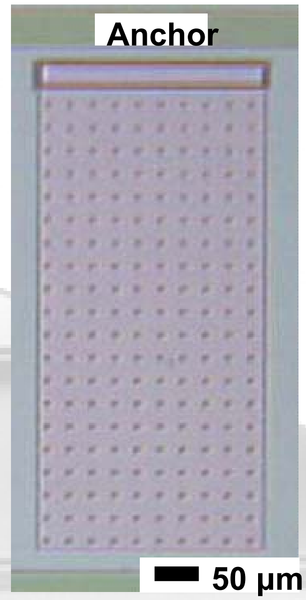

Cantilevers

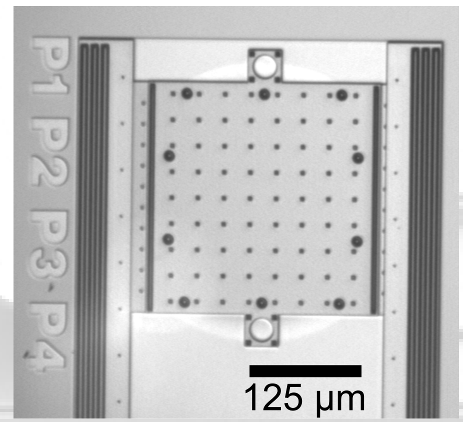

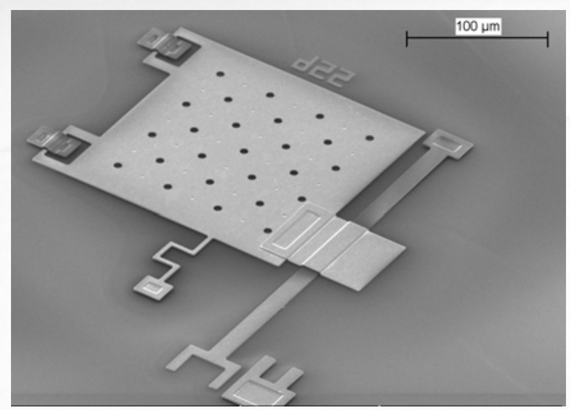

Sliders

Flaps

Sandia National Laboratories

Optical Actuation

- Actuator output typically increases with input optical power
- Unfortunately, so does the risk of damage and device failure
- Improved performance obtained by:
  - **maximizing output**
  - **reducing damage risk**
- We must have a fundamental understanding of device behavior in order to improve designs.

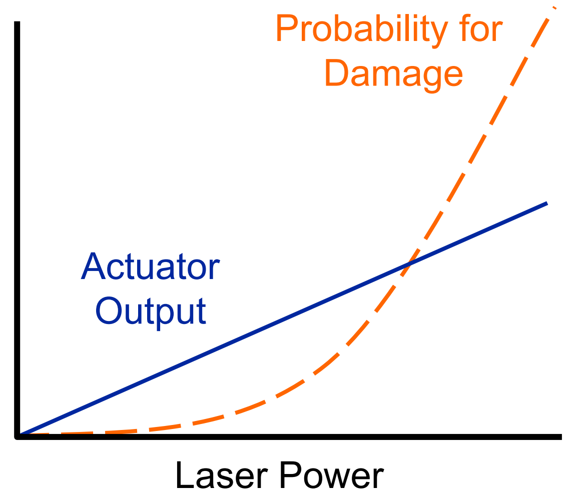

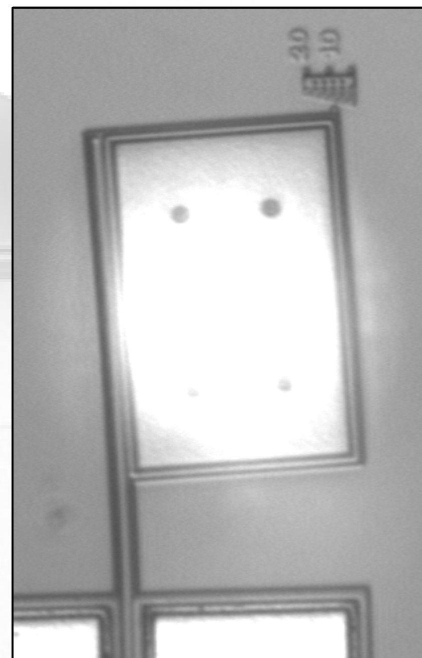

Laser Powered Thermal Actuators
Design of Experiments

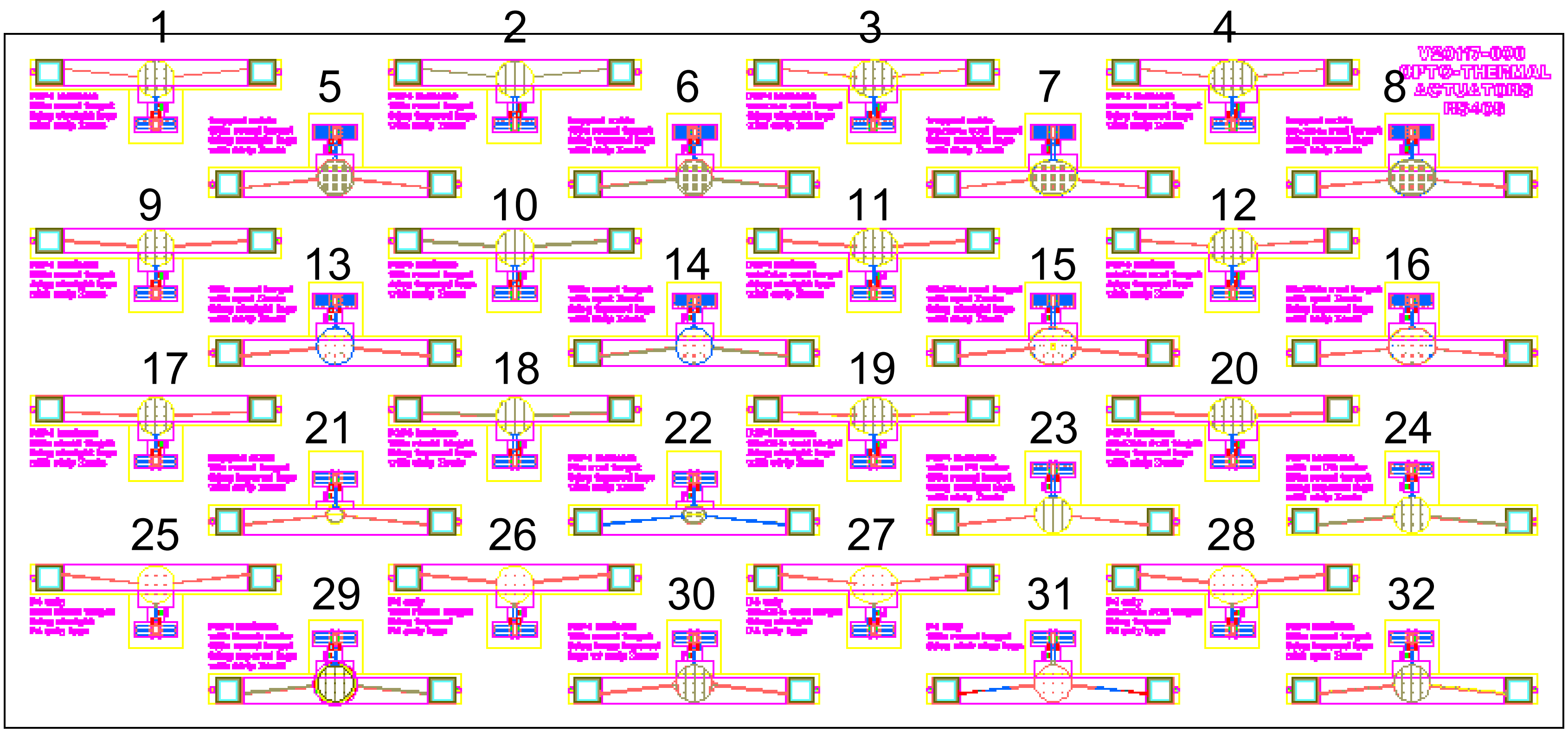

- Varied target design, target size, leg design and composition, and leg angle

Phinney, Klody, Sackos, and Walraven, *Proc. of SPIE*, Vol. 5343, pp. 81-88, 2005.

Laser Powered Thermal Actuator Target Cross Sections

- 4 different target designs were fabricated
- Poly3 and Poly4 are each 2.25 μm thick
- Oxide layer is 2.0 μm thick
- Distance to Poly3 layer to substrate is approx. 6.75 μm
- Distance to Poly4 layer to substrate is approx. 11.0 μm

Poly3-Poly4 laminate

Poly3-Poly4, trapped oxide

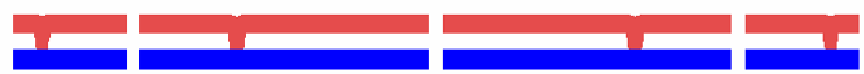

Poly3-Poly4, no trapped oxide

Poly4 only

Phinney and Serrano, *Sensors and Actuators A*, **134**, pp. 538-543, 2007.

Sandia National Laboratories

Experimental Methods

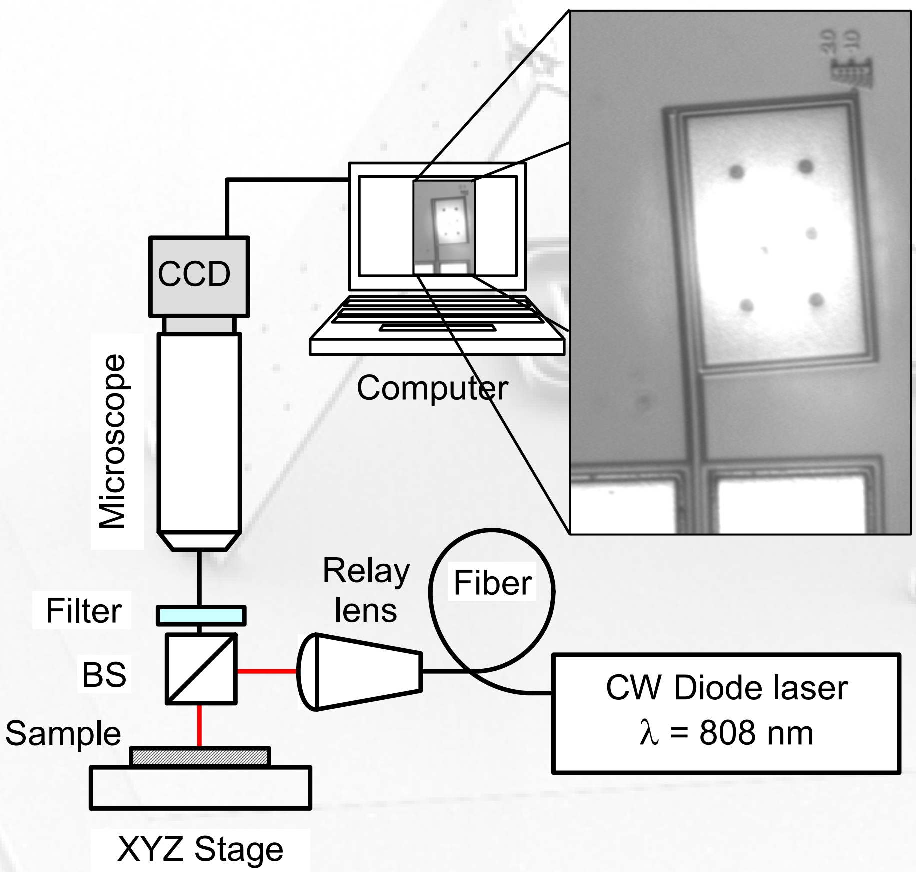

- 808 nm CW fiber coupled laser heating of MEMS
- 100 μm diameter spot on sample
- Variable laser power, up to 1 W
- Various actuator designs and MEMS structures tested
- Displacement performance and robustness evaluated through image analysis

Sandia National Laboratories

Experimental Details
Initial Laser Damage Experiments

- Two dice were tested for a total of 64 actuators tested (two of each design).
- Displacement was measured for the bent-beam thermal microactuators from the images taken by the computer.
- Displacement was roughly the same (around 6 μm) for all actuators.
- However, damage levels varied substantially from essentially no damage to high amounts of damage.

Phinney, Klody, Sackos, and Walraven, *Proc. of SPIE*, Vol. 5343, pp. 81-88, 2005.

Optically Powered Thermal Actuator Damage Characteristics

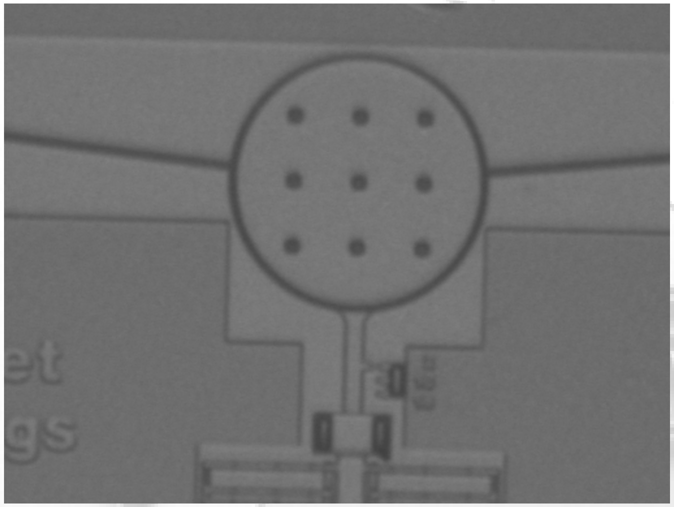

Poly3-Poly4 laminate actuator: No Damage

Poly3-Trapped Oxide-Poly4 actuator: Low Damage

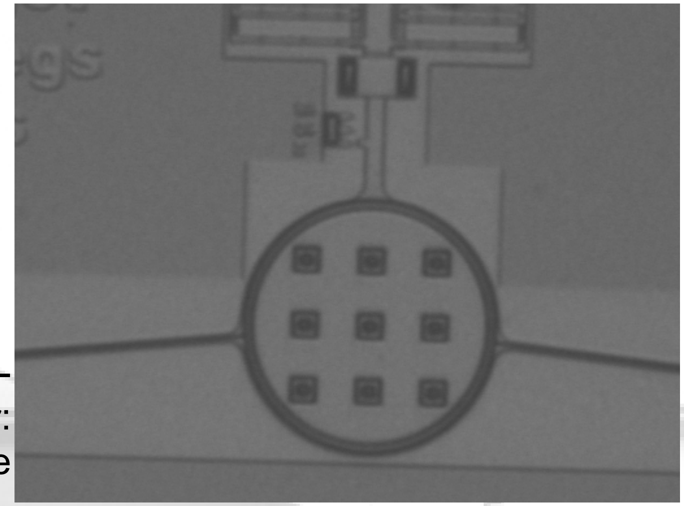

150 μm

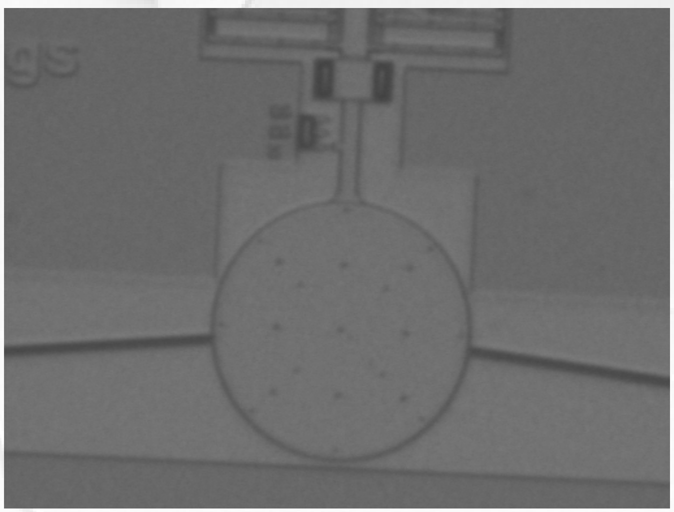

150 μm

Varying amounts of damage observed when actuator targets irradiated by a laser at 808 nm at three power levels: 150 mW, 250 mW, and 350 mW

Poly3-Air Gap- Poly4 actuator, connecting posts are 2 μm by 2 μm: High Damage

Summary of Laser Damage

Target Design	Number of Actuators Tested	Level of Detectable Post-Test Damage		
		None	Low	High
P3P4 laminate	36	23	11	2
P3P4 with trapped oxide	10	4	6	0
P3P4 with air gap	8	0	0	8
P4 only	10	0	0	10

Phinney, Klody, Sackos, and Walraven, *Proc. of SPIE*, Vol. 5343, pp. 81-88, 2005.

FIB Cross Sections of Parts

P3P4 Laminate Prior to Laser Irradiation

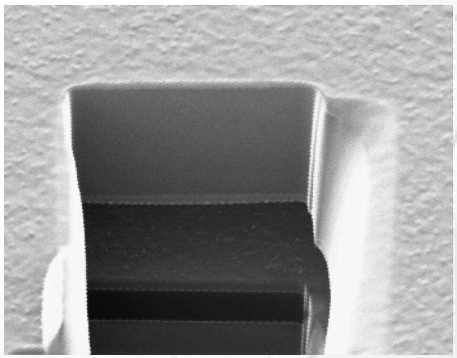

P4-Trapped Oxide-P3 Prior to Laser Irradiation

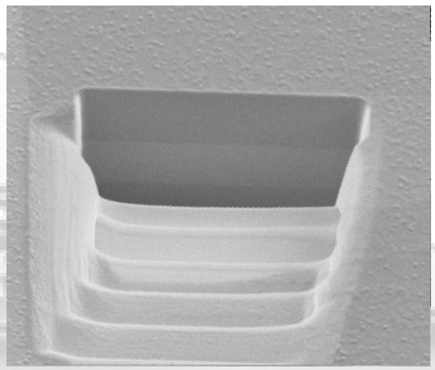

P3P4 Laminate After Laser Irradiation Showing No Damage

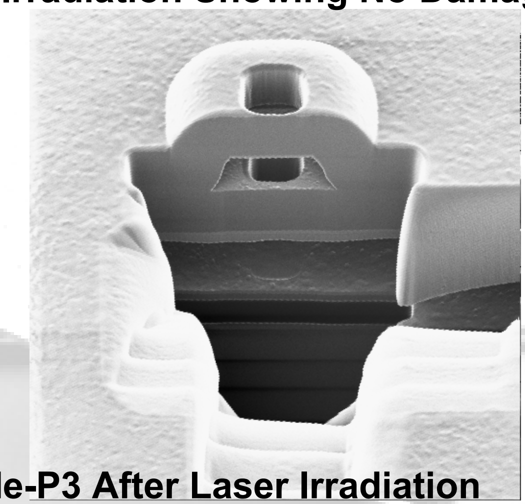

P3P4 Laminate After Laser Irradiation with Low Amount of Visible Damage

Damage is mostly superficial in this area (depth is less than a micron)

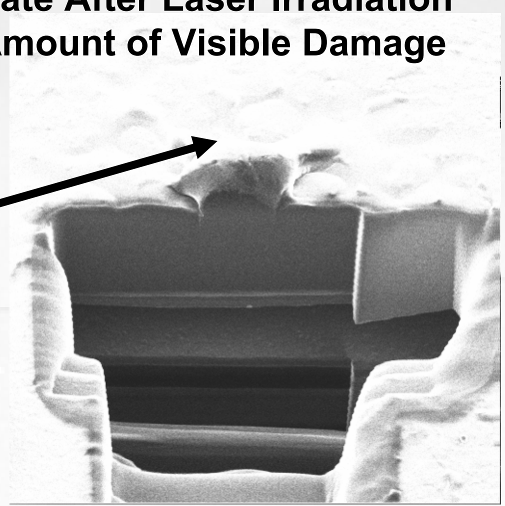

P4-Trapped Oxide-P3 After Laser Irradiation with Low Amount of Visible Damage

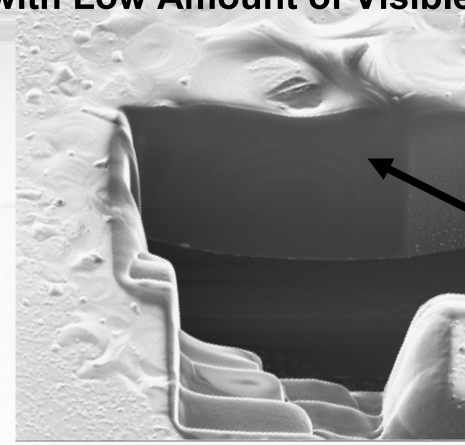

Damage and apparent bending is observed all the way through the poly layer

Sandia National Laboratories

Damage Characterization for Subsequent Laser Damage Experiments

- Extent of damage on target surface critical for device reliability
- To compare ovals and circles, normalize damage width, L_D, by target width, L_T, or calculate damage fraction, ratio of damage area divided by target area
- Evaluate damage extent as a function of power, irradiation time

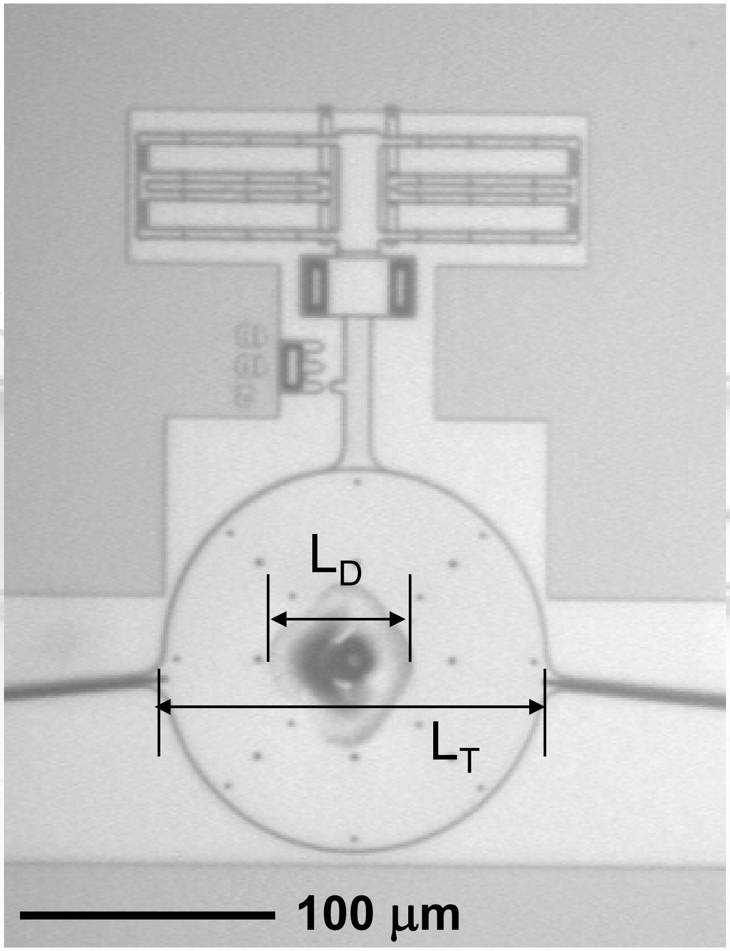

Laser Damage: Two Regimes

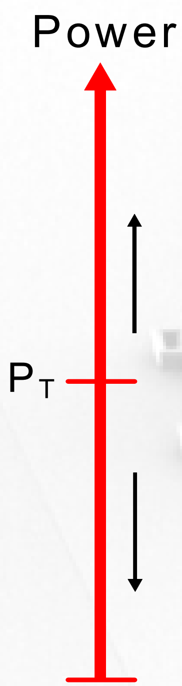

- Occurrence of damage depends on laser power
- Two regimes of damage were observed
  - Immediate damage: damage occurs immediately upon irradiation; higher laser powers
  - Prolonged exposure: damage occurs after irradiation over a period of time; lower laser powers
- Indication of both short- and long-term phenomena occurring during laser irradiation

Immediate Damage

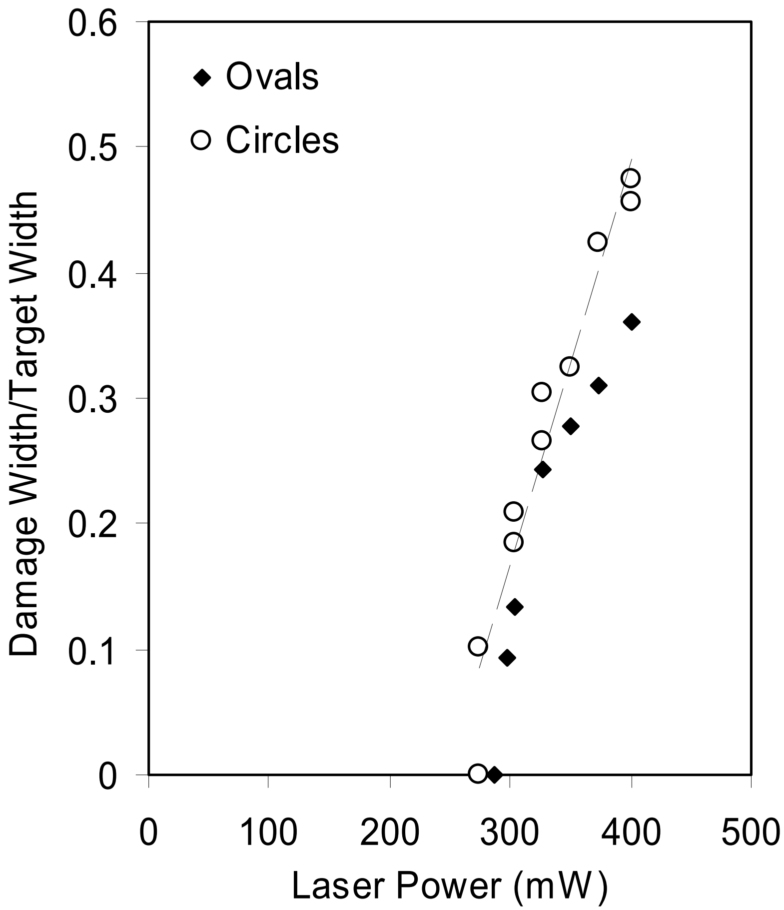

- No detectable delay between laser irradiation and surface damage
- Damage extent increases linearly for laser powers greater than 300 mW on circular and oval targets

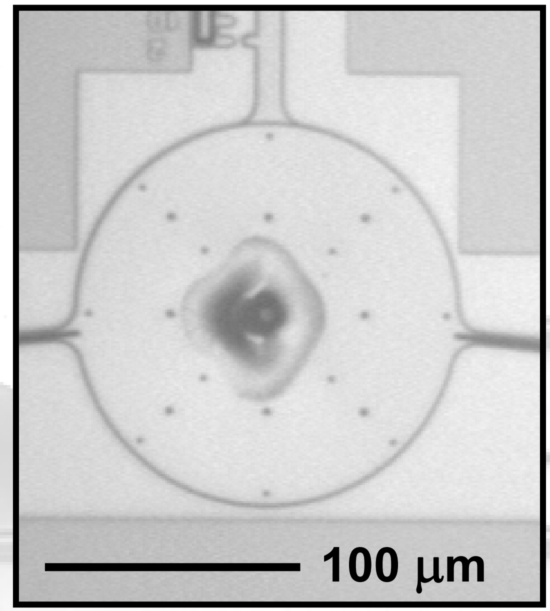

- Threshold power for immediate damage:
  - ~275 mW (circular)
  - ~295 mW (oval)

Serrano, Phinney, and Brooks, 2005, *Proc. of InterPACK'05*, ASME, IPACK2005-73322, pp. 1-6.

Sandia National Laboratories

Effect of Post Size

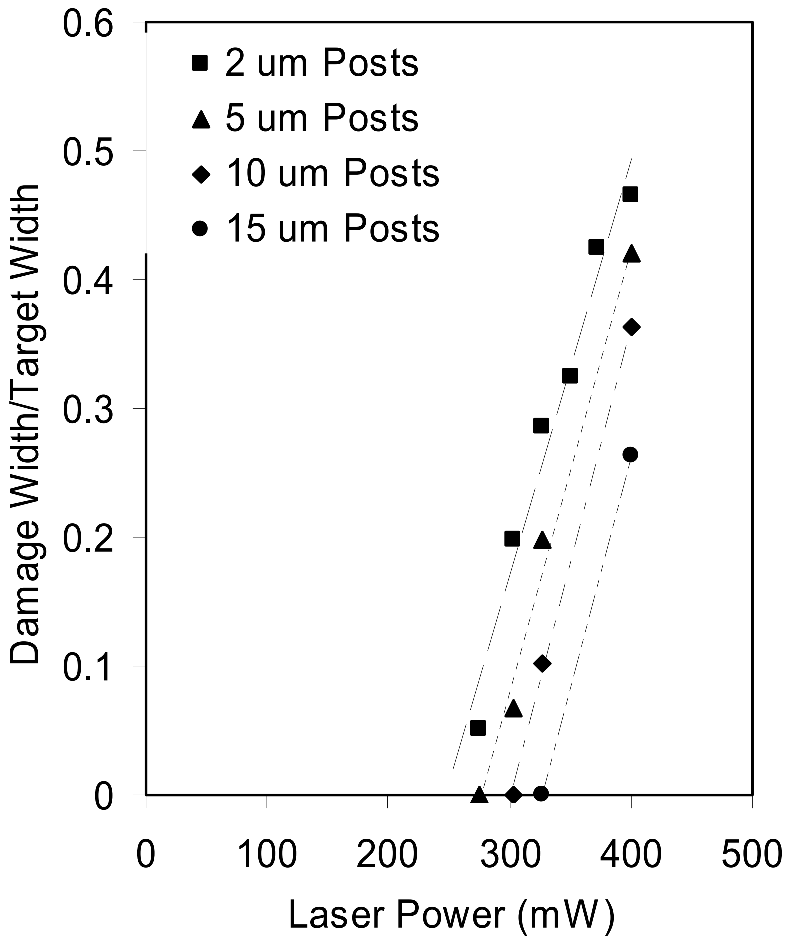

- Threshold power for immediate damage shifted to greater laser powers and longer time-scales
- Targets with 15 x 15 μm^2 posts withstood 16 min. w/o damage

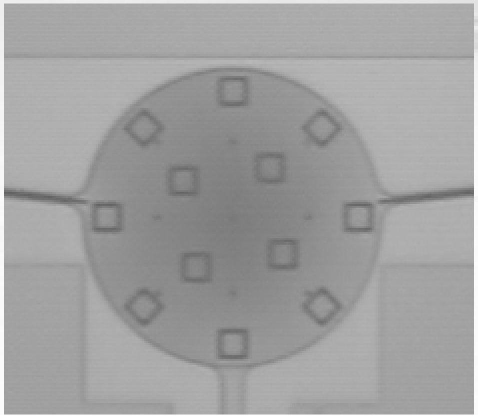

P=326 mW, t_D ~ 600 s

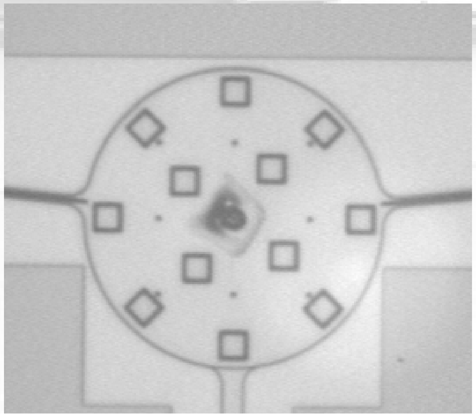

P=400 mW, t_D ~ 0 s

Bent-Beam Actuators

- Displacement is ~5-6 μm with minimal dependence on laser power
- Robustness to damage is key for device reliability

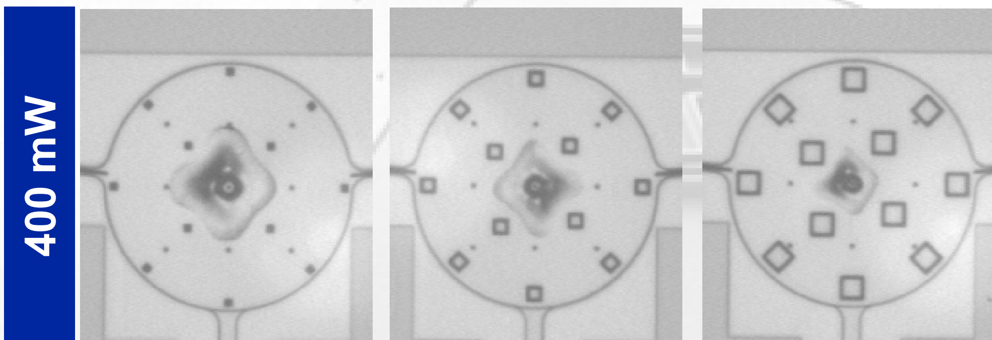

5 μm posts | 10 μm posts | 15 μm posts

- Increasing target thermal mass shifts damage to higher powers; cannot prevent it entirely
- Threshold power for damage can be estimated from damage size

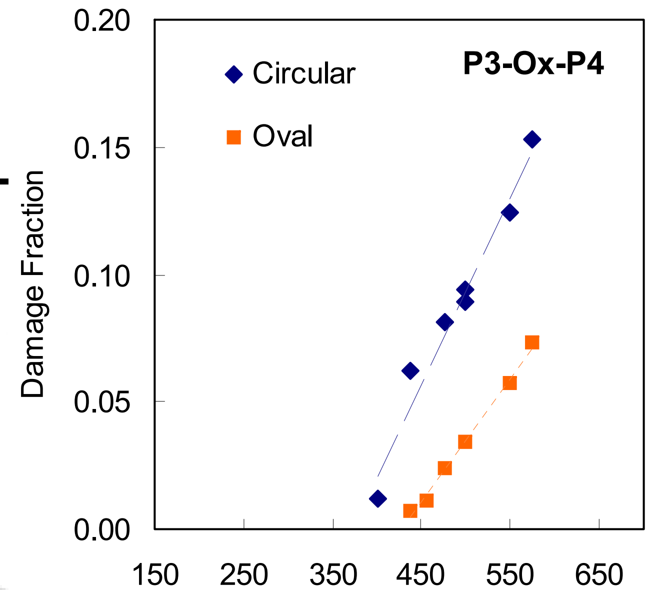

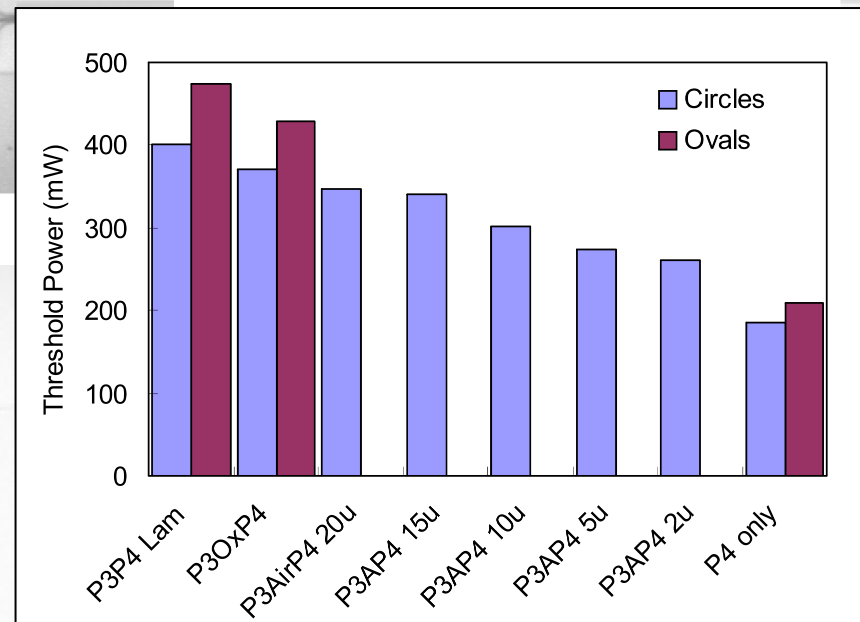

Phinney and Serrano, *Sensors and Actuators A*, **134**, 538-543, 2007.

Flexure Thermal Microactuators

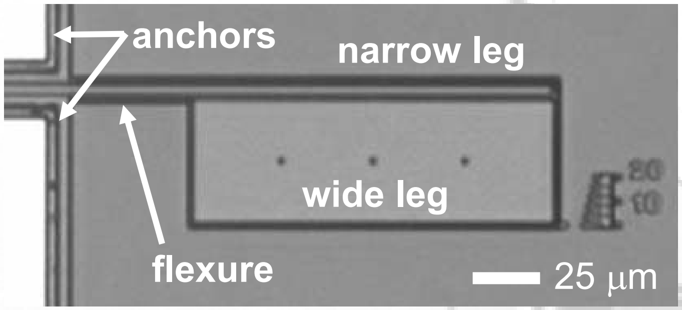

- Actuator designs
  - **Composition: P4-only or P3-P4 laminate**
  - **Narrow leg: 2.5 x 200 μm**
  - **Wide leg: 2.5 x (50/100) μm**
  - **50 μm flexure element**
  - **2.5/5.0 μm leg-leg distance**

- Dissimilar thermal expansion between hot and cold sides used to generate motion
- Compared to ET flexure actuators
  - Larger wide leg which serves as target for laser
  - Wide leg is “hot” side of actuator
  - Motion is in the opposite direction
  - Different failure mechanism

Serrano and Phinney, 2006, *Proc. ASME IMECE*, IMECE2006-14950, pp. 1-6.

Target Composition

- Displacement is linear with power up to initiation of surface damage
- Maximum displacement similar for both compositions
- After damage, displacement recedes slightly (P34) or remains constant
- P4-only actuators significantly more robust than previous studies; possibly due to interference

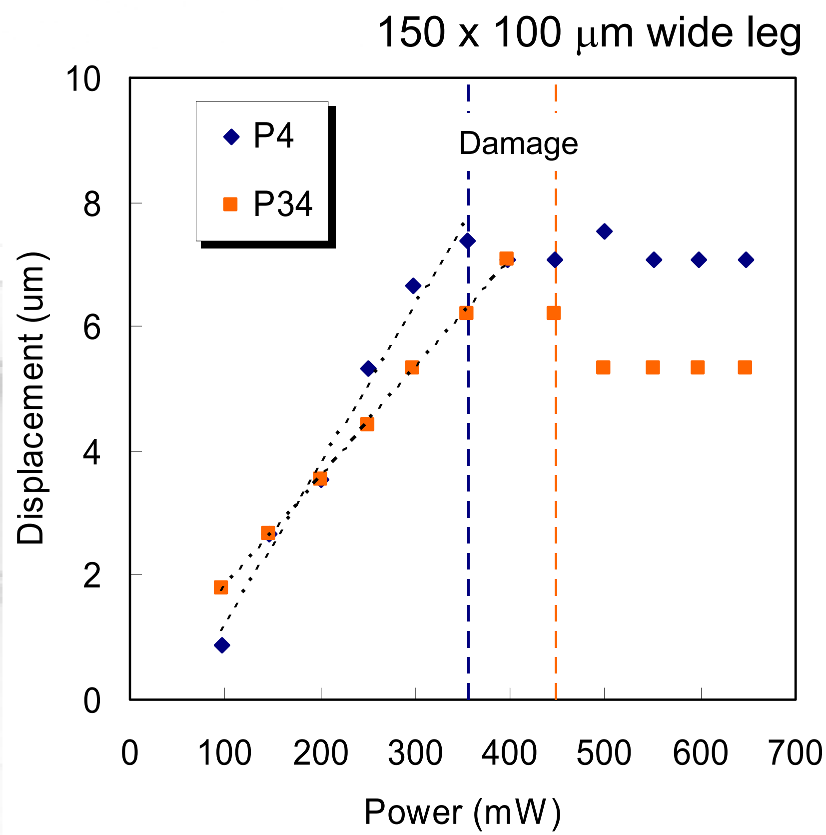

Serrano and Phinney, *JMEMS,* **17,** 166-174, 2008.

Performance and Laser Damage

- Linear displacement with laser power up to initiation of damage
- Damage compromises structural integrity of device and recession in the displacement

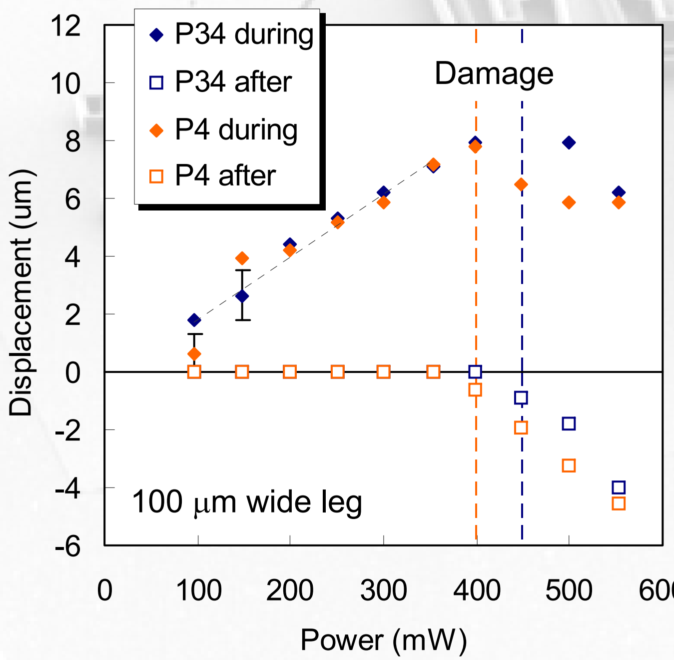

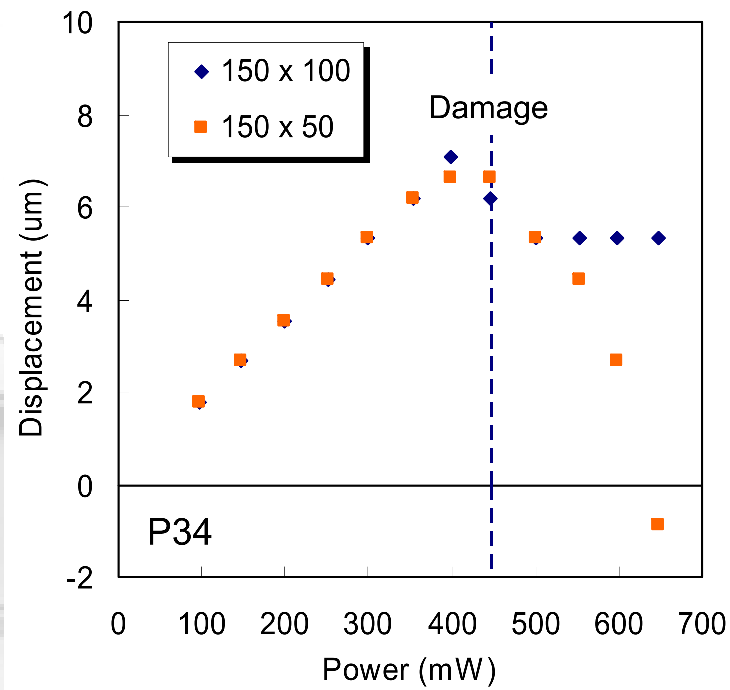

- Strain relaxation during damage results in additional thermal contraction when unpowered and recession of return position.

Serrano and Phinney, *JMEMS*, **17,** 166-174, 2008.

Sandia National Laboratories

Effects of Layers and Underlying Vias

Slider Design

Top View

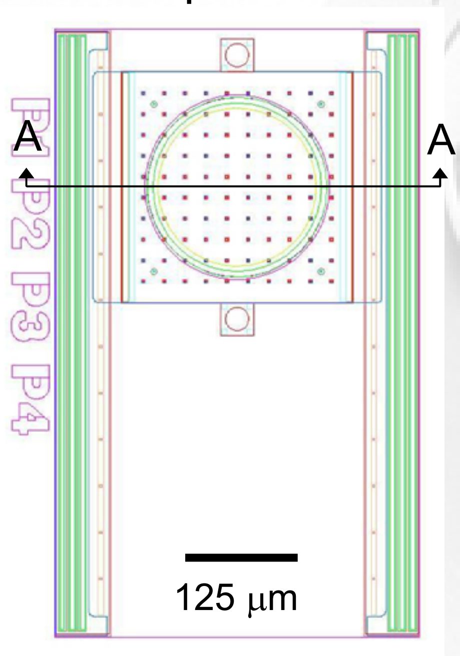

cross section A-A

substrate via (hole)

Before Laser Heating

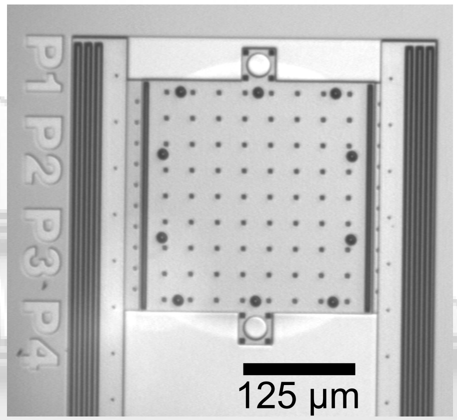

After Laser Heating

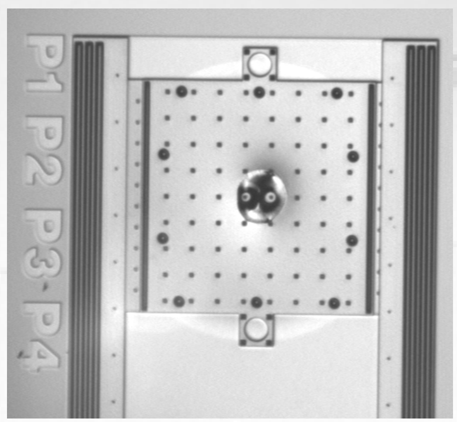

Thresholds for Damage for Polysilicon Sliders over a Substrate Via and over an Intact Substrate – 808 nm laser

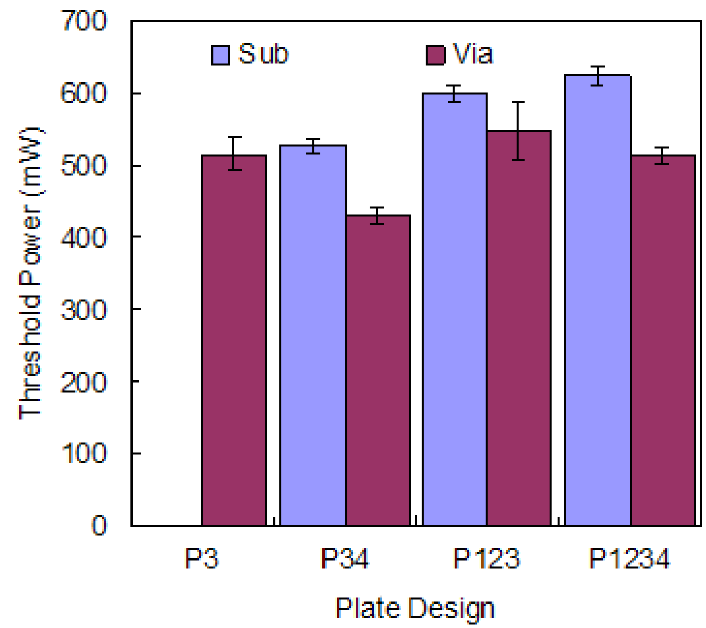

Flap Design and Fabrication

Poly1 flap

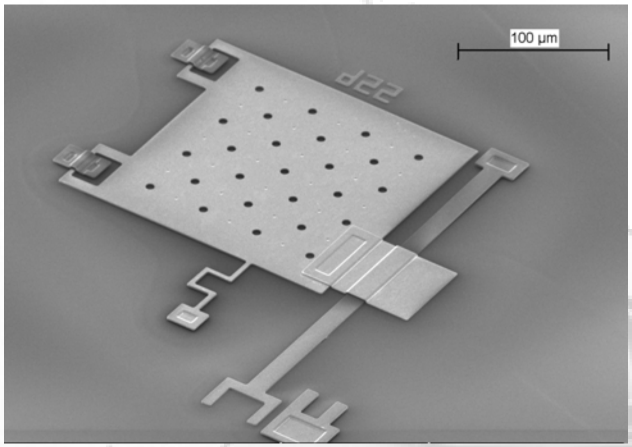

before being flipped

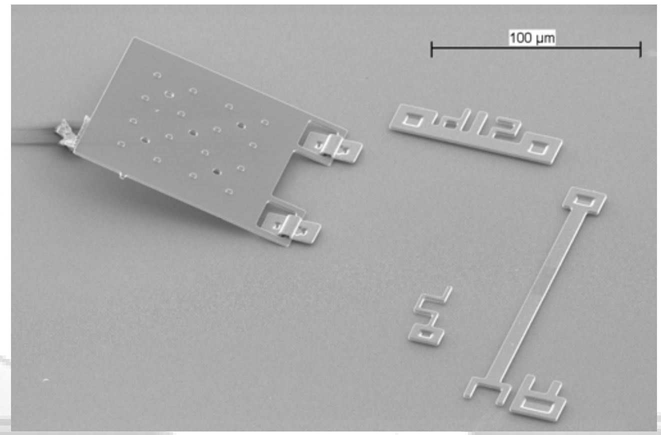

after being flipped

Poly2 flap

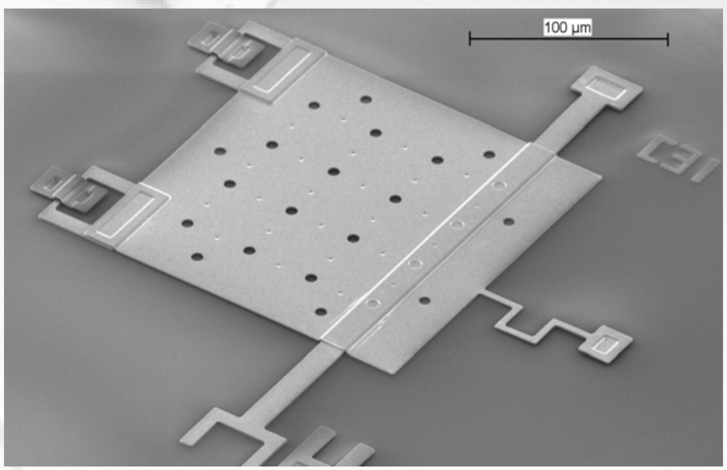

before being flipped

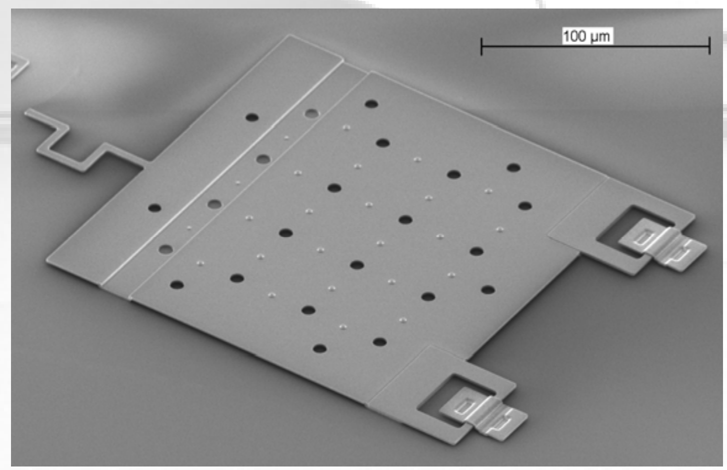

after being flipped

Xue, Koppaka, Phinney and Mackin, *Proc. 2004 SEM X*, Paper No. 305, pp. 1-7, 2004.

Sandia National Laboratories

Sacrificial Surface Micromachining

Multi-User MEMS Process (MUMPs™)

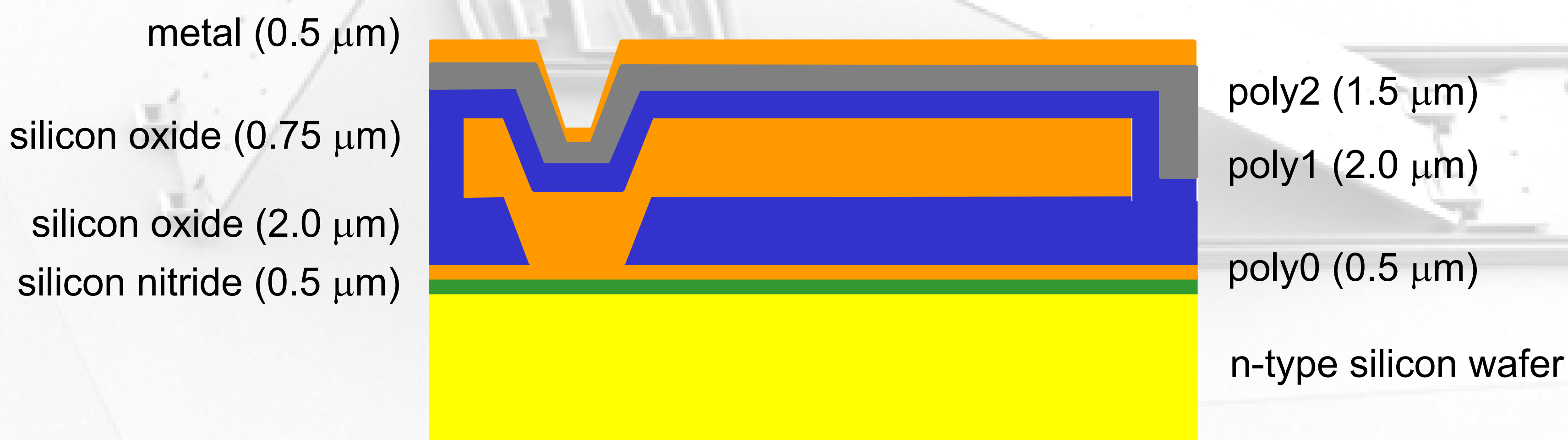

Sandia National Laboratories

Laser Irradiation

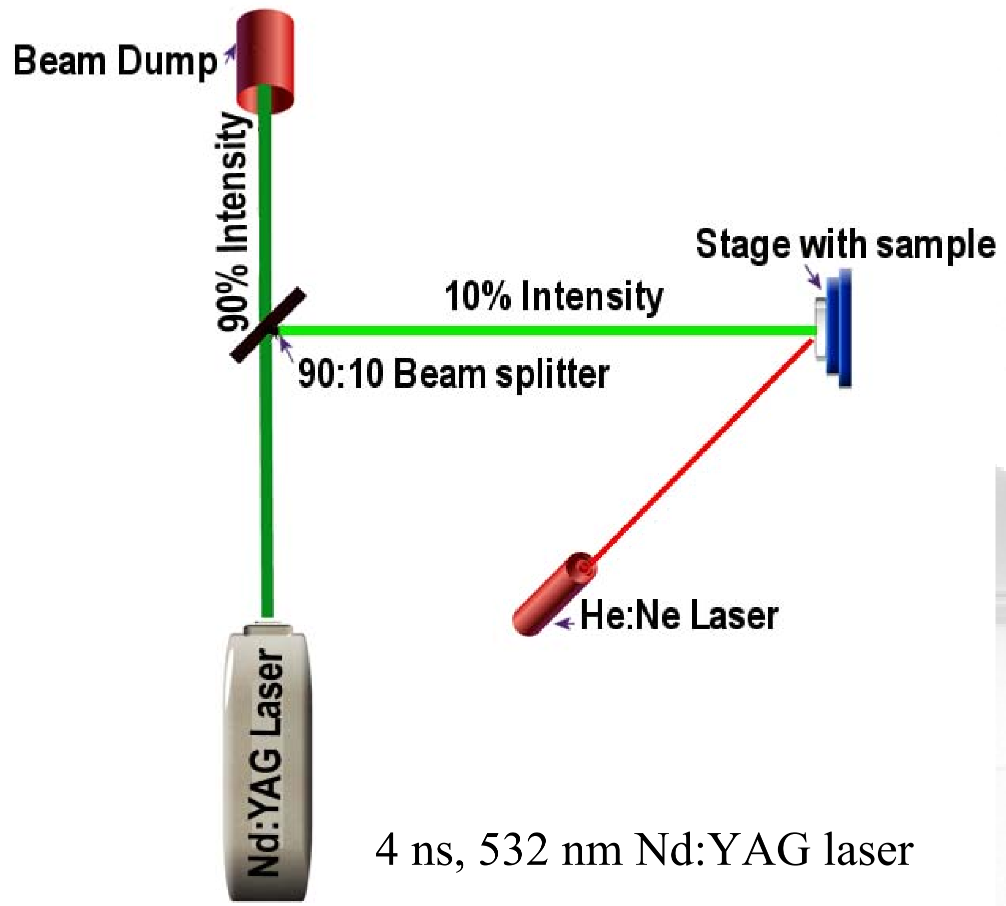

4 ns, 532 nm Nd:YAG laser

Sandia National Laboratories

Surface Topography

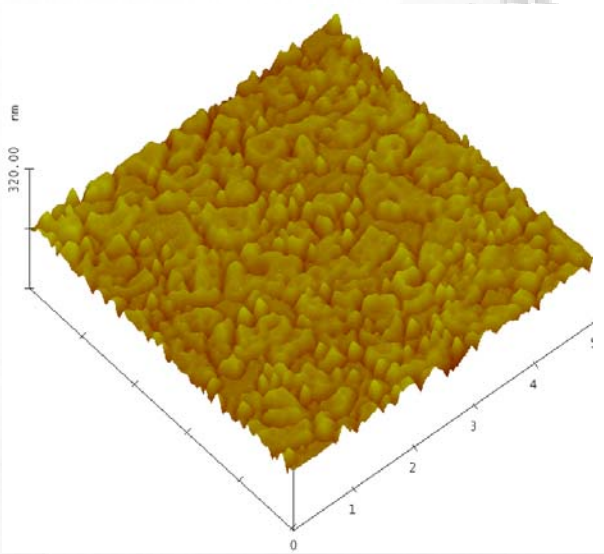

0 mJ/cm²

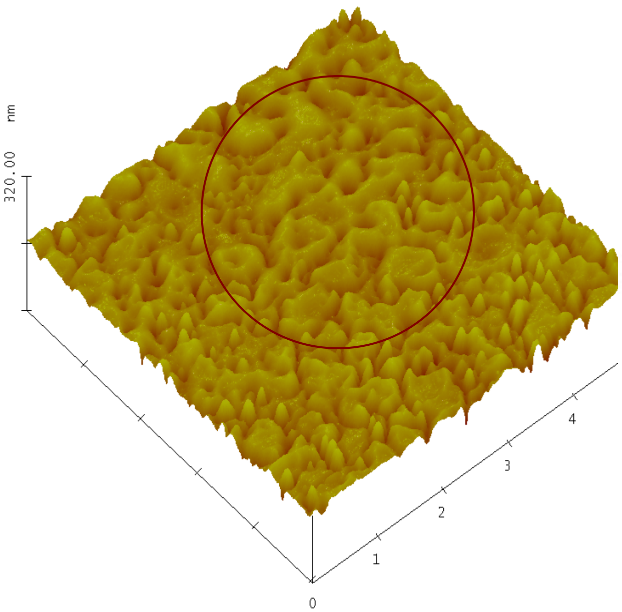

70 mJ/cm²

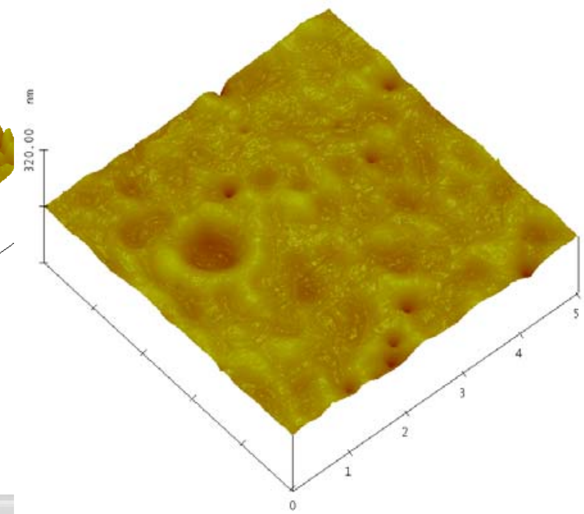

80 mJ/cm²

5 μm x 5 μm AFM images of the top surfaces of **poly2 flaps** before and after laser irradiation (Thickness: 1.5 μm)

Xue, Koppaka, Phinney and Mackin, *Proc. 2004 SEM X*, Paper No. 305, pp. 1-7, 2004.

Surface Parameters

Root mean square (RMS) roughness: $\sigma = \sqrt{\frac{\sum (z_i - \bar{z})^2}{N}}$

Reduced skewness: $S = \frac{1}{N\sigma^3} \sum \left(z_i - \bar{z}\right)^3$

Reduced kurtosis: $K = \frac{1}{N\sigma^4} \sum \left(z_i - \bar{z}\right)^4$

Gaussian distribution, $S \approx 0$ and $K \approx 3$

Surface Roughness Parameters of Poly2

Fluence (mJ/cm^2)	Top poly2 flap			Bottom poly2 flap		
	RMS (nm)	Skewness (*S*)	Kurtosis (*K*)	RMS (nm)	Skewness (*S*)	Kurtosis (*K*)
Before irradiation	9.76±0.56	-0.40±0.08	3.42±0.07	1.92±0.31	-0.11±0.16	2.96±0.15
40	10.34±0.71	-0.48±0.16	3.61±0.18	1.82±0.15	0.11±0.10	2.96±0.31
50	10.89±0.13	-0.56±0.08	3.76±0.02	1.90±0.20	0.05±0.23	2.89±0.22
60	10.84±0.58	-0.62±0.05	4.14±0.17	1.83±0.28	0.13±0.21	3.02±0.17
70	11.10±0.73	-0.79±0.04	4.63±0.02	1.96±0.16	0.01±0.02	2.84±0.17
80	**4.93±0.06**	**-0.93±0.01**	**6.68±0.18**	1.93±0.15	0.04±0.10	2.86±0.10

Surface Roughness Parameters

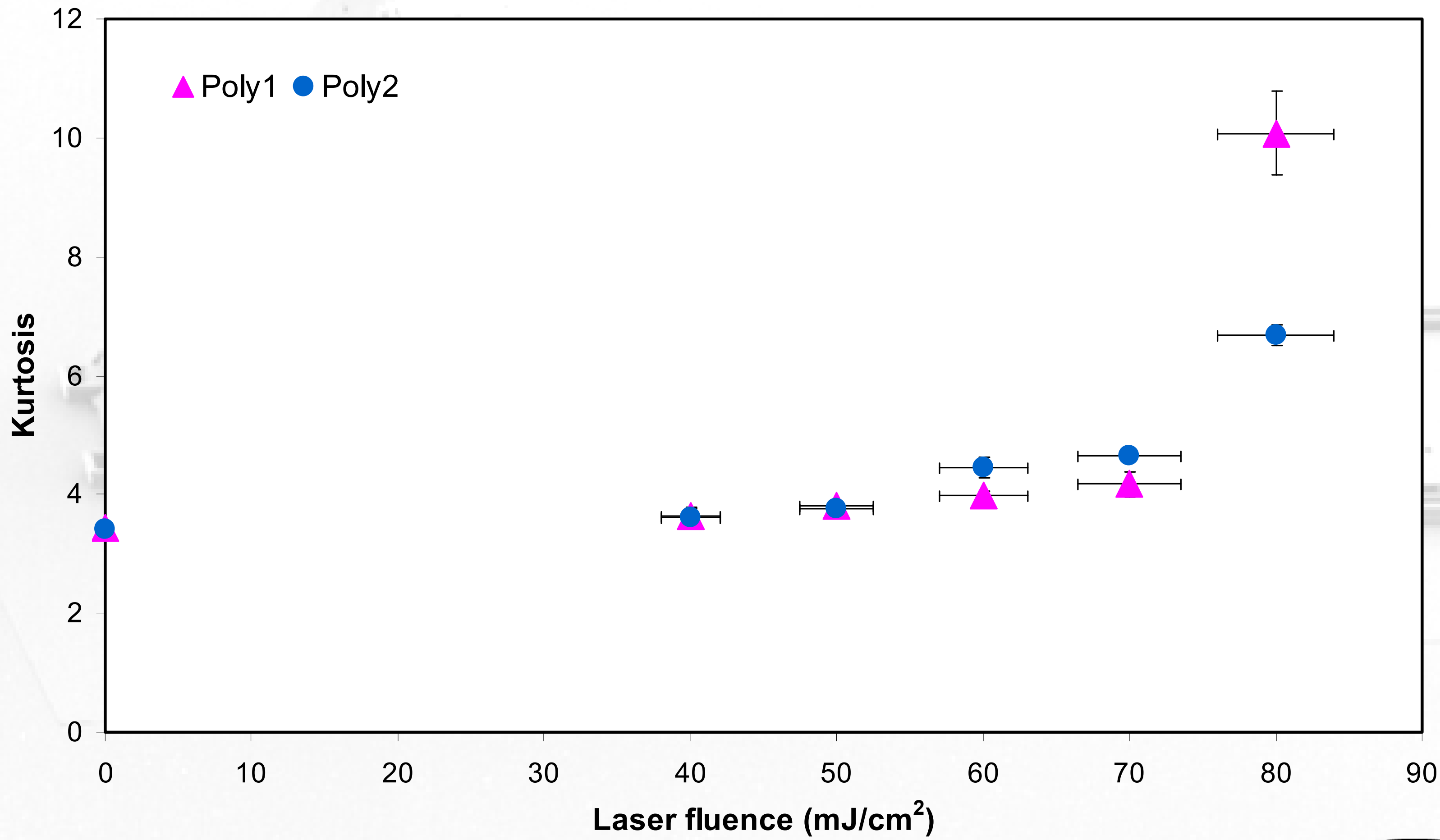

Xue, Koppaka, Phinney and Mackin, *Proc. 2004 SEM X*, Paper No. 305, pp. 1-7, 2004

Sandia National Laboratories

Experimental Static Interferometry Test Setup and Cantilever Design

polysilicon cantilever

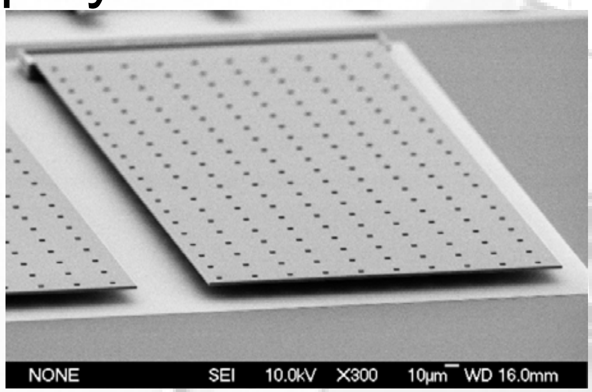

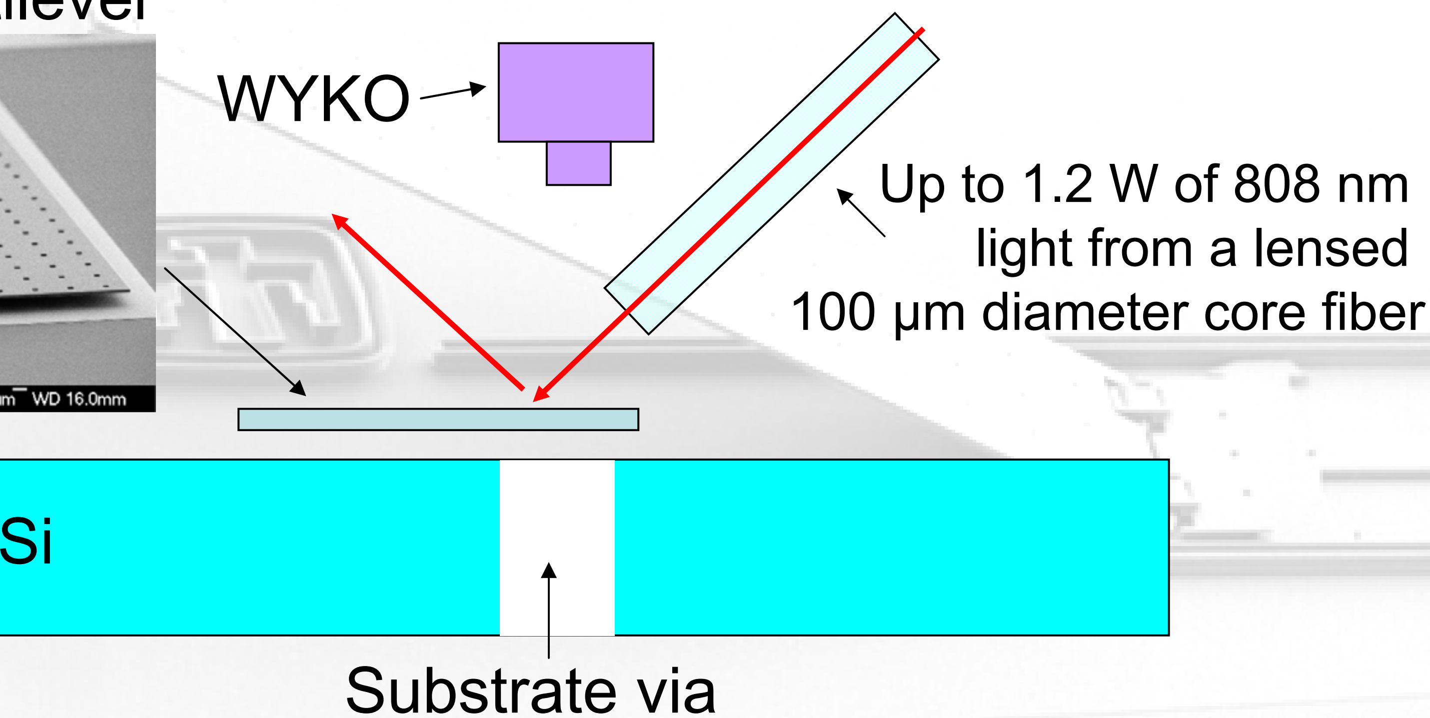

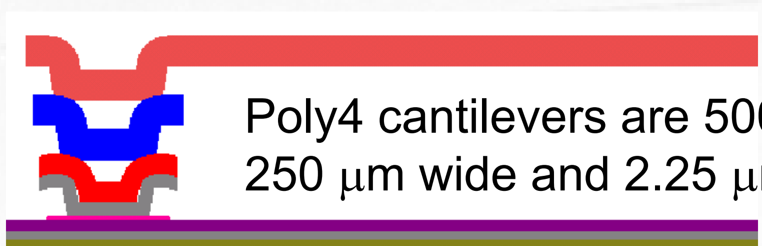

Poly4 cantilevers are 500 µm long,
250 µm wide and 2.25 µm thick

Approximate Laser Spot Location and Size

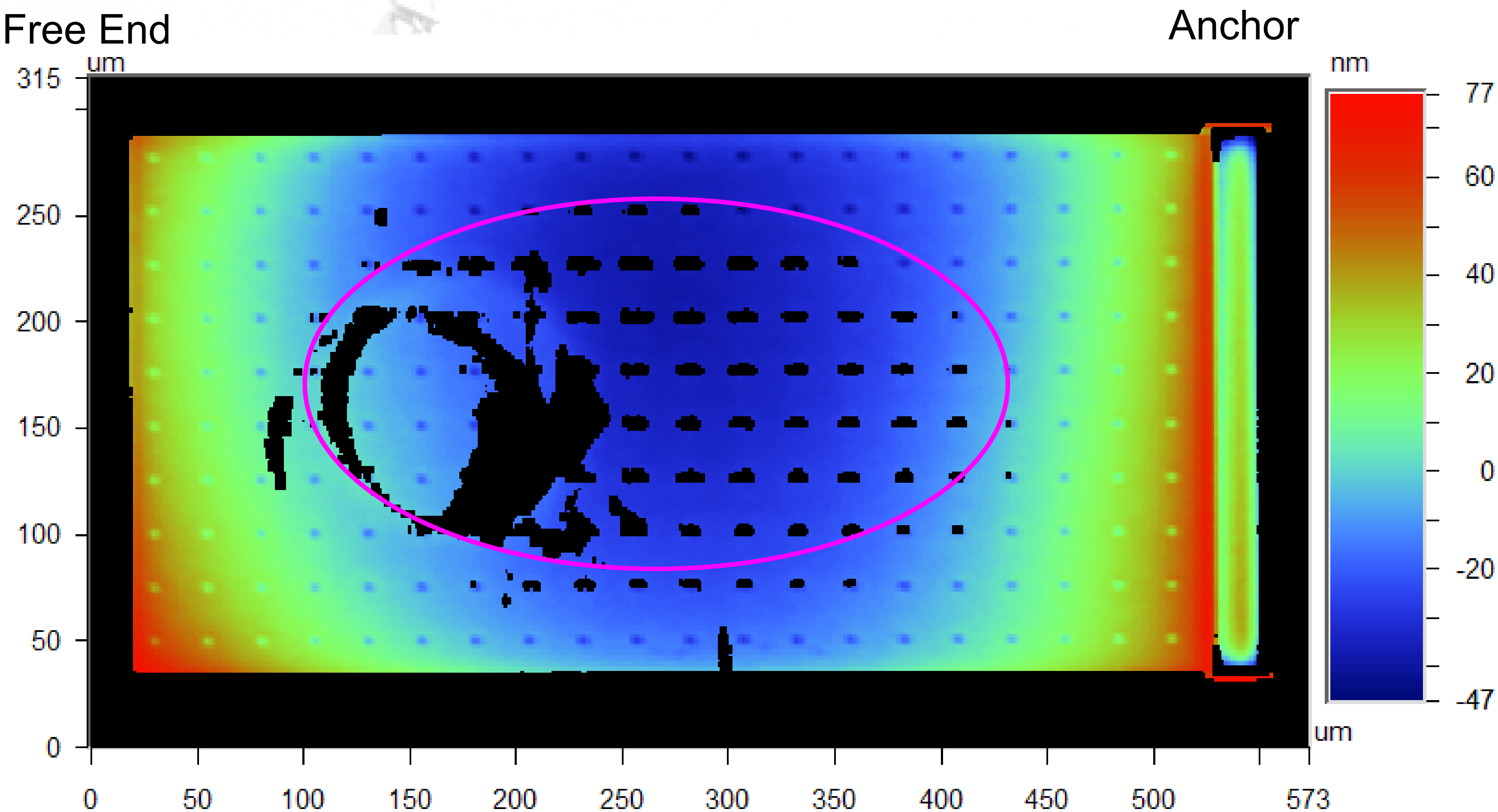

Sandia National Laboratories

Poly4 Cantilever with via during Laser Illumination (fixed scale)

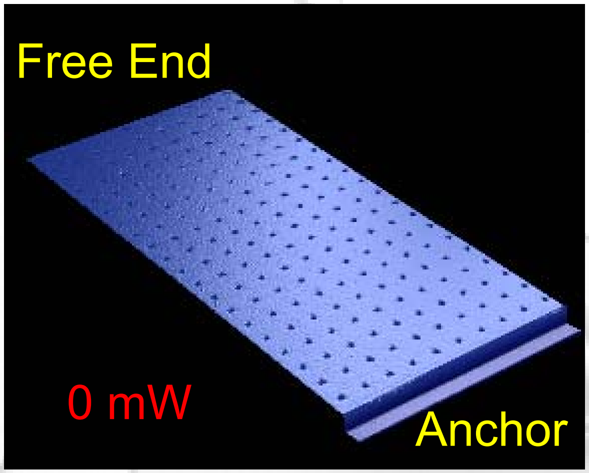

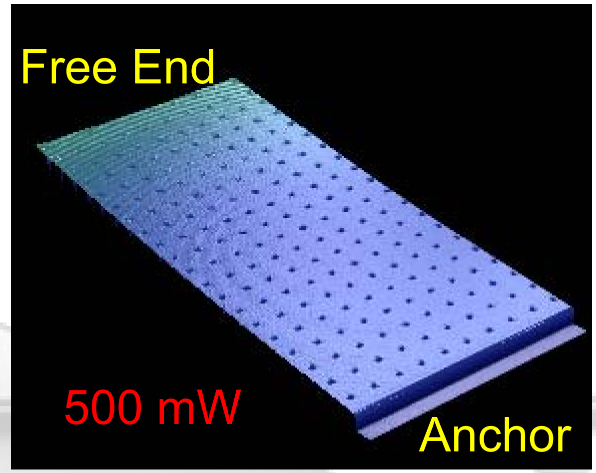

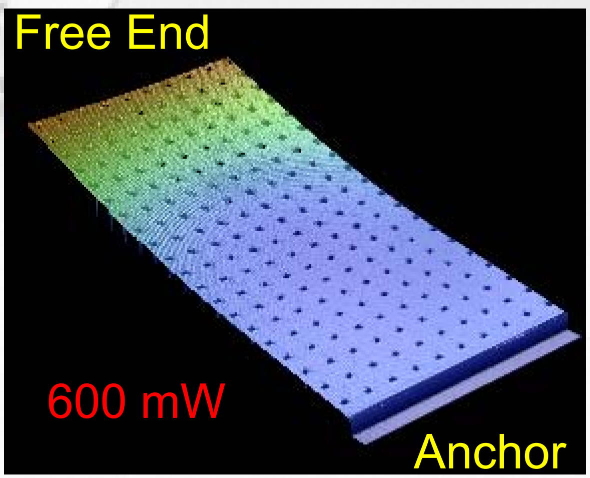

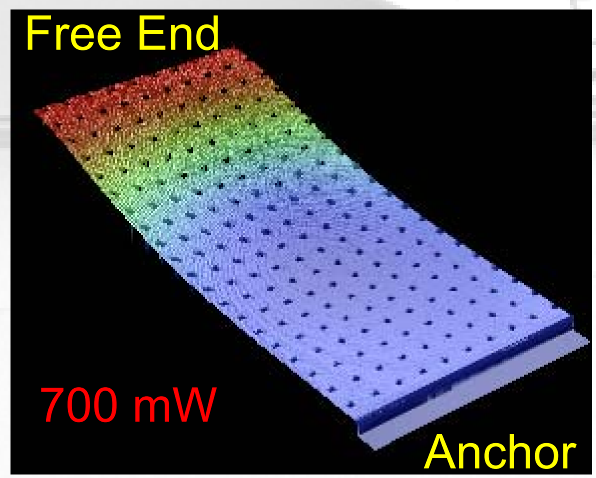

Phinney, Spahn, and Wong, *Proc. of SPIE*, Vol. 6111, pp. 611108, 2006.

Poly4 Cantilever with via after Laser Illumination (floating scale)

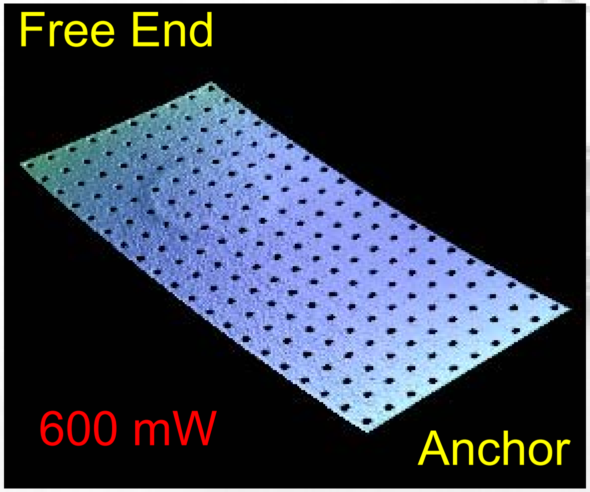

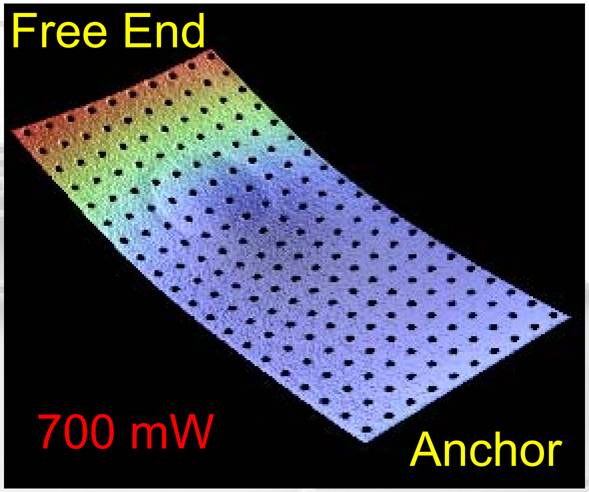

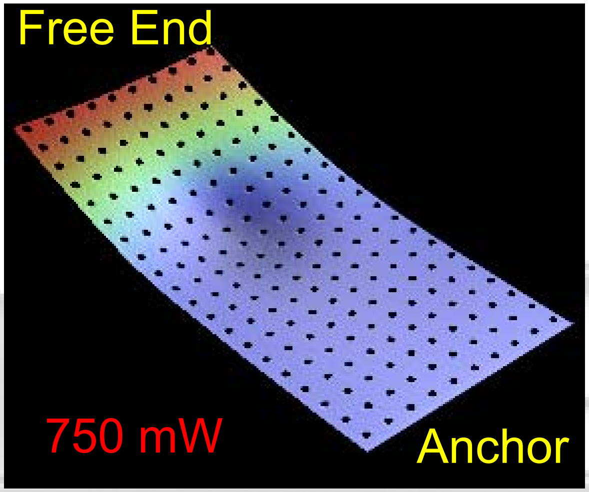

Vertical scale 4.5x of previous two pictures (-0.5 μm to 1.6 μm)

Phinney, Spahn, and Wong, *Proc. of SPIE*, Vol. 6111, pp. 611108, 2006.

X Profile for Poly4 Cantilever with via during Laser Illumination

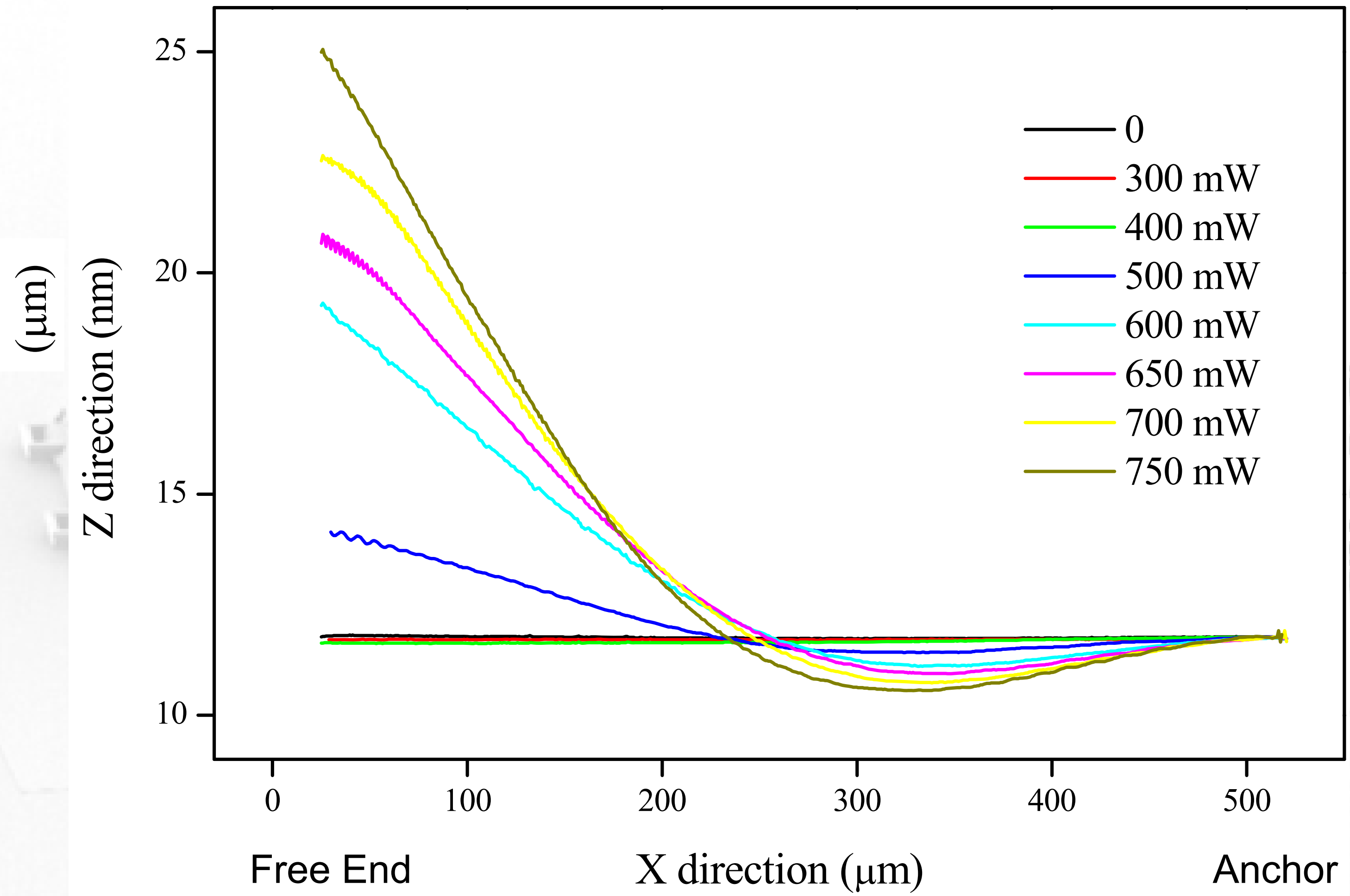

Phinney, Spahn, and Wong, *Proc. of SPIE*, Vol. 6111, pp. 611108, 2006.

X Profile for Poly4 Cantilever with via after Laser Illumination

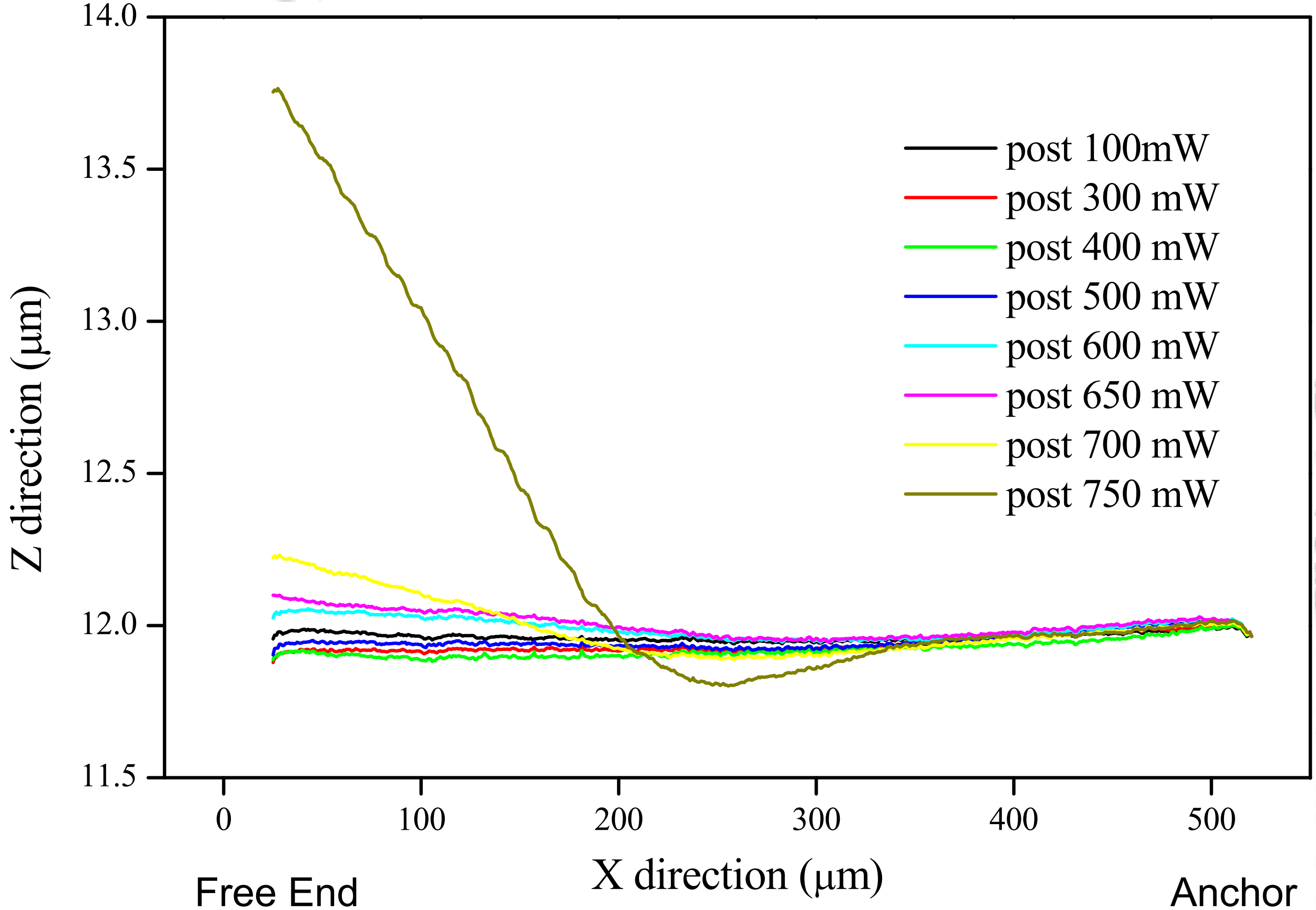

Phinney, Spahn, and Wong, *Proc. of SPIE*, Vol. 6111, pp. 611108, 2006.

X Profile R_t for Poly4 Cantilever with via as a Function of Laser Power

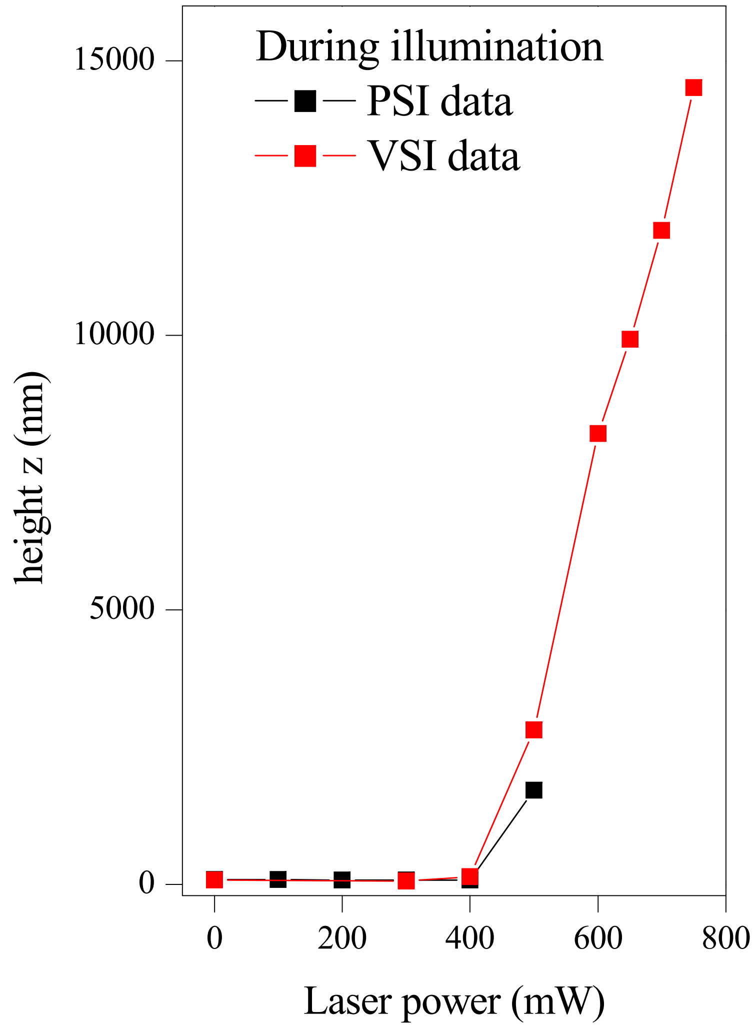

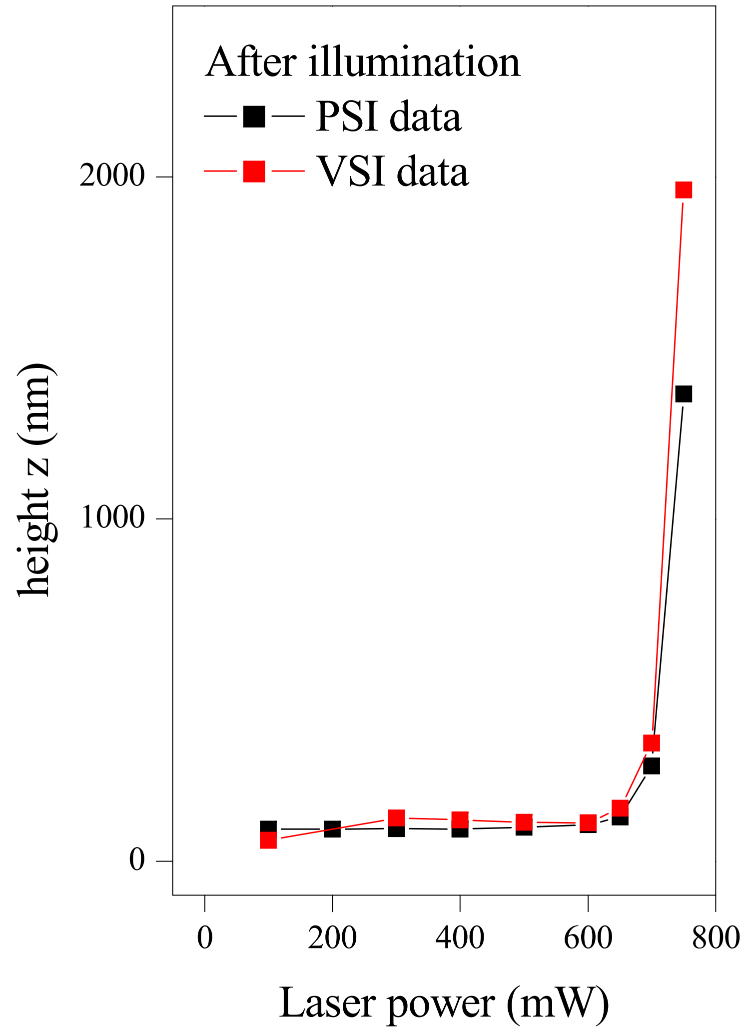

Sandia National Laboratories

Prolonged Exposure Damage

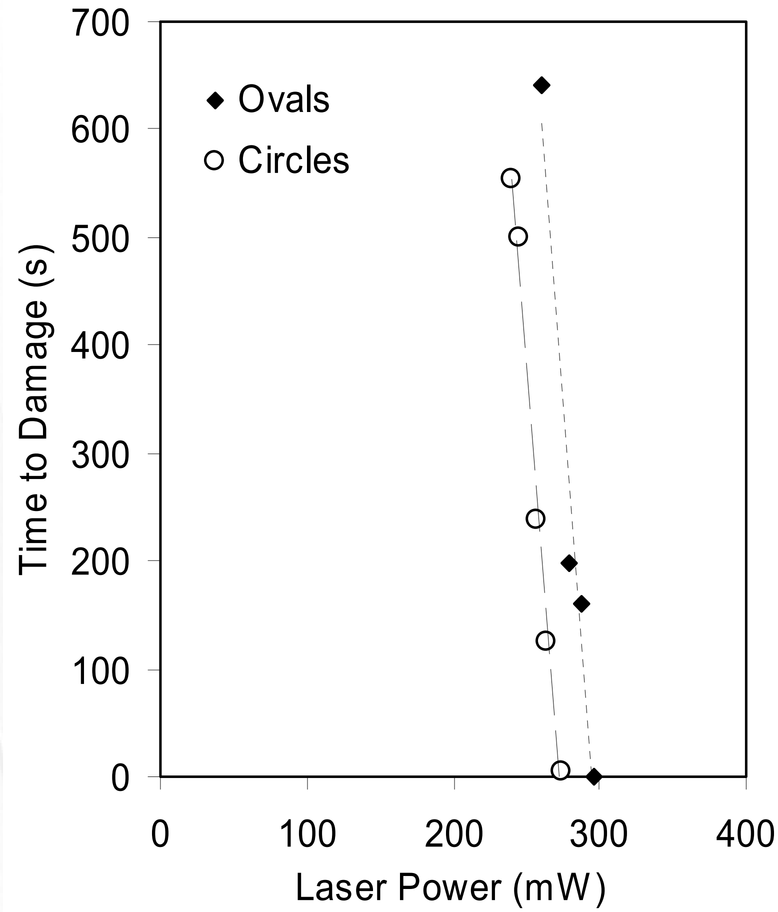

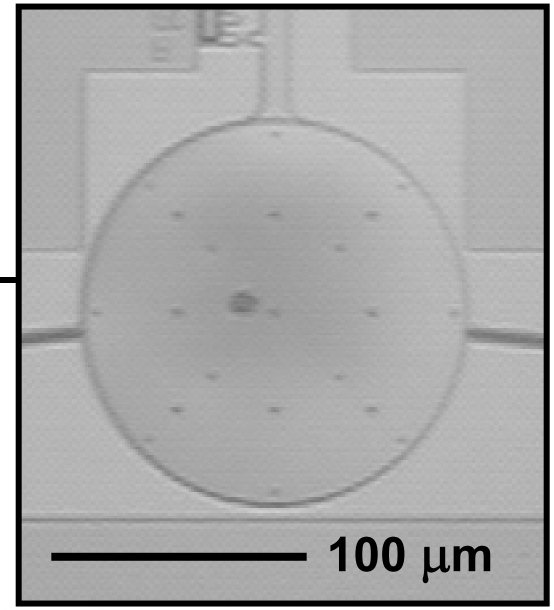

- Damage extent is small compared to immediately damaged actuator
- Exposure time before damage critical for device survivability
- Sharp increase in damage time as power is lowered
- Exposures times beyond 5 minutes result in warping/discoloration of target surface
- Damage possibly caused by material and/or property changes due to surface annealing

Sandia National Laboratories

Timed Exposure

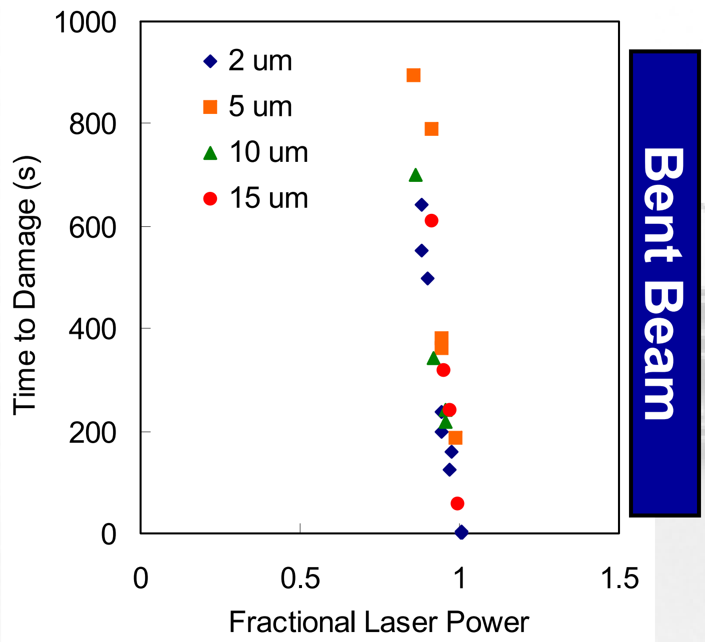

- Bent beam actuators can still suffer damage if operated near the damage threshold
- Properties (n, k, Λ) can change enough near threshold to cause overheating and damage

- Flexure actuators operated below damage threshold hold displacement
- If damaged, displacement recession can continue for several minutes

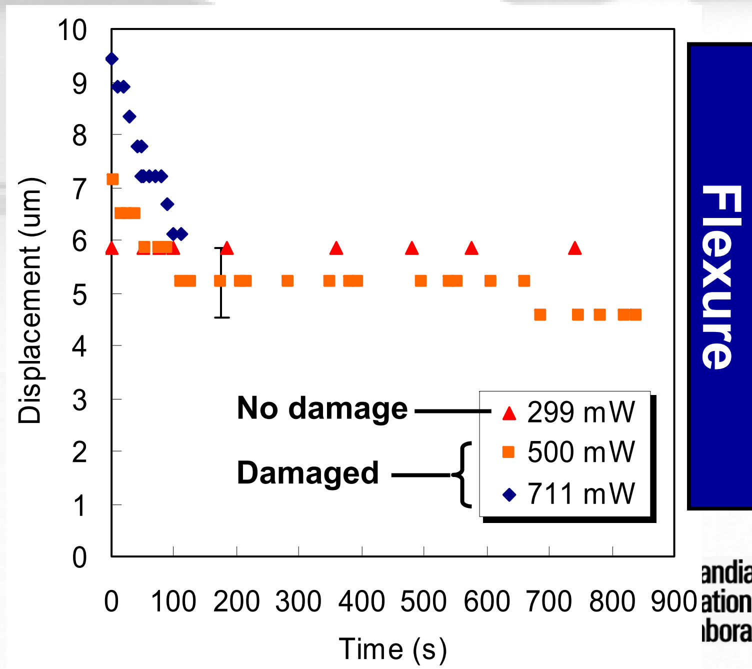

Microthermometry Using Raman Spectroscopy

Renishaw Raman Instrument

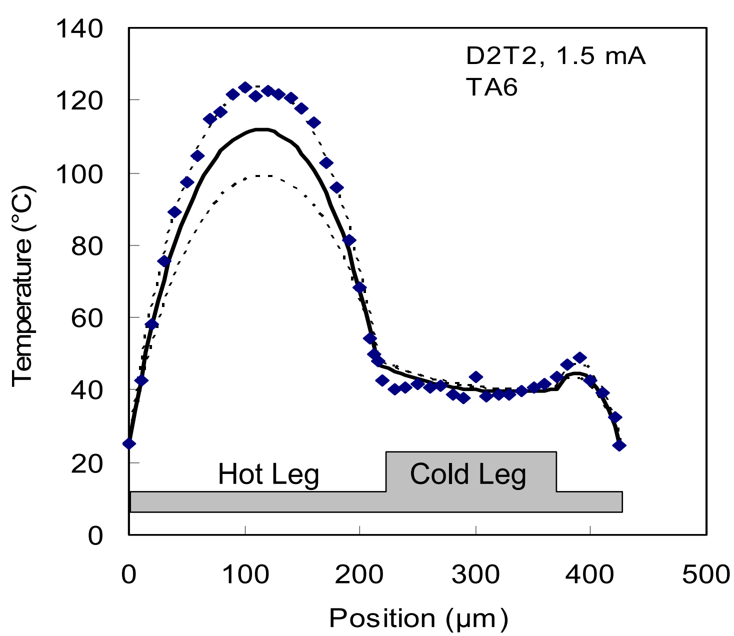

Raman Spectra from PolySi Part

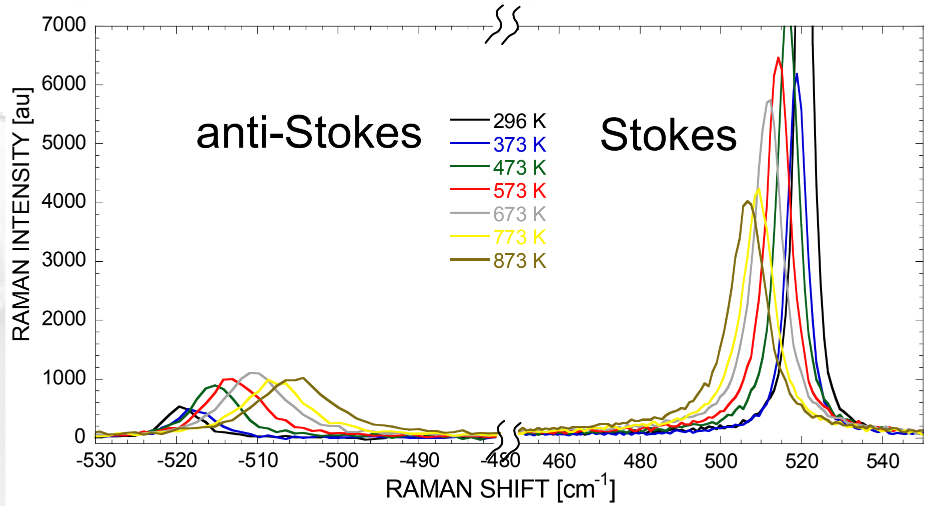

First temperature profiles for MEMS electrically heated thermal microactuators:

- Bent-beam (Kearney, Phinney, and Baker, *JMEMS*, **15**, 314-321, 2006.)
- Flexure (Serrano, Phinney, and Kearney, *JMM*, **16**, 1128-1134, 2006.)

Sandia National Laboratories

Experimental Setup

Heating Laser

- 808 nm CW laser, fiber-coupled to a 100 µm core fiber
- Laser focused with 1:1 relay lens mounted on XYZθ stage
- Angle of incidence fixed at 60° to the sample normal; results in 200 µm x 100 µm elliptical spot

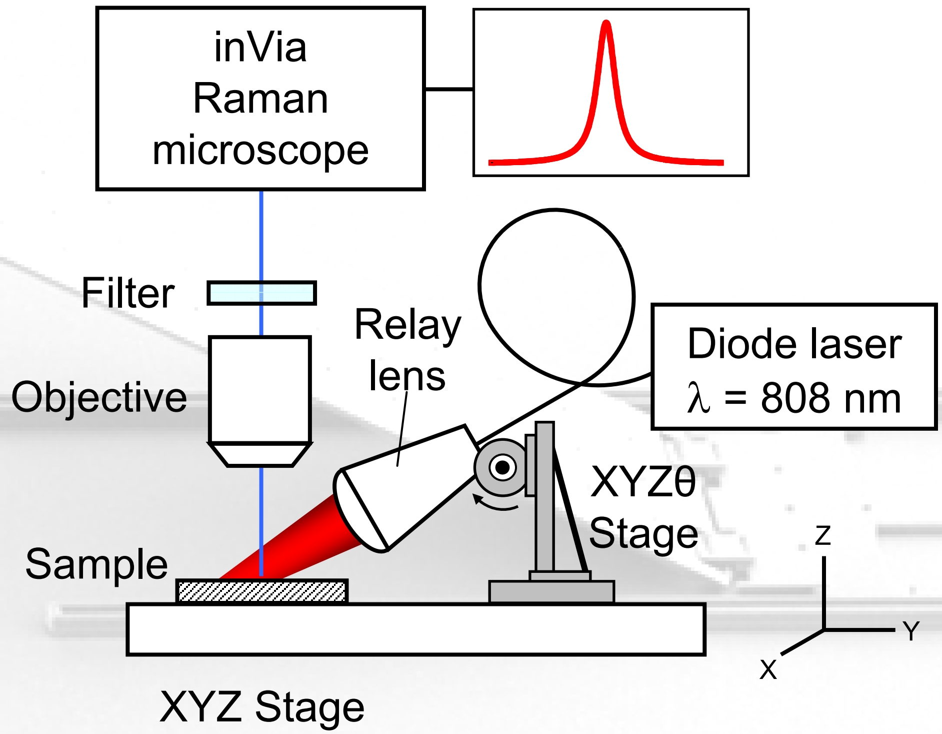

Raman microscope

- 488 nm Ar^+ laser focused with 20x, 0.42 NA objective; resolution better than 1.5 µm
- IR filter blocks scattered IR light with minimal loss to Raman signal from sample (λ_{Raman} ~ 500 nm)
- Laser heating set-up designed to operate within physical constraints of Raman microscope

Sandia National Laboratories

Optically-Powered Flexure Actuator

- Steady temperature increase along narrow leg
- Target temperature uniform at ~375°C up to middle, then decreases as flexure is approached
- Upper-right corner is hottest point on actuator due to device motion and longest conduction pathway

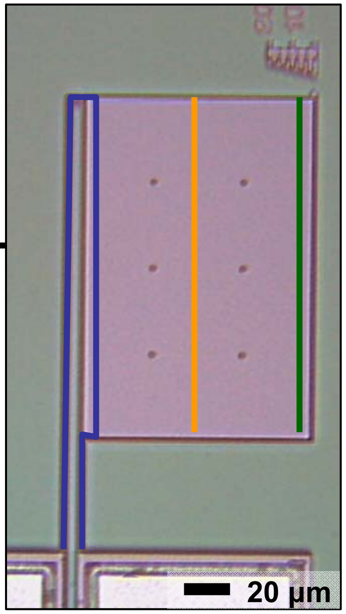

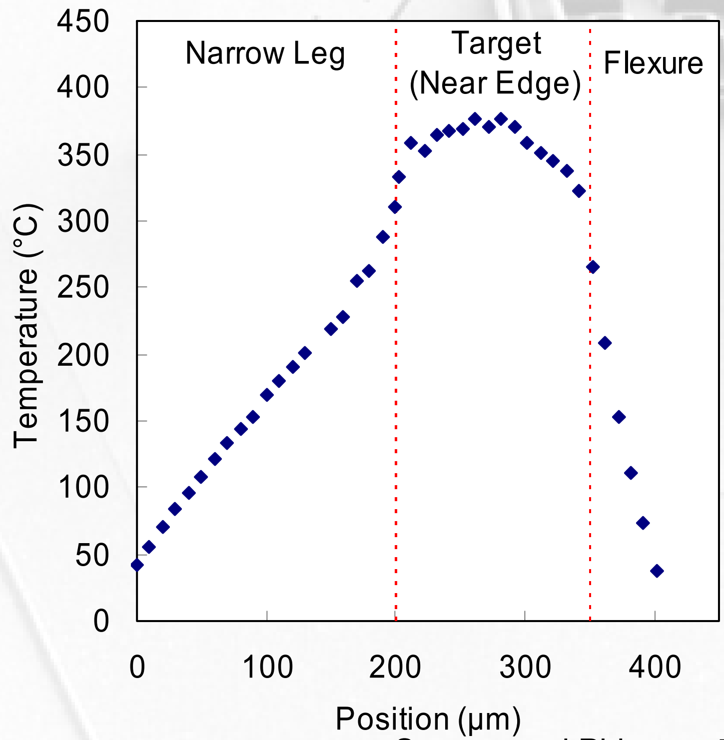

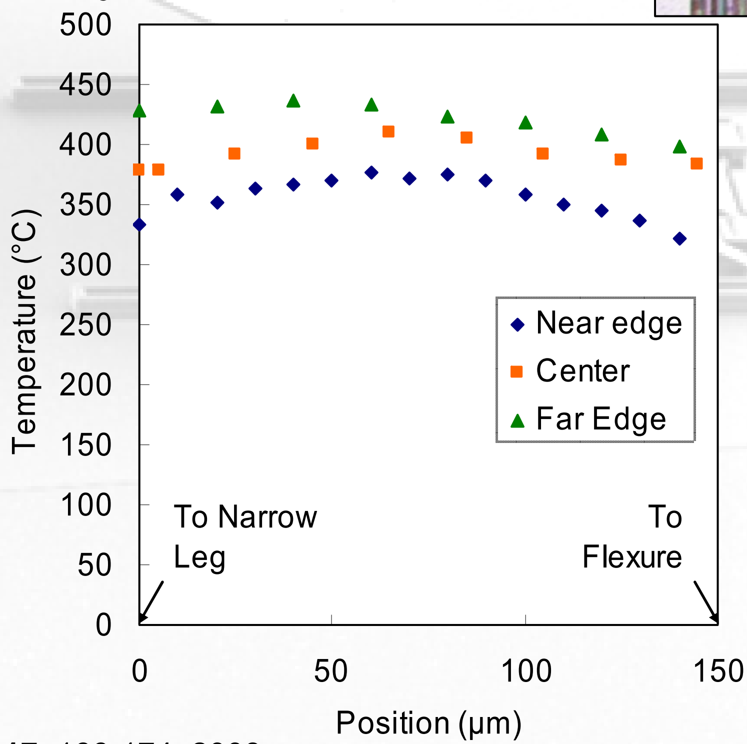

Serrano and Phinney, *JMEMS*, **17**, 166-174, 2008.

Sandia National Laboratories

Cantilever Plate

- Irradiated with 314 and 532 mW, with the laser spot centered on the plate
- Temperature measured across width and length of plate at 20 μm intervals

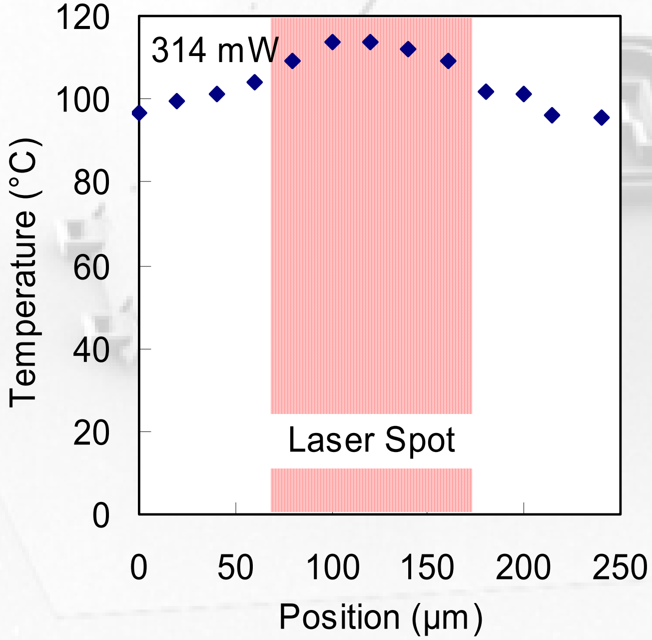

Across width

- Symmetric temperature profile
- Almost uniform temperature across plate with slight increase within laser spot
- Peak temperature of 115°C at 314 mW

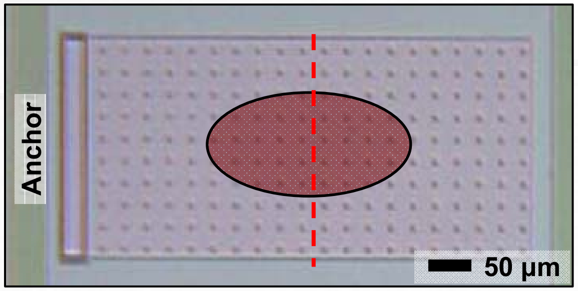

Serrano and Phinney, *Proc. InterPACK2007*, IPACK2007-33571, 2007.
Serrano, Phinney, and Rogers, *IJHMT*, **52**, 2255-2264, 2009.

Sandia National Laboratories

Cantilever Plate

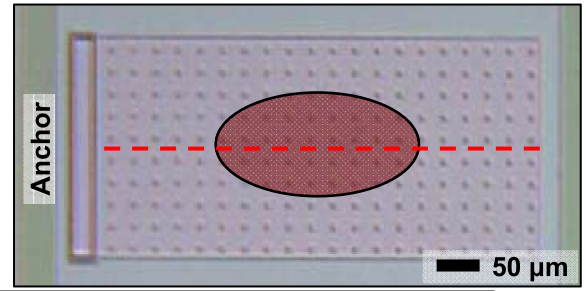

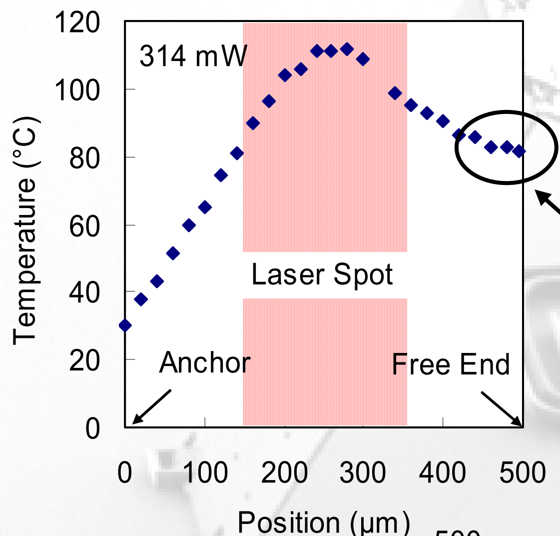

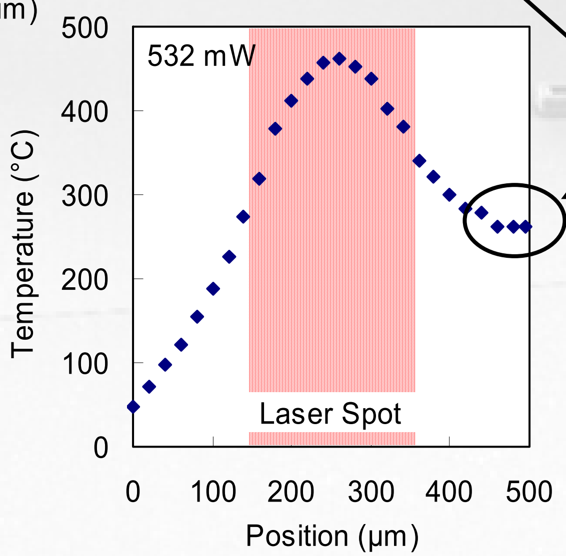

Across length

- Effect of different boundary conditions clearly evident
- Pronounced increase within irradiated region
- Peak temperature of 460°C at 532 mW

Adiabatic edge observed at free end, validating extended surface model assumptions

Temperature Variation with Laser Power

- Center temperature is ~linear with power < 400 mW and temperatures < 200°C
- In the vicinity of 440 mW, temperature "jumps" by 200°C to over 400°C
- Temperature remains linear with power for higher powers

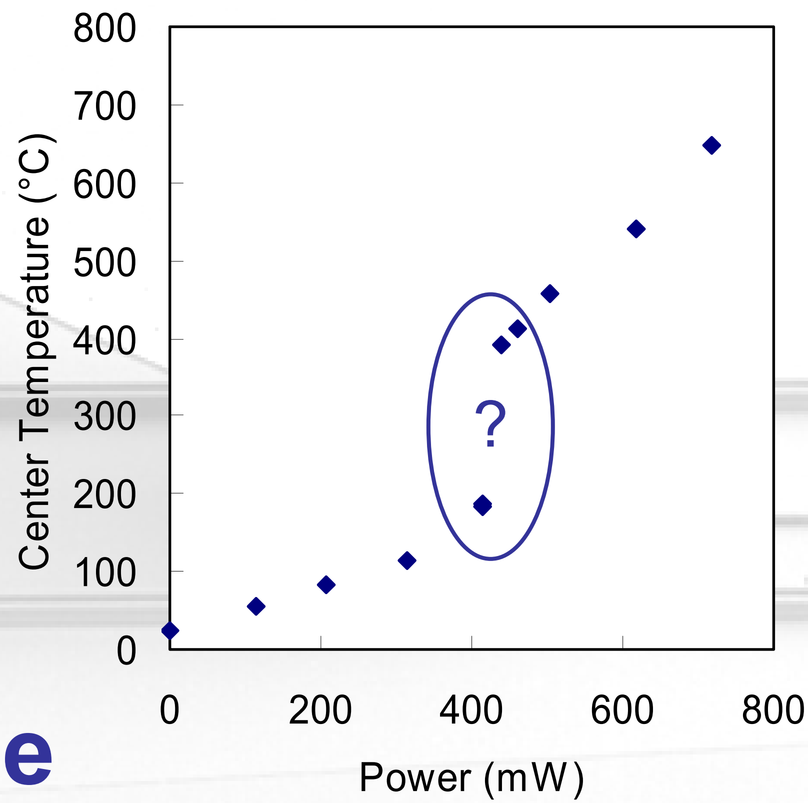

Why the abrupt jump?

Serrano and Phinney, *Proc. InterPACK2007*, IPACK2007-33571, 2007.
Serrano and Phinney, *JMEMS,* **17,** 166-174, 2008.

Optical Energy Absorption in MEMS: Poly4 Layer

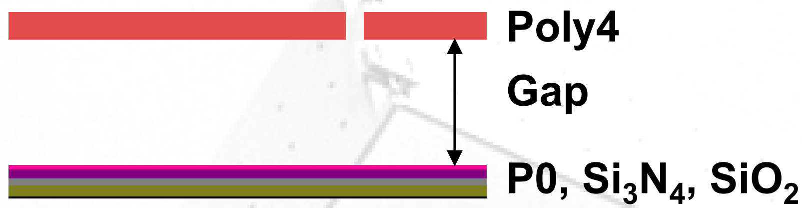

- Thin film interference affects absorption in multi-layered PolySi MEMS that consist of semi-transparent layers with thicknesses less than penetration depth (808 nm, p.d. ~7 μm, thickness ~2 μm)
- Optical absorption, absorptance, calculated from Fresnel relations.
- Optical absorption strongly depends on film and gap thicknesses with standard processing thickness and gap variations leading to >100% change in optical energy absorption.
- Energy absorption can be affected by component deflection during operation.

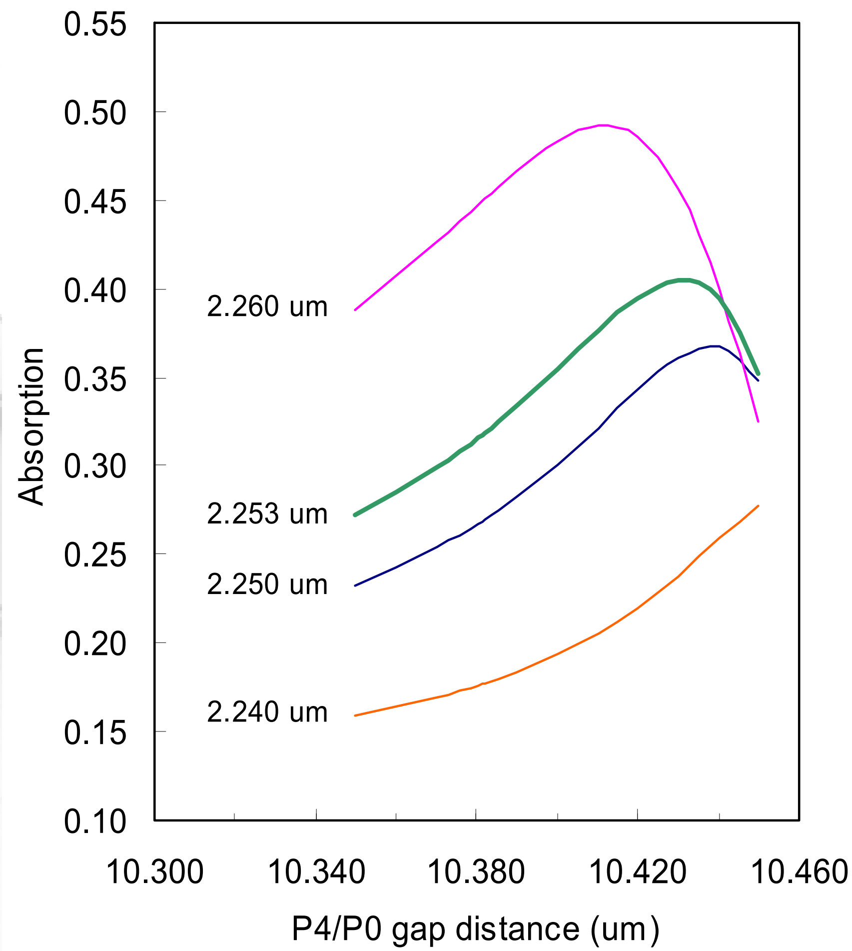

Optical Property Modeling for Cantilever Plate

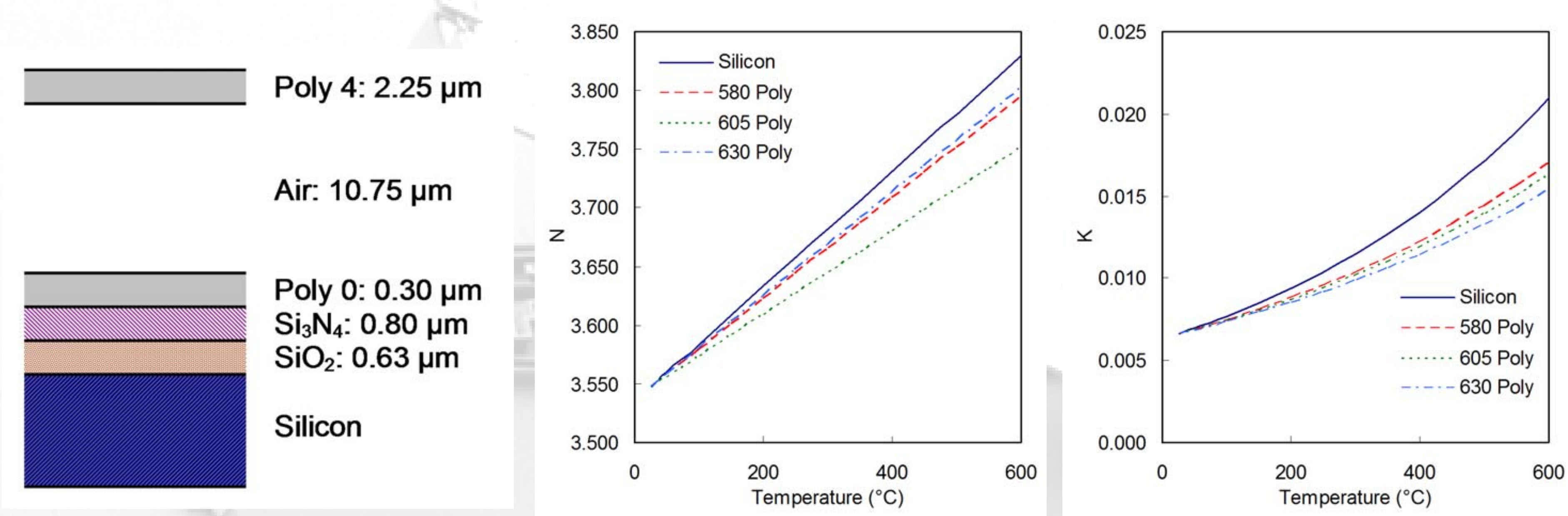

- Real and imaginery refractive indices of Si and PolySi are a function of temperature
- Multiple layers considered in a modular technique adapted from the LTR method of Mazilu, Miller, and Donchev (*Applied Optics*, **40** (36), 6670-6676, 2001). This technique allows extraction of the optical properties for individual layers.

Serrano, Phinney, and Rogers, *IJHMT*, **52**, 2255-2264, 2009.

Optical-Thermal Phenomena

Small Thickness **+** **T-dependant refractive index** **=** **T-dependant absorption**

Flat absorption at lower T leads to initial linear temperature increase

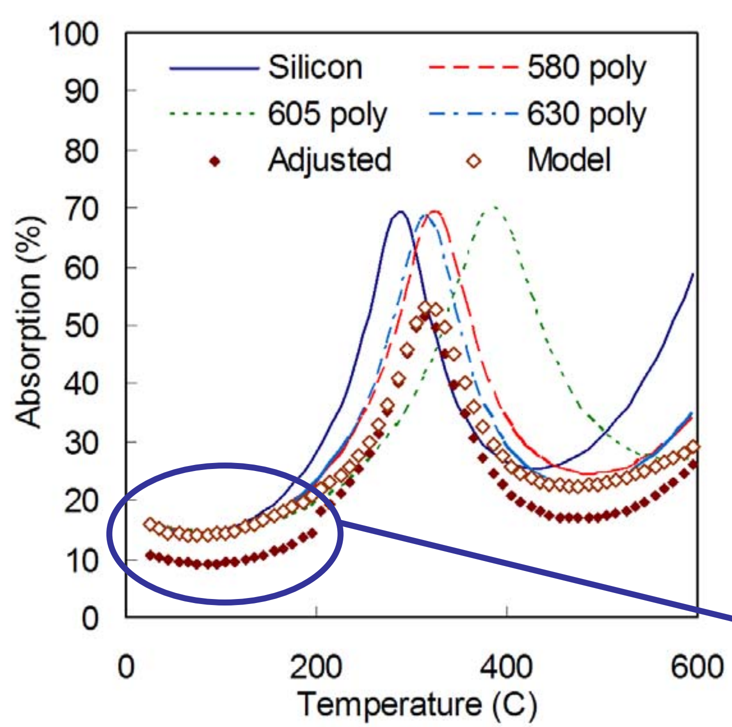

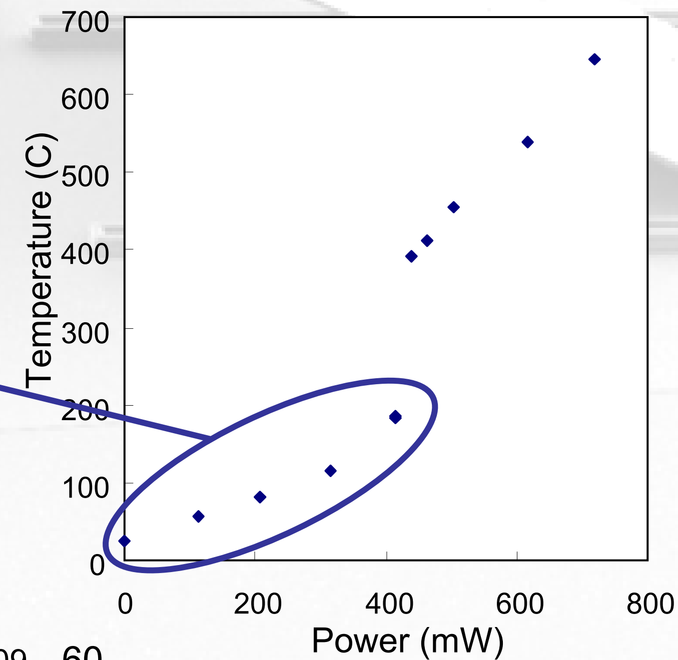

Cantilever plate: 60° incidence; 808 nm; literature temperature dependence for optical constants

Serrano, Phinney, and Rogers, *IJHMT*, **52**, 2255-2264, 2009.

Sandia National Laboratories

Optical-Thermal Phenomena

Small Thickness **+** **T-dependant refractive index** **=** **T-dependant absorption**

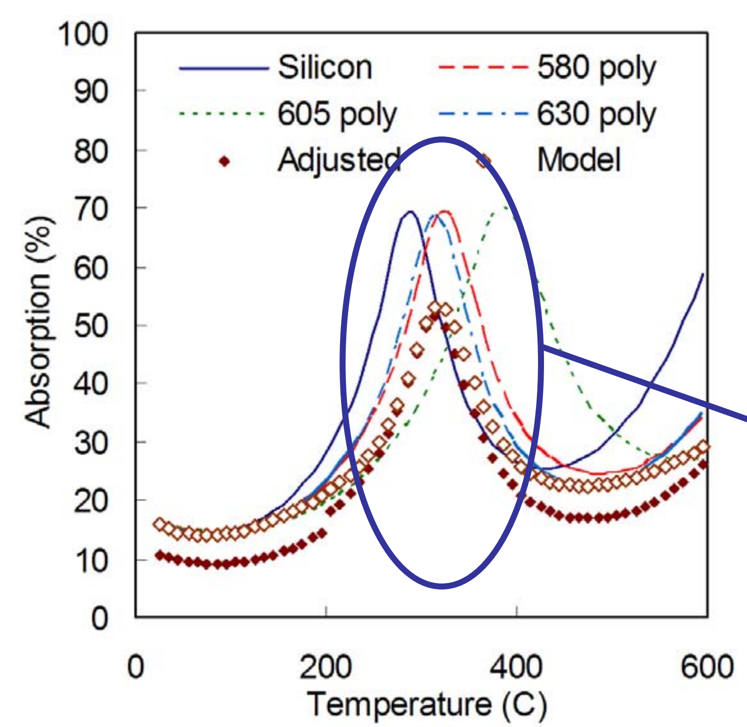

Cantilever plate: 60° incidence; 808 nm; literature temperature dependence for optical constants

Flat absorption at lower T leads to initial linear temperature increase

Absorption peak leads to “positive feedback” effect:

forbidden T’s

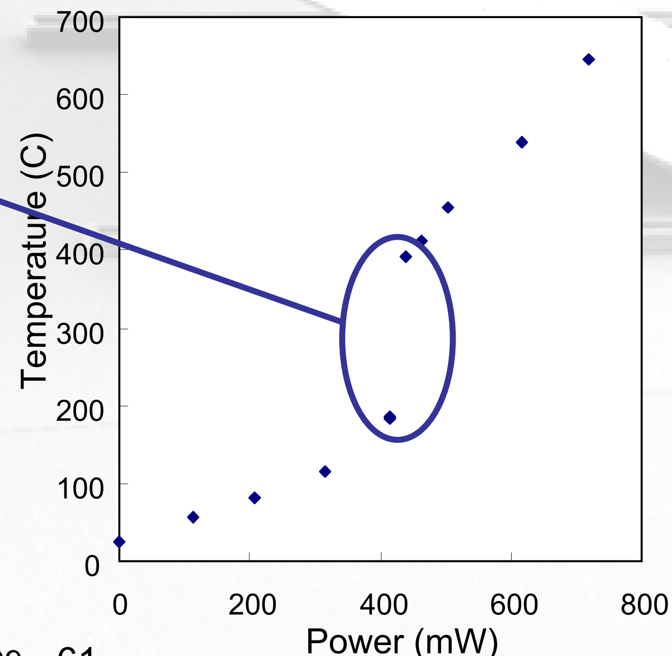

Serrano, Phinney, and Rogers, *IJHMT*, **52**, 2255-2264, 2009.

Simulating Optical-Thermal Phenomena

- Coupled optical-thermal phenomena must be considered for accurate device modeling
- Requires knowledge of *n*(T) and *k*(T)

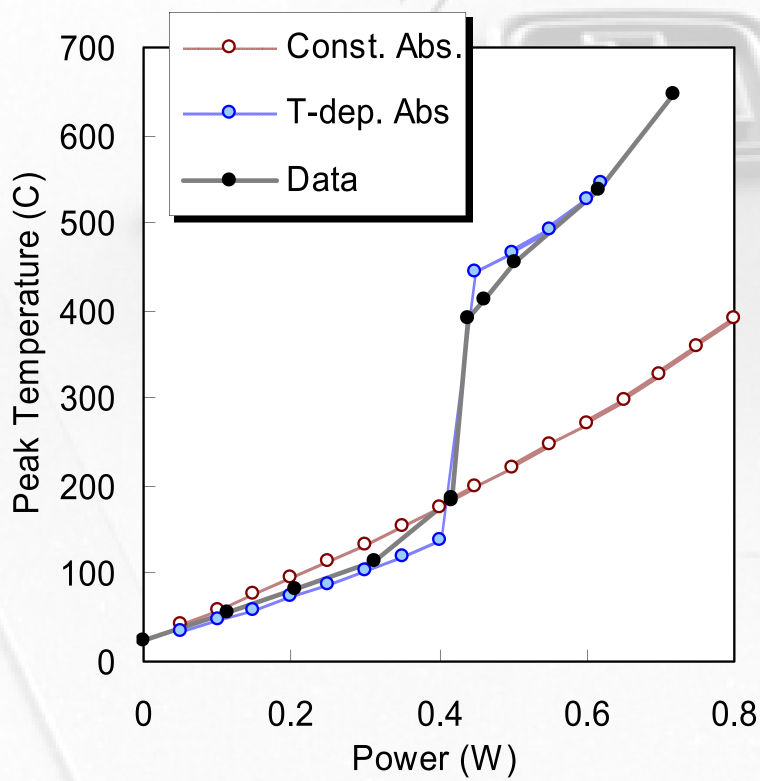

- With fixed absorption, model fails to reproduce temperature jump and under-predicts peak temperature at higher powers
- Including optical effects into thermal model improves model results and also predicts temperature jump

Sandia National Laboratories

Comparison of Experiments and Simulations for Laser-Heated Cantilever

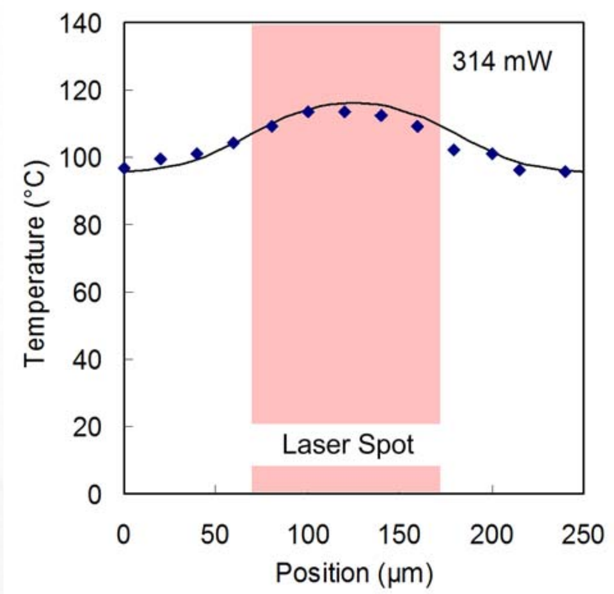

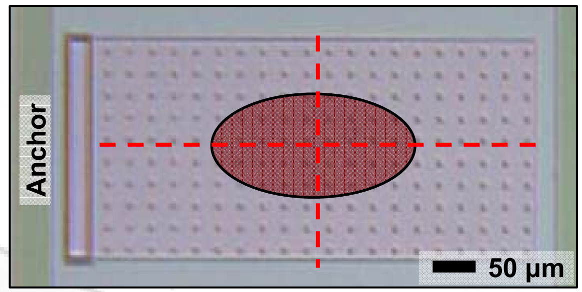

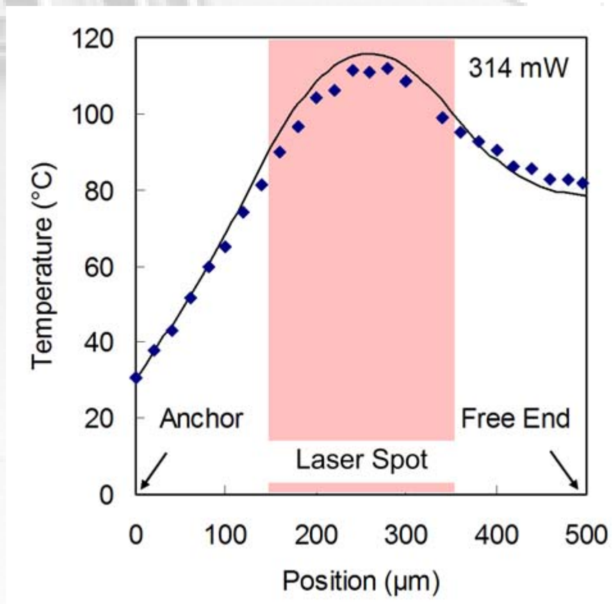

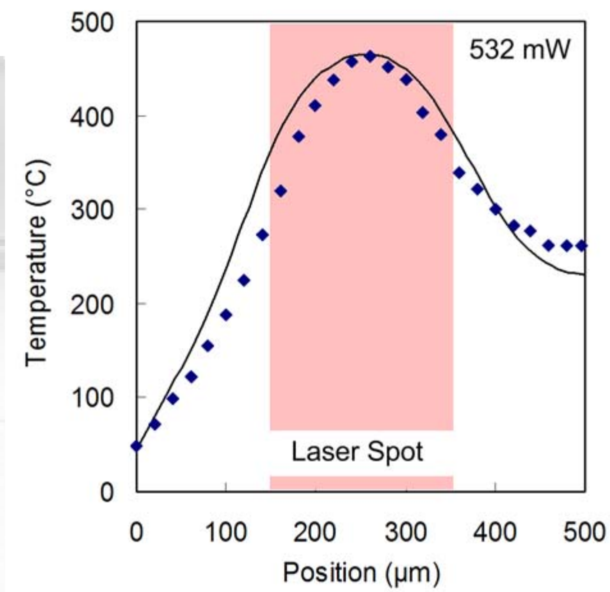

Serrano, Phinney, and Rogers, *IJHMT*, **52**, 2255-2264, 2009.

Simulating Optical-Thermal Phenomena

- Coupled optical-thermal phenomena must be considered for accurate device modeling
- With temperature-dependant absorption in model, temperature jump is also predicted

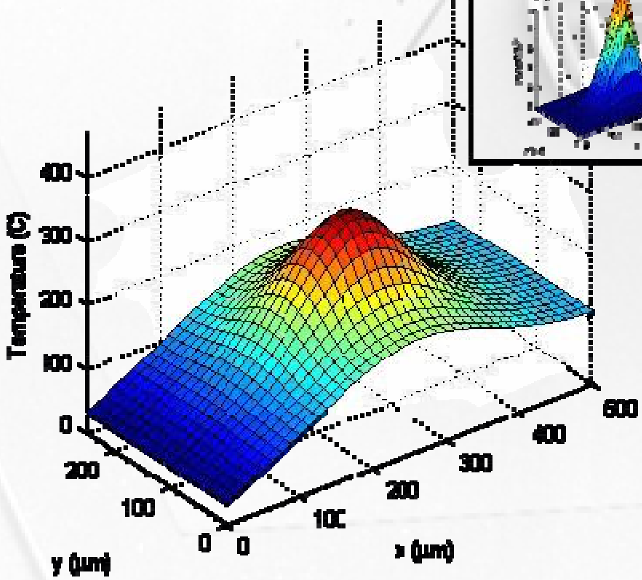

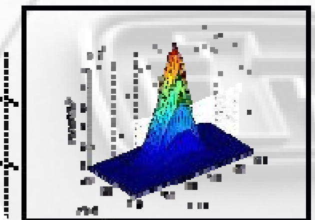

- Non-uniform absorption across surface drives system towards equilibrium much faster than without

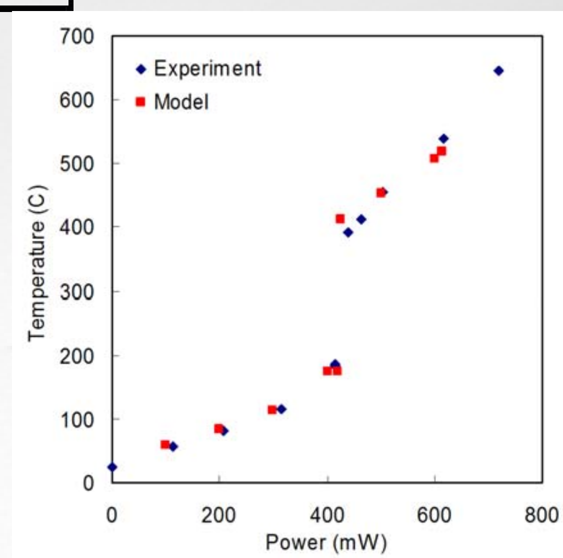

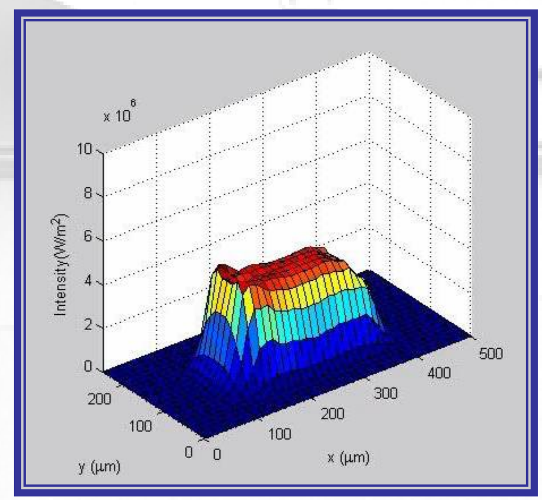

Serrano, Phinney, and Rogers, *IJHMT*, **52**, 2255-2264, 2009.

Sandia National Laboratories

Effects of Laser Wavelength

Maps of the ratio of the absorptance of a single layer PolySi slider irradiated over a substrate to the absorptance of one irradiated over a via for different gap heights and PolySi thicknesses. The experimentally determined thresholds for laser power for the two wavelengths are also shown.

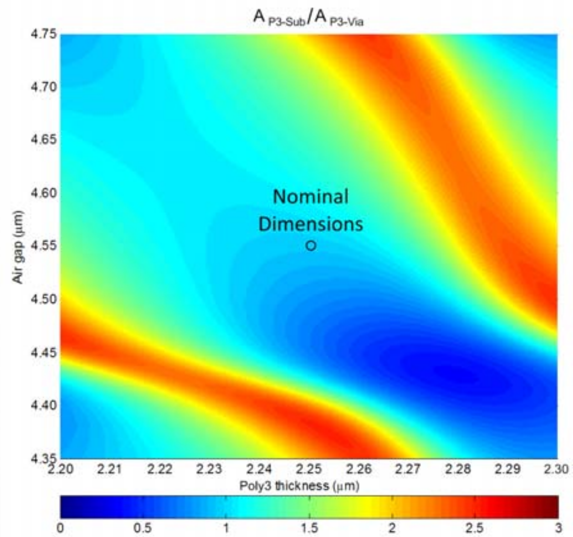

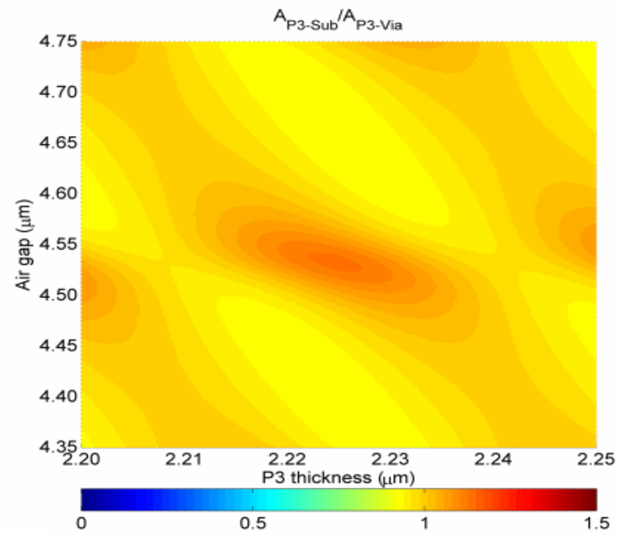

532 nm

808 nm

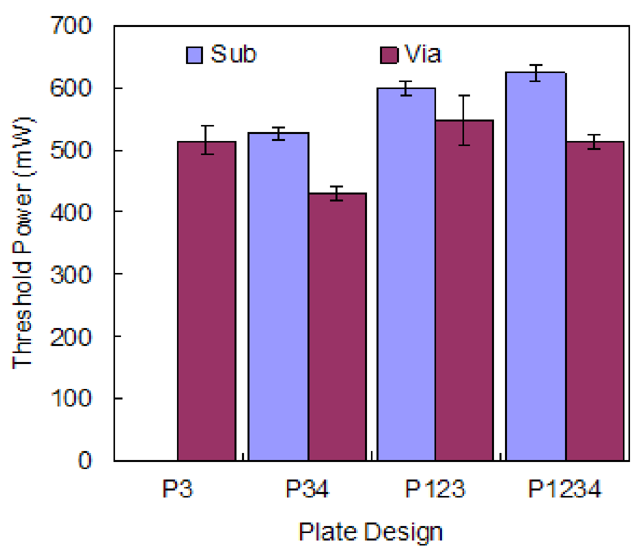

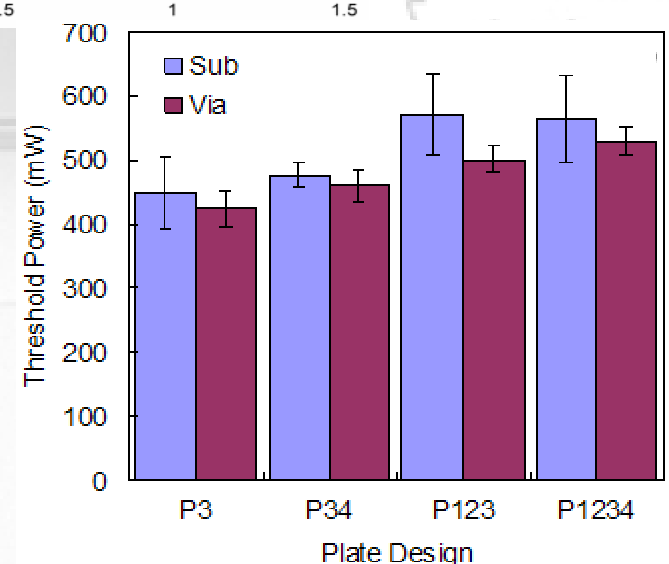

Serrano and Phinney, and Rogers, *J. of Micro/Nanolithography, MEMS, and NEMS*, in review, 2009.

Benefits of Large-Scale Models

- **Increasing complexity of model reduces number of adjustable parameters**
  - **model air → eliminate convection coefficient**
  - **model bondpad → eliminate fixed end temperature**
- **Effect of other parameters can be investigated**
  - **gap**
  - **thermal conductivity**
  - **release holes**

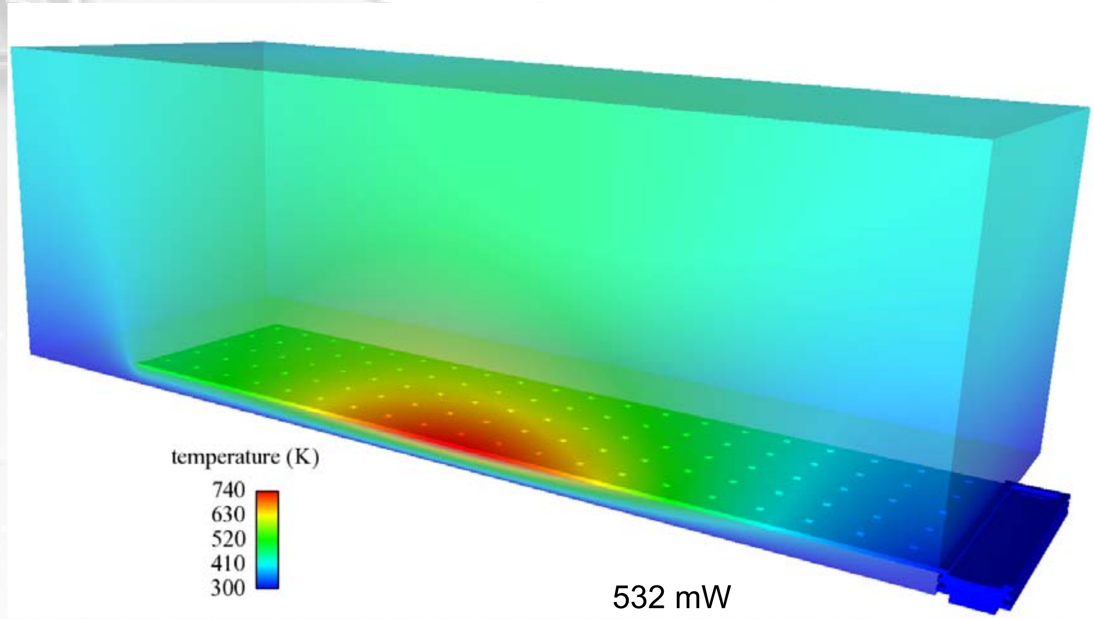

2D – 3D Comparison

- **3D simulation performed with remaining parameters fixed**
- **Generally improved agreement**
  - **except at free end**

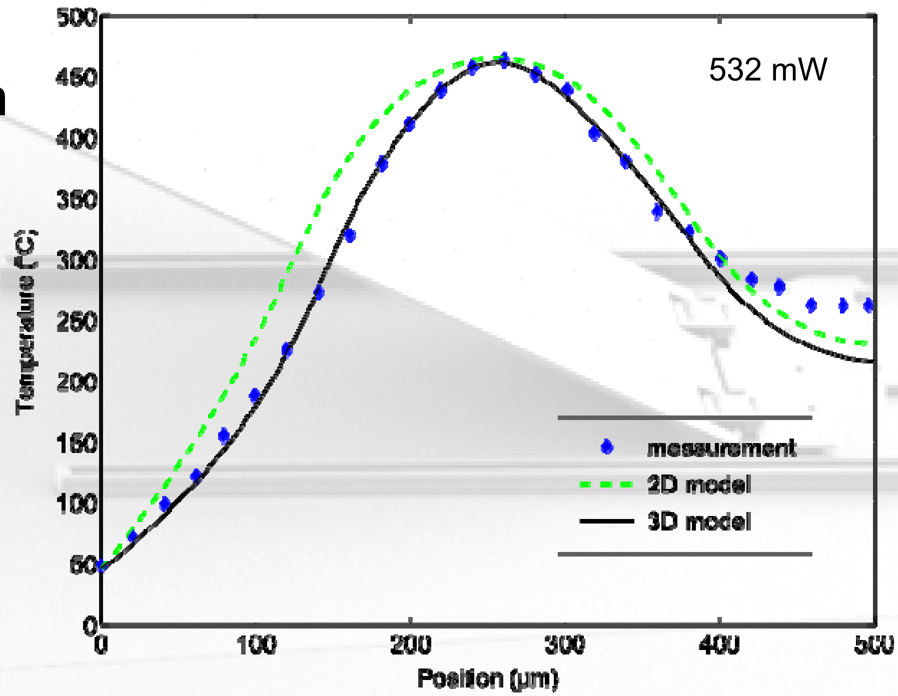

Sandia National Laboratories

Effect of Changing Models

- **Absorptance**
  - **"Model" case more comparable to measurements than "Adjusted" case**
- **Thermal conductivity model**
  - **avoids extrapolation above 300 ºC**
  - **fits previous work on SUMMiT structure**
- **No adjustable parameters**
- **Still reasonable agreement**
  - **overpredict max T**

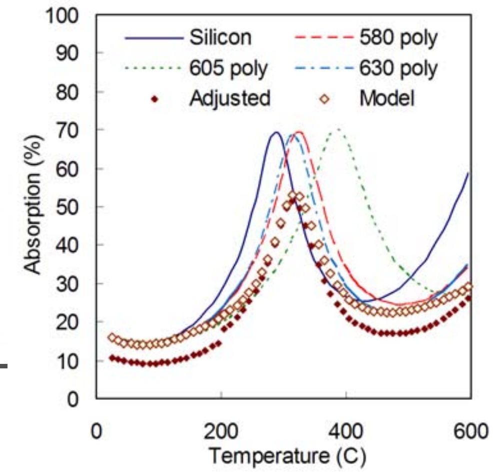

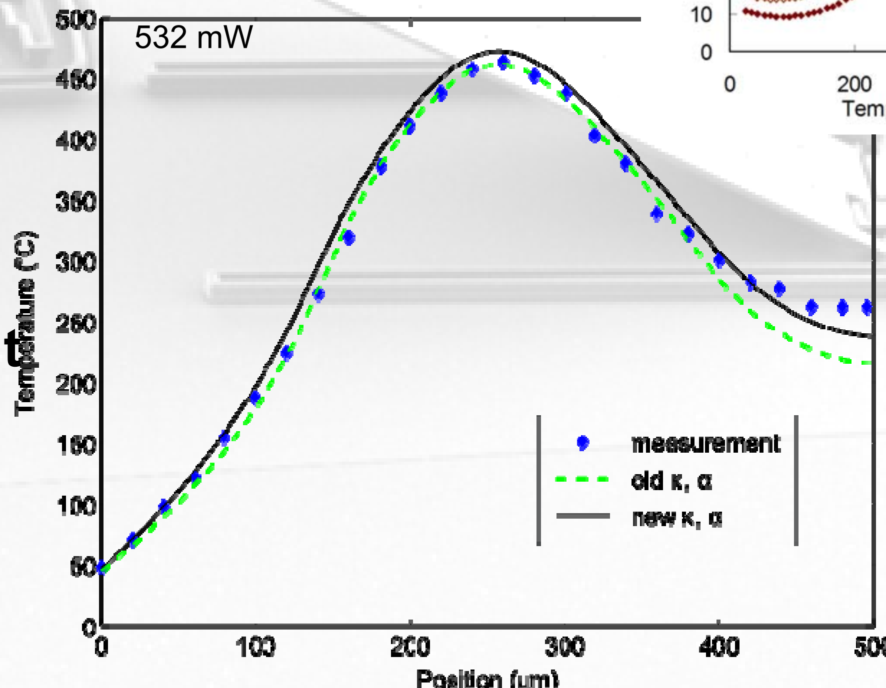

Sandia National Laboratories

Strong Effect on Temperature Jump

- First temperature jump occurs ~100mW early
- Predicted slope too high before jump and too low after it
- Need measured absorption data
- Need better geometric information
- Must evaluate possibility of structural deformation

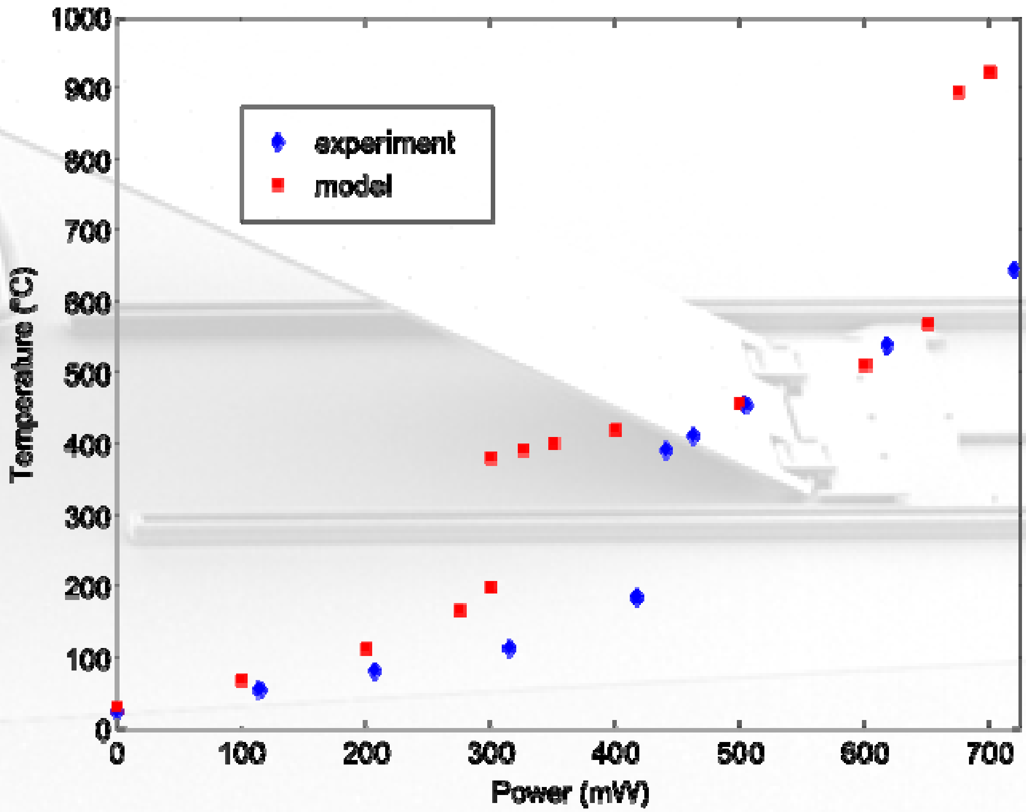

Sandia National Laboratories

Temperature Calculations: Time Scales of Heat Transfer

- Characteristic Time (Fo=1)

$$t_c \equiv \frac{L_c^2}{\alpha_{PolySi}}$$

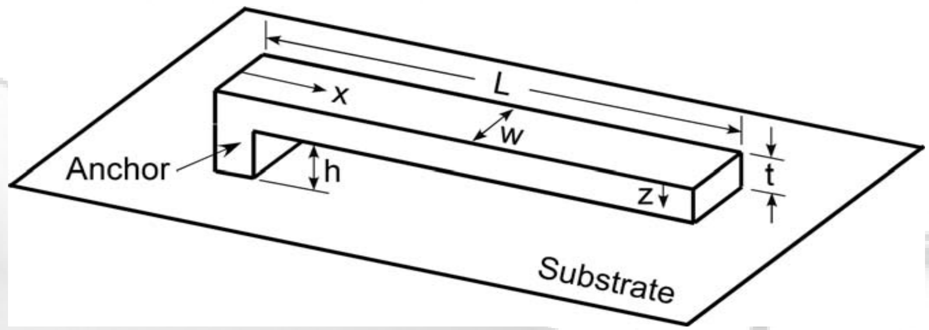

Direction	L_c [μm]	t_c
z	2-2.5	200 ns
x	500-2000	20-200 ms

$$\alpha_{PolySi} = 1.76(10^{-5})\ \mathrm{m^2/s}$$

Temperature Distribution in the z-direction after Laser Irradiation

- Finite Difference Equation

$$T_n^{P+1} = 2Fo_z(T_{n\pm1}^P) + \frac{S\Delta t}{C} + (1 - 2Fo_zBi_z - 2Fo_z)T_n^P$$

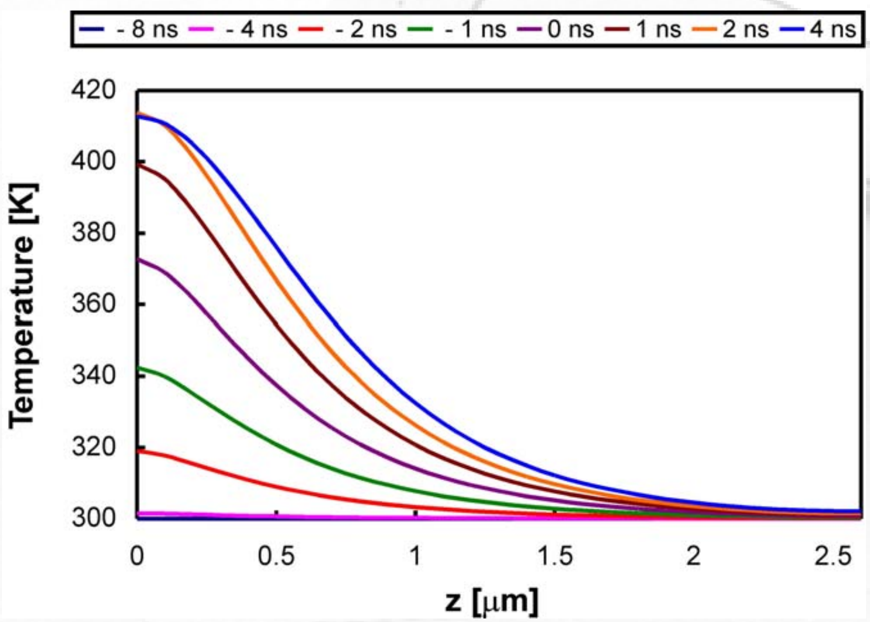

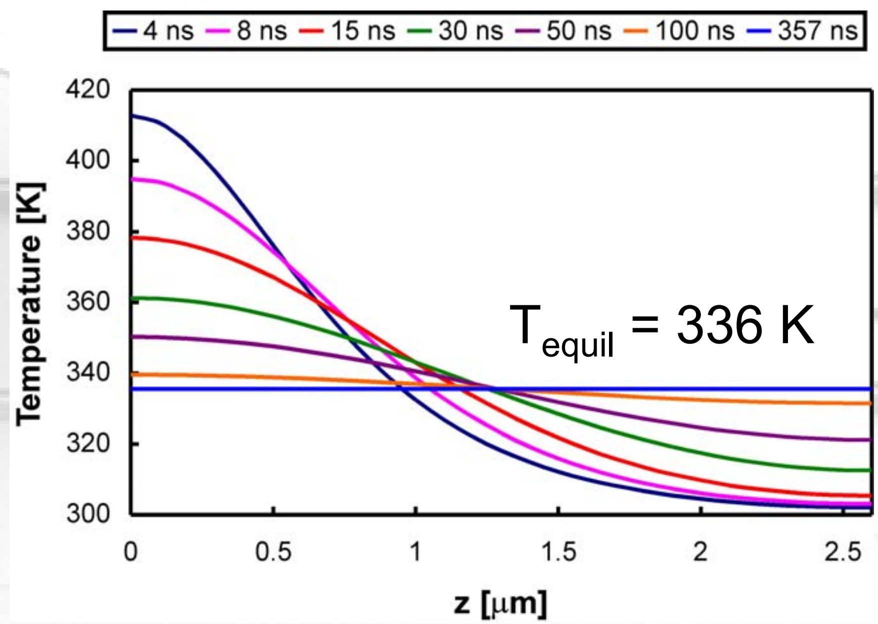

Heating t_p = 4 ns, J = 25 mJ/cm² **Equilibration**

Rogers and Phinney, 2004, *Numerical Heat Transfer, Part A*, Vol. 45, pp. 737-750

Temperature Distribution along the Length after Laser Irradiation

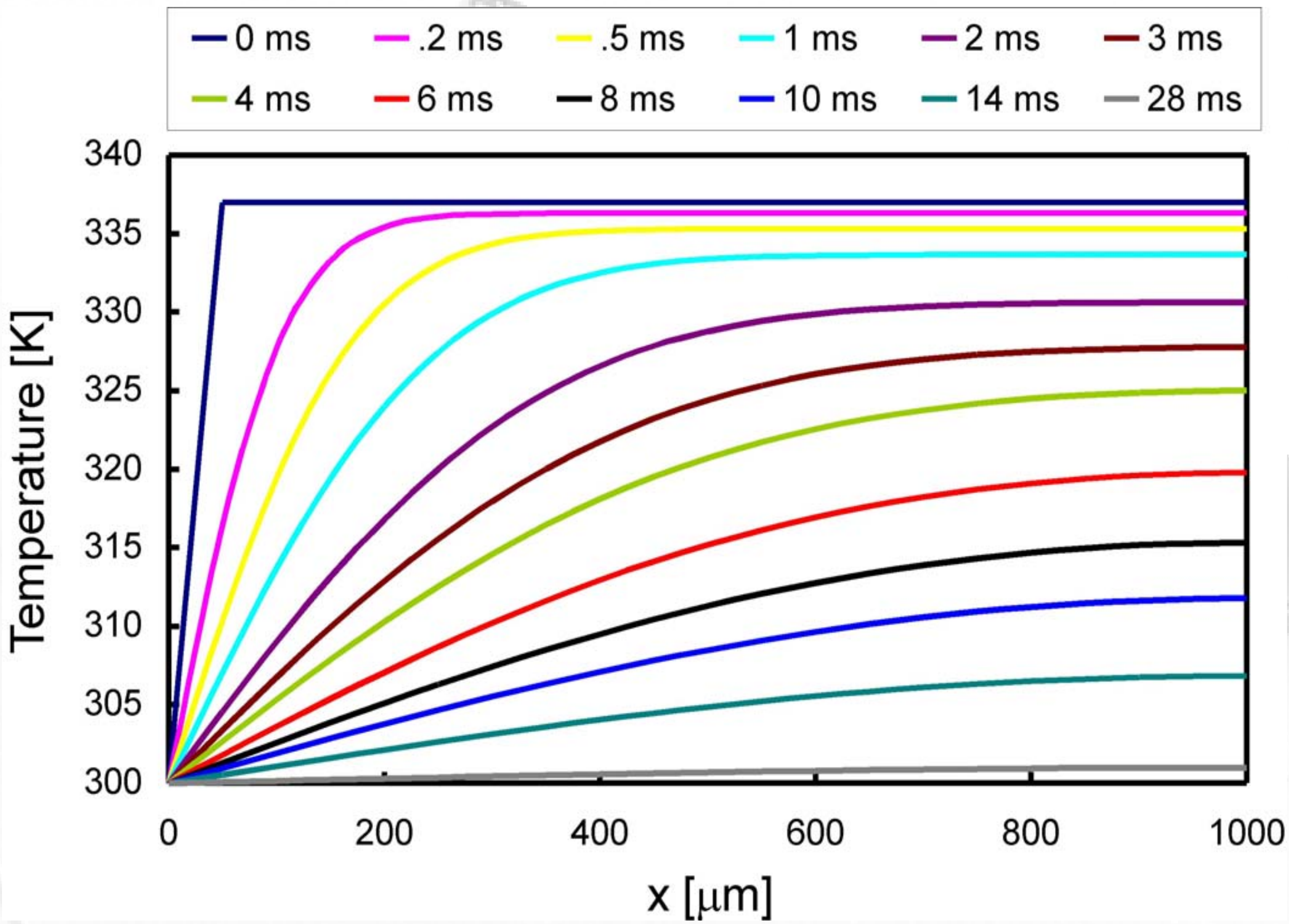

Polysilicon
L = 1000 μm
w = 30 μm
t = 2.5 μm
J = 25 mJ/cm^2
T_{init} = 337 K
h = 150 W/m^{2}K

Rogers and Phinney, 2004, *Numerical Heat Transfer, Part A*, Vol. 45, pp. 737-750.

Sandia National Laboratories

Temperature Distribution along the Length after Laser Irradiation

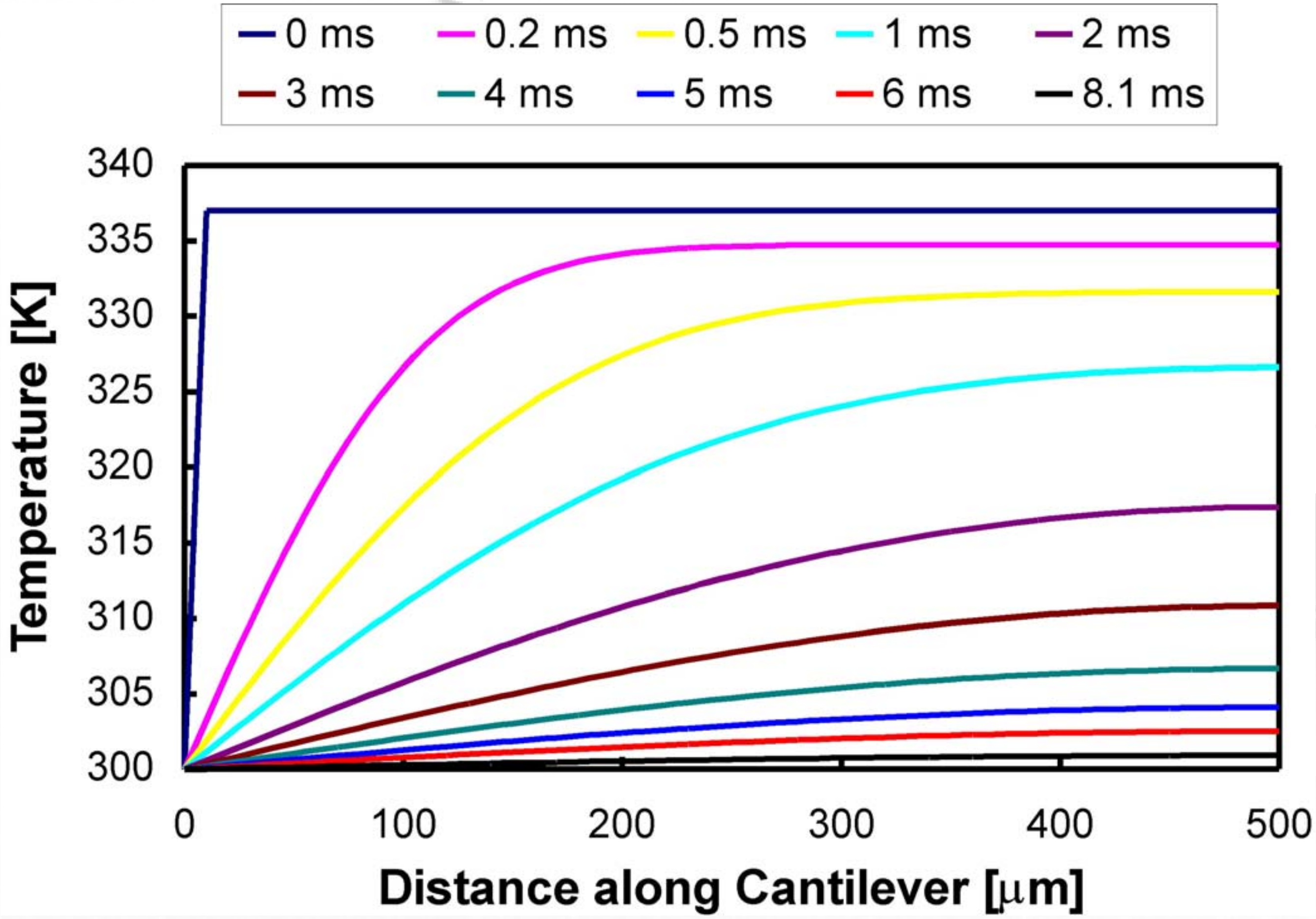

Polysilicon
L = 500 μm
w = 30 μm
t = 2.5 μm
J = 25 mJ/cm^2
T_{init} = 337 K
h = 150 W/m^{2}K

Rogers and Phinney, 2004, *Numerical Heat Transfer, Part A*, Vol. 45, pp. 737-750.

Effect of Energy Loss to the Environment on Cooling Time

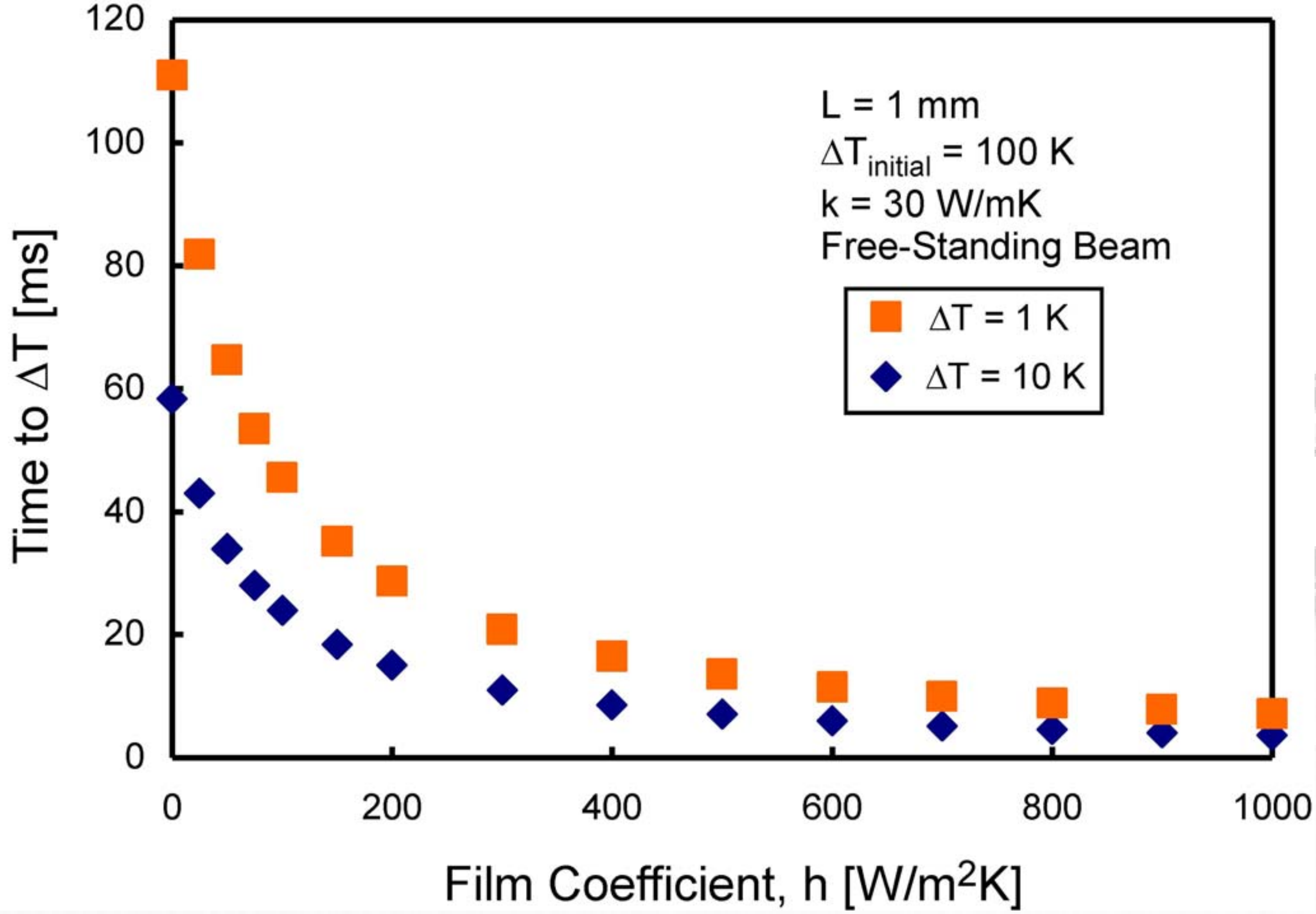

Rogers and Phinney, 2004, *Numerical Heat Transfer, Part A*, Vol. 45, pp. 737-750.

Laser Selection for the Repair Process

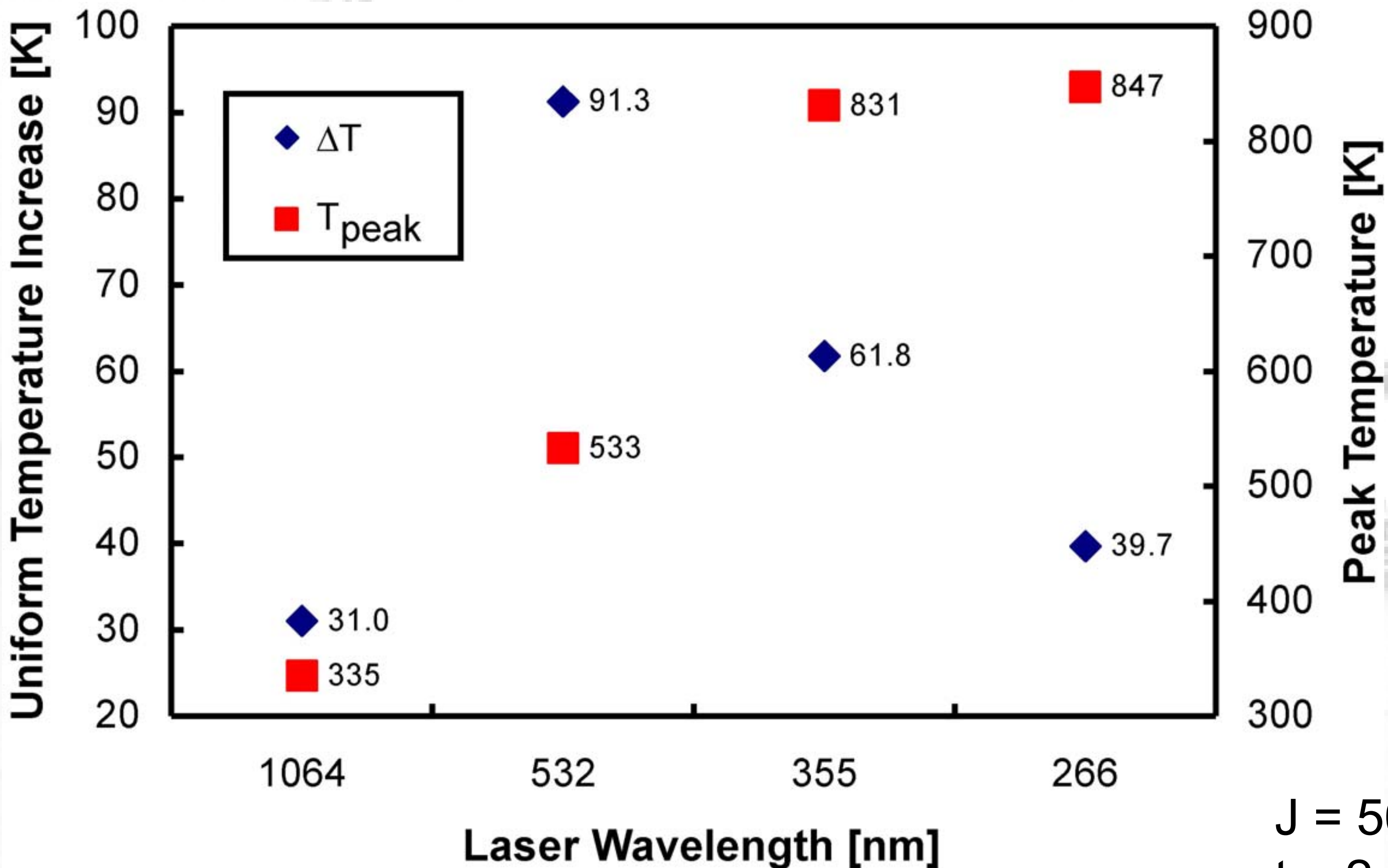

J = 50 mJ/cm^2
t = 2.0 μm

Sandia National Laboratories

Laser Parameters to Repair a 2.6 μm Thick Microcantilever to 1000 μm for an Adhesion Energy of 0.25 mJ/m^2

Material	$L_{0,\ initial}$ (μm)	ΔT (K)	λ (nm)	Fluence (mJ/cm^2)	T_{peak} (K)
Al	404	4.6	532	38	310
Si_3N_4	632	9.4	266	310	310
SiC	576	25.3	266	65	330
PolySi	504	24.3	532	17	379

Comparison of Measured and Calculated Tip Deflection

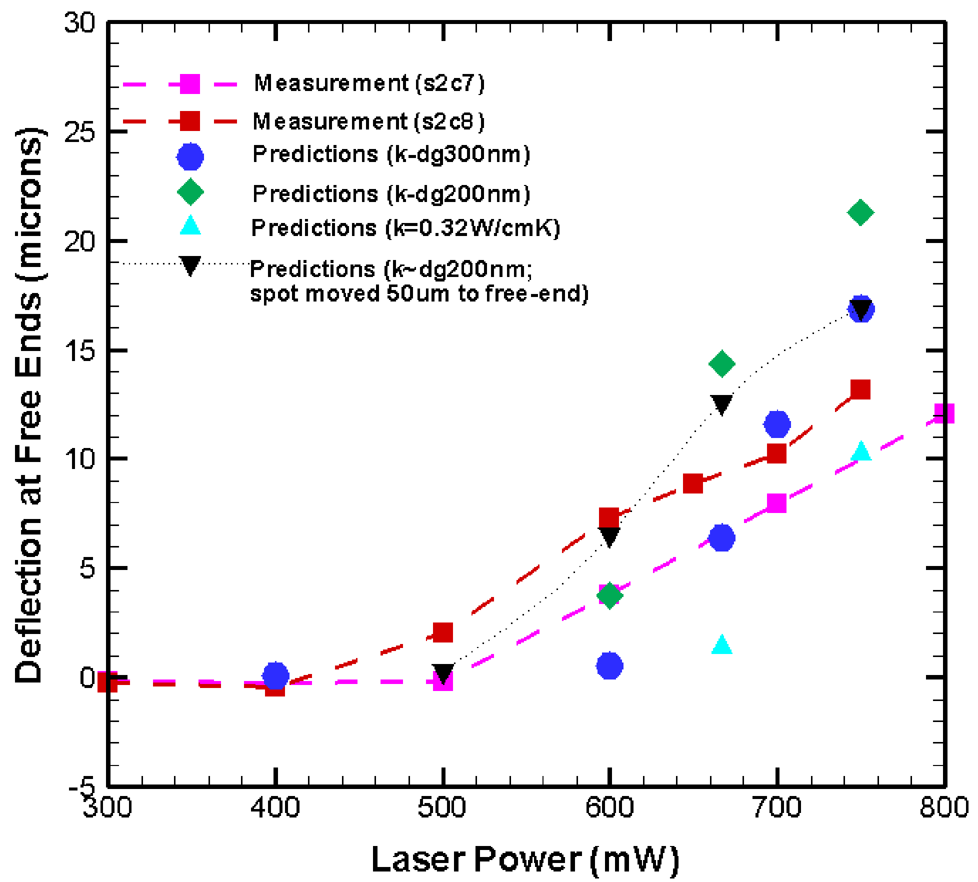

- Large uncertainties with material properties: k, CTE, absorptivity
- Validated models are necessary for design and optimization.

Sandia National Laboratories

Effect of Initial Deformation and Laser Spot Location

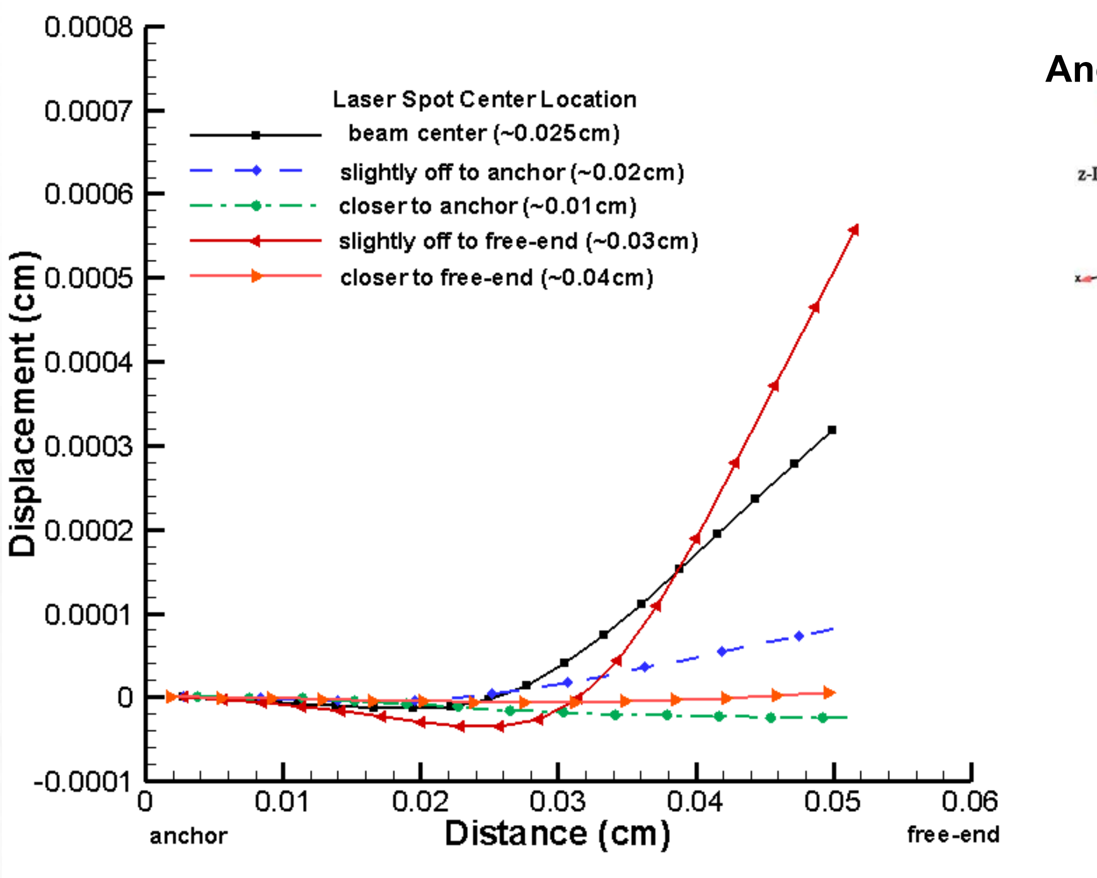

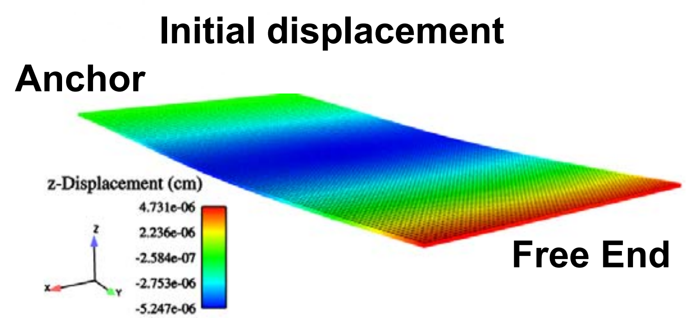

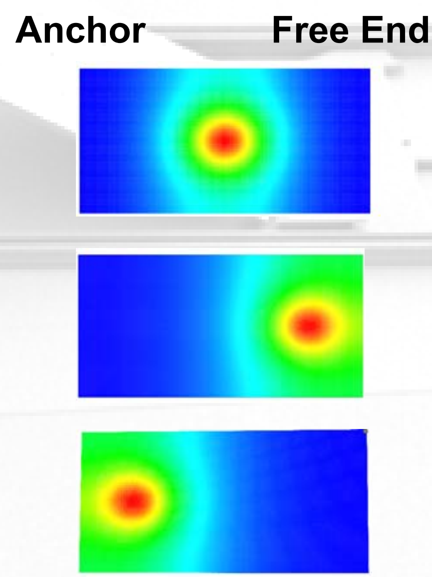

- No deformation predicted if initial strain is not included.
- Laser spot location can determine the magnitude and direction of deformation.

Sandia National Laboratories

Variation of Tip Deflection with Laser Power

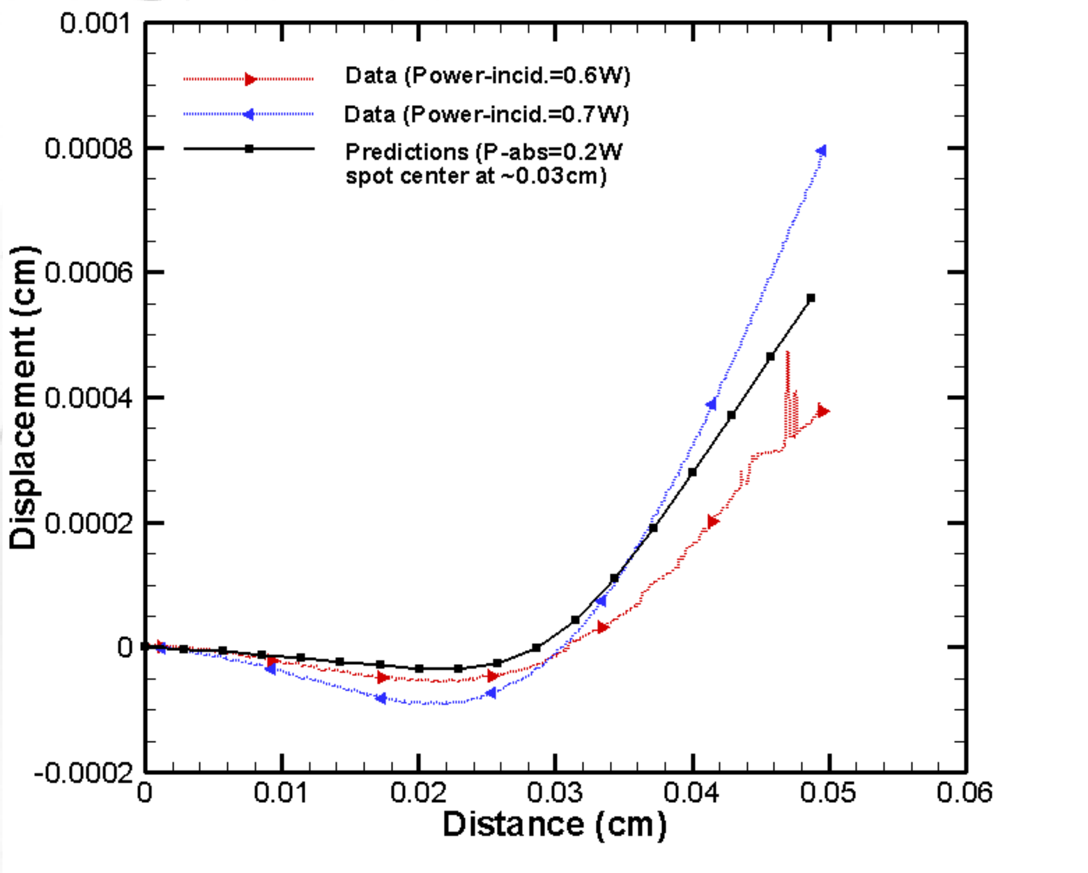

- Laser with spot size of 100 μm diameter and 45 degree inclined angle
- Approximately 30% of optical energy being absorbed
- Significant deformation occurred at above 0.5 W (T-max > 1000 K)

Sandia National Laboratories

Thermometry
(System Diagnostic)

- Infrared imaging / Pyrometry
- micro-Raman imaging
- Thermoreflectance
- Near-field optical thermometry
- Scanning thermal microscopy – non-optical method, not discussed

IR Imaging / Pyrometry

- Simplest Optical Thermometer
- Requirements
  - Microscope with IR-transmissive objective
  - IR Camera with appropriate spectral range
    - Lower Temperatures → Longer Wavelengths
  - Knowledge of device emissivity
  - IR band-pass filters and/or monochromator
- Advantages
  - IR detectors easily accessible
  - Simplest and least costly method to implement (if detectors avail.)
  - Full-field 2-D imaging
  - Transient data possible

Limitations

Spatial Resolution limited to several microns at best

Large bias errors due to reflection of radiation when $e < 1$

Device "surface emissivity" often must be known

Assumes radiation is still a "surface" phenomenon

Low signal levels in case of a reflective surface (mirror)

IR Imaging of a Microswitch

Laser shining on an micro-optical shutter

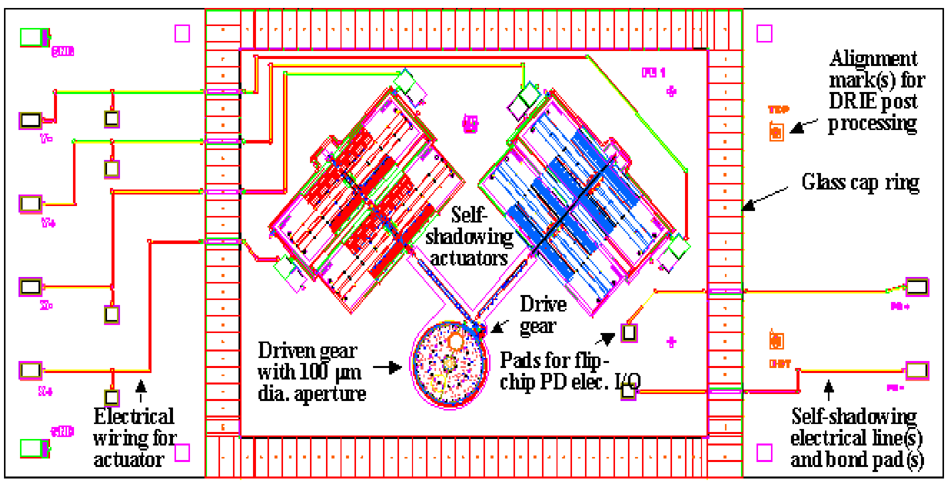

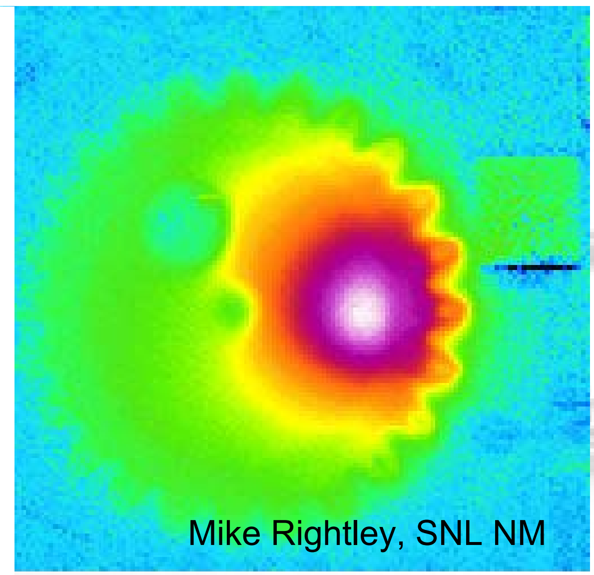

Infrared Image of Laser-Heated Optical Shutter

Temperature Measurements Using Raman Microscopy – Description

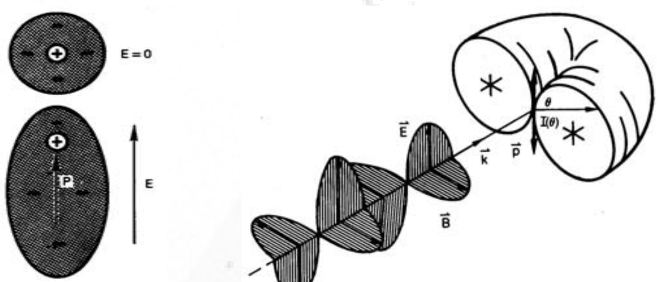

Light Scattering by a Laser-Induced Dipole

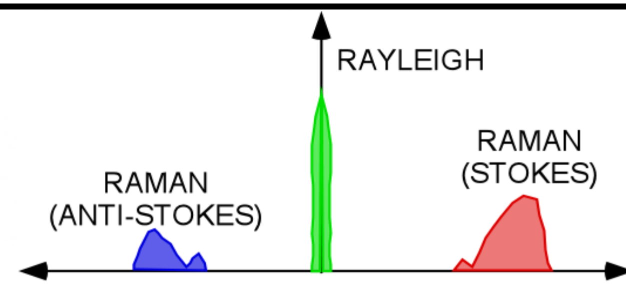

Light Scattering Spectrum

- Light is scattered by <u>inducing</u> a <u>radiating dipole</u> in the scattering medium. $E_s \sim P$
- The scattered light field, E_s is proportional to the strength of the induced dipole moment, *P*.

$$E_s \sim P \sim \alpha \, E_L \sim \alpha \cos \omega t$$

- The polarizability, α, is a measure of how readily a medium is "polarized" (how easily light induced dipoles) and α can be expanded in terms of the equilibrium and 'vibrating' positions of the molecules in the scattering medium, in this case a solid-state lattice.

$$\alpha = \alpha_o + (\partial\alpha / \partial Q) Q$$

- If the lattice vibrates at a certain allowed phonon frequency, Ω, then $Q \sim \cos \Omega t$ and

$$E_s \sim \alpha_o \cos \omega t + (\partial\alpha/\partial Q) \, [\cos(\omega + \Omega)t \; + \cos(\omega - \Omega)t]$$

Rayleigh Scattering — Raman Scattering

Micro-Raman Probing of Polysilicon

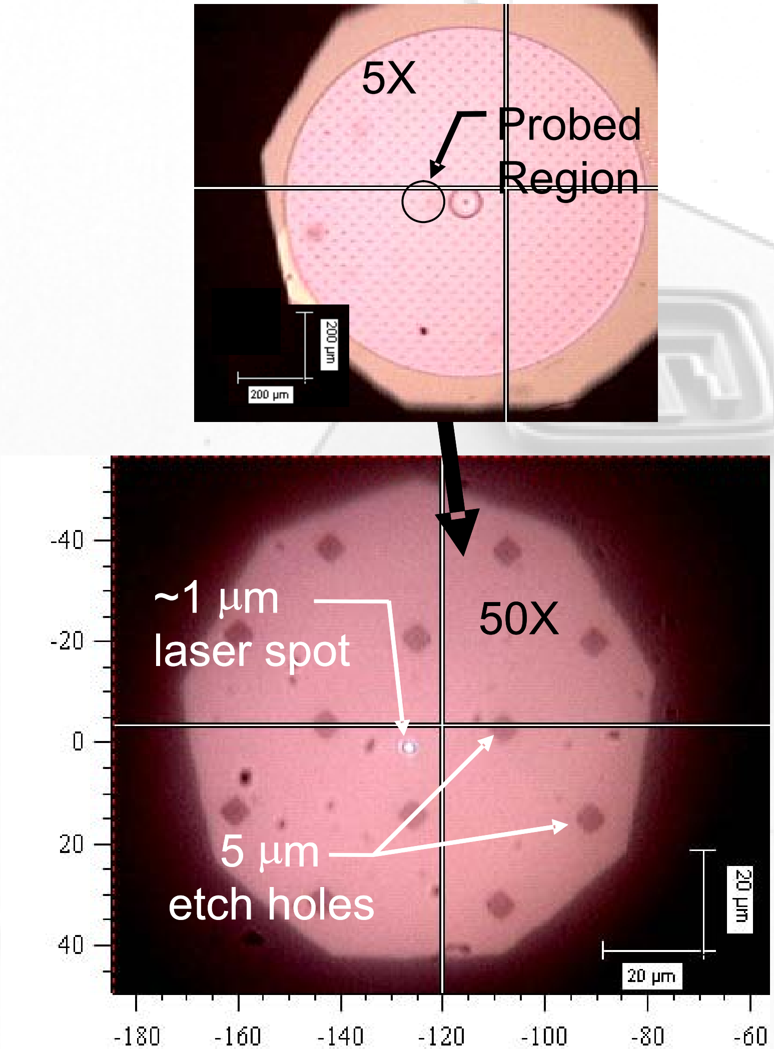

Polysilicon Surface under Raman Microscope

Laser-Illuminated Sample in Hot Stage

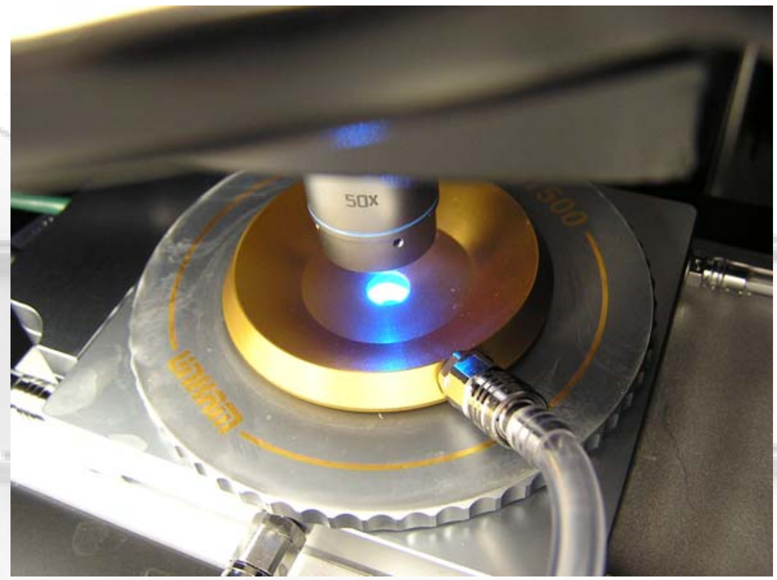

Sandia National Laboratories

Polycrystalline Silicon Raman Spectra: Temperature Sensitivity

- Temperature-dependent information extracted from PolySi Raman Spectra.
- Stokes (red-shifted) peak position – Shifts with increasing temperature due to lattice expansion.
- Stokes linewidth (full-width at half maximum) – increases with temperature due to increased optical phonon relaxation time.
- Ratio of Stokes to anti-Stokes (blue-shifted) areas -- Increased with temperature as a result of increasing population of thermally excited optical phonons.
- Some of these properties may also depend on stress and/or doping.

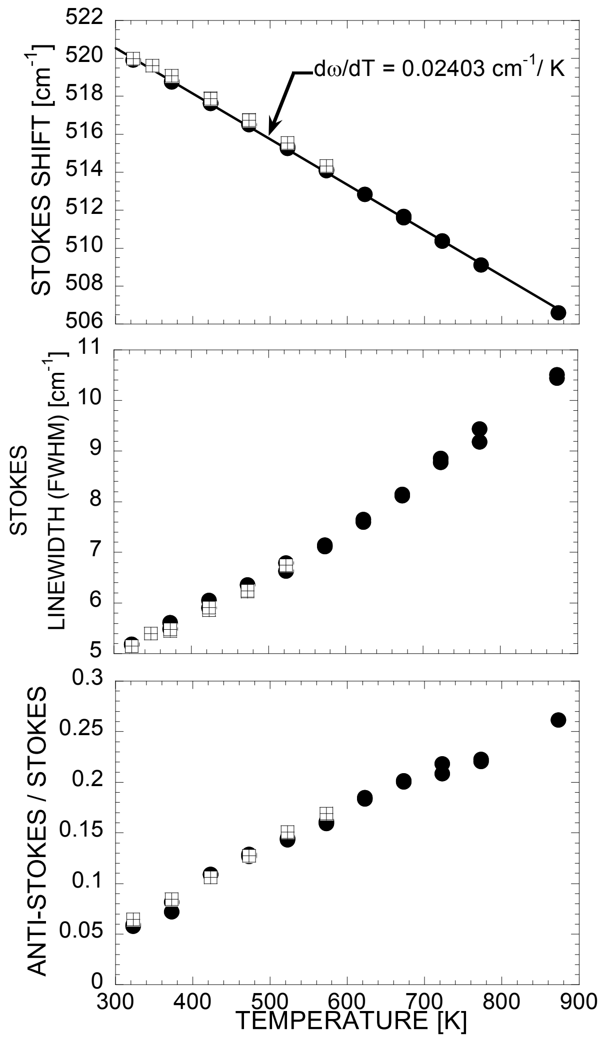

Temperature Sensitive Properties

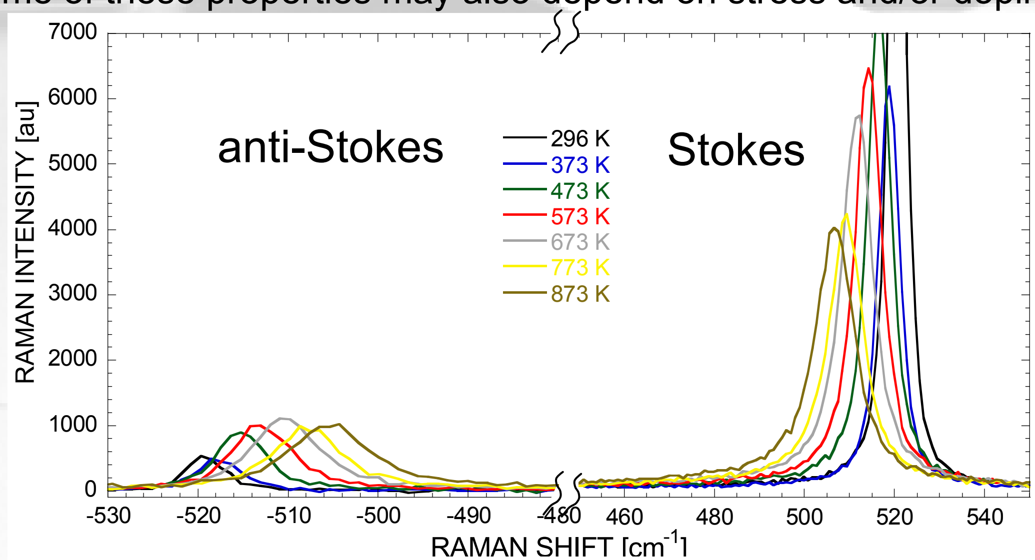

Raman Spectra from PolySi Part

Sandia National Laboratories

MEMS Thermal Actuators

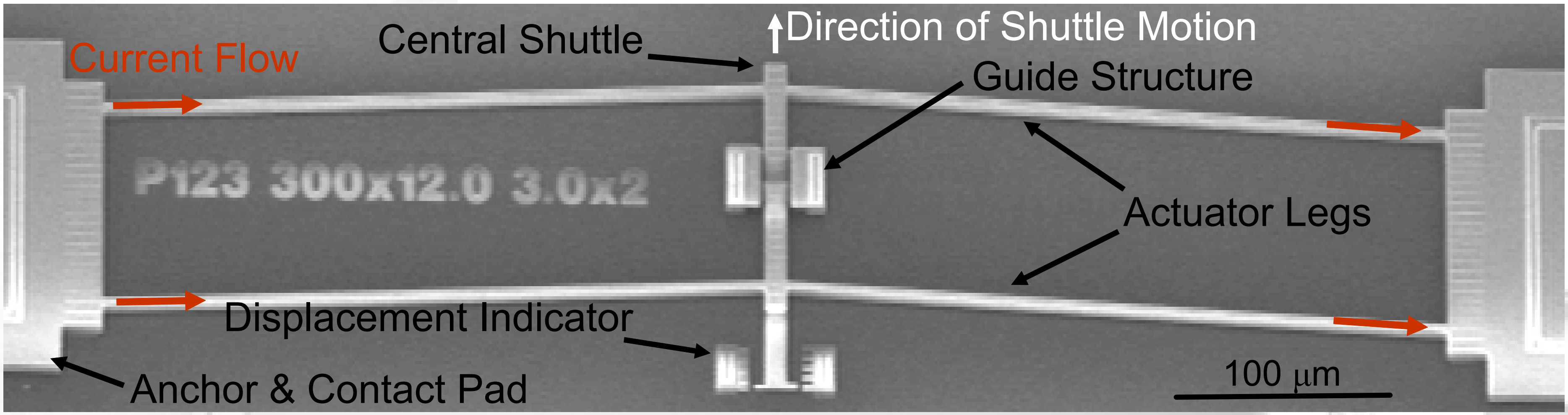

- Utilizes constrained thermal expansion due to Joule heating to achieve motion.
- Operates at low voltages and higher currents (12 V 20 mA typical) compared to other MEMS actuators.
- Capable of relatively high output forces (2.5 mN) and displacements (over 50 μm).

(M. Baker, Sandia National Laboratories, NM)

Sandia National Laboratories

Raman Thermometry of a Thermal Actuator

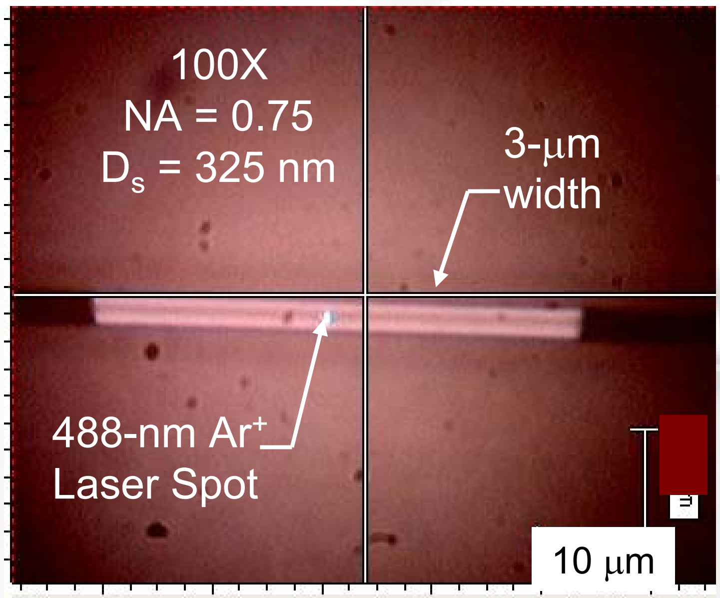

Actuator Linkage Under Raman Microscope

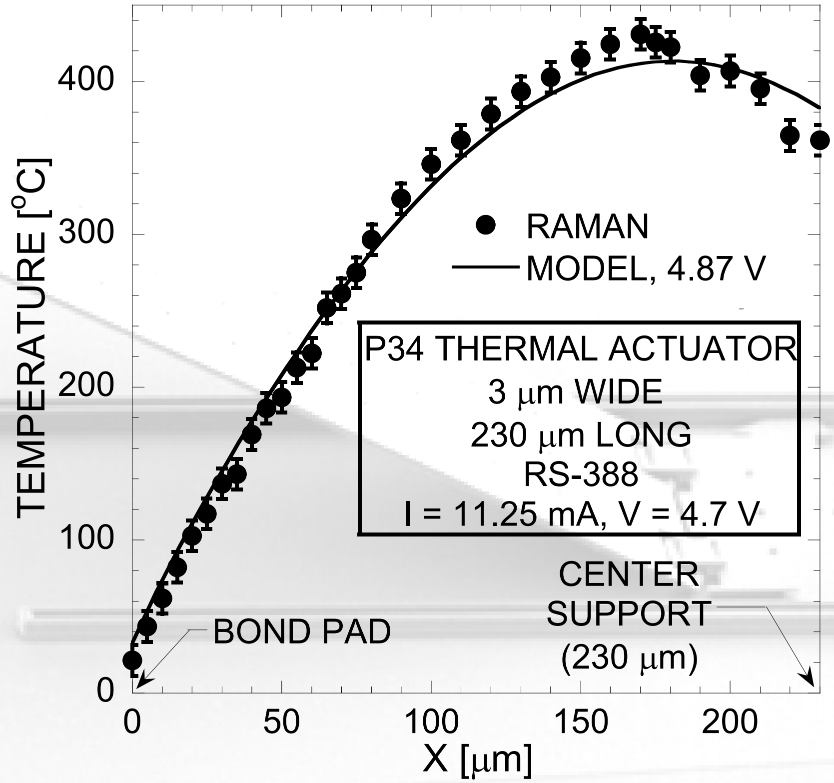

- To our knowledge, these were the first known data for such actuators, which are being studied in parallel by research groups at Brigham Young and Wisconsin
- The outstanding spatial resolution and unambiguous nature of the Si Raman signature are a significant improvement over IR methods

(Kearney, Phinney, and Baker, *JMEMS*, **15**, 314-321, 2006; Serrano, Phinney, and Kearney, *JMM*, **16**, 1128-1134, 2006)

Thermoreflectance

- Technique
  - Monitor the change in the reflected optical signal from a surface and relate it to the temperature of a surface
- Advantages
  - Submicron spatial resolution possible
  - Visible or UV applied light source instead of IR thermal radiation Reasonably simple to implement
  - Moderate cost
- Limitations
  - Calibration of surface reflectance required
  - Low values of reflectance coefficient $C_{tr} \sim 10^{-4}$ to 10^{-5} K^{-1} limits sensitivity
  - Scanning, AC-coupled measurements required. Dynamic range of CCDs is insufficient for 2-D imaging
  - Absolute calibration is difficult so that differential temperatures are most readily achieved

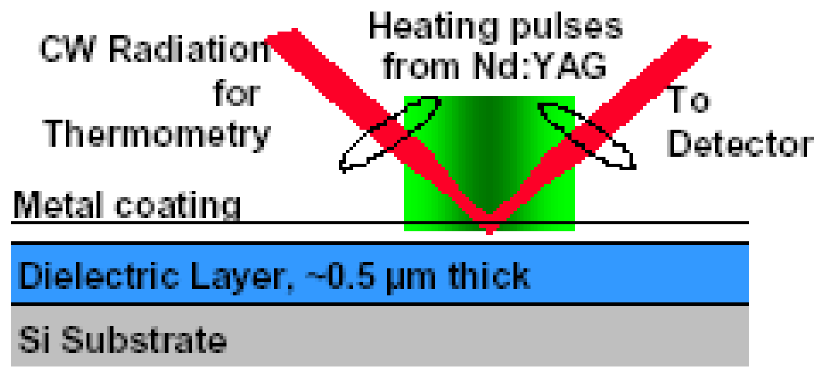

Thermoreflectance Concept

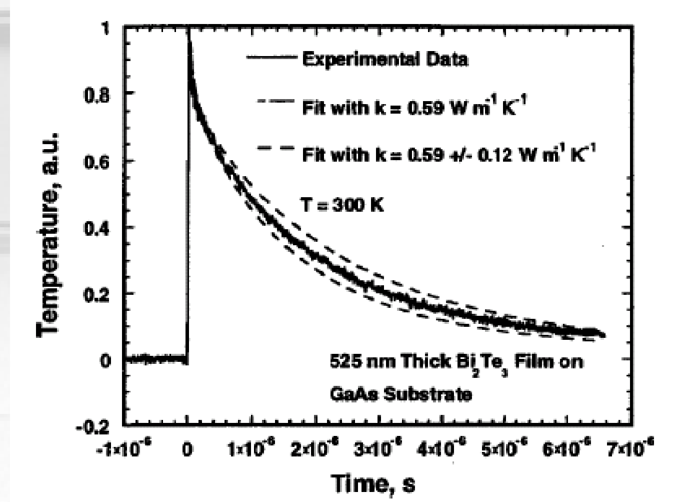

Time-Resolved Reflectance Signal

M.N. Touzelbaev et al., *J. Applied Phys.*, **90**(2), 763, 2001.

Thermoreflectance

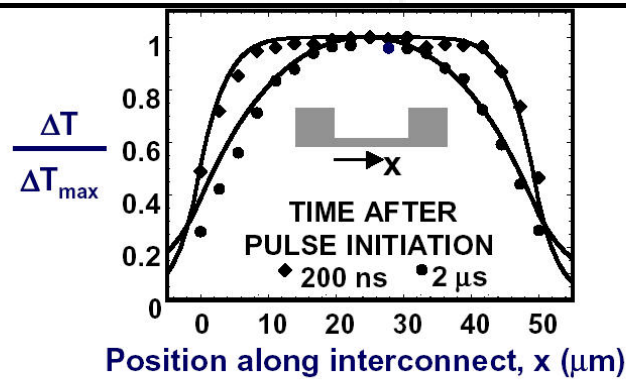

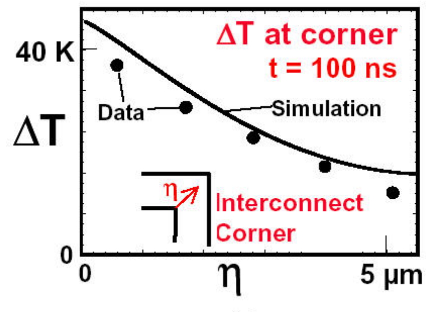

Temperature Mapping of an Interconnect (Ju and Goodson, 1997, 1998)

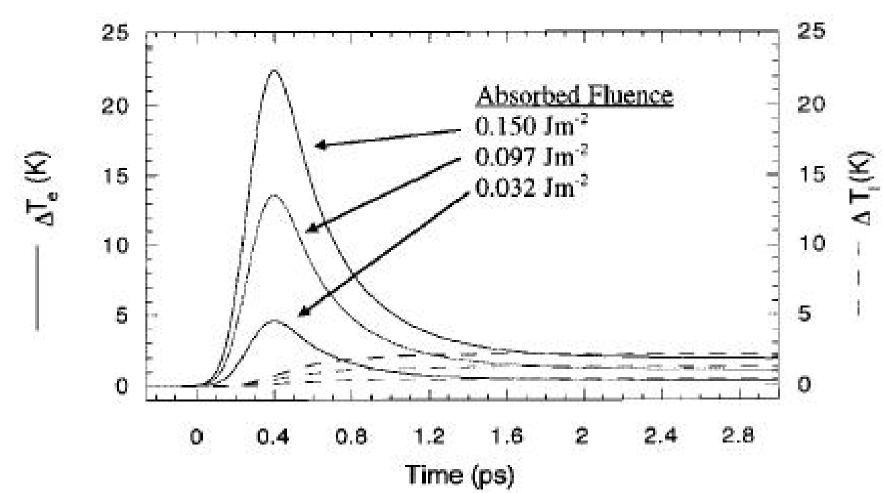

Electron Relaxation for 200nm Pt film.

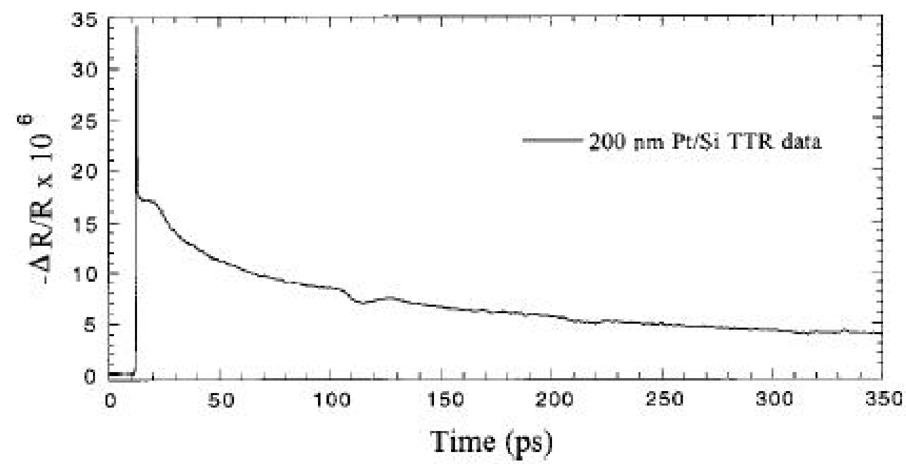

Thermoreflectance Data for Pt/Si films

P. Norris et al., Rev. Sci. Inst., 2003.

Sandia National Laboratories

Near-Field Optical Thermometry

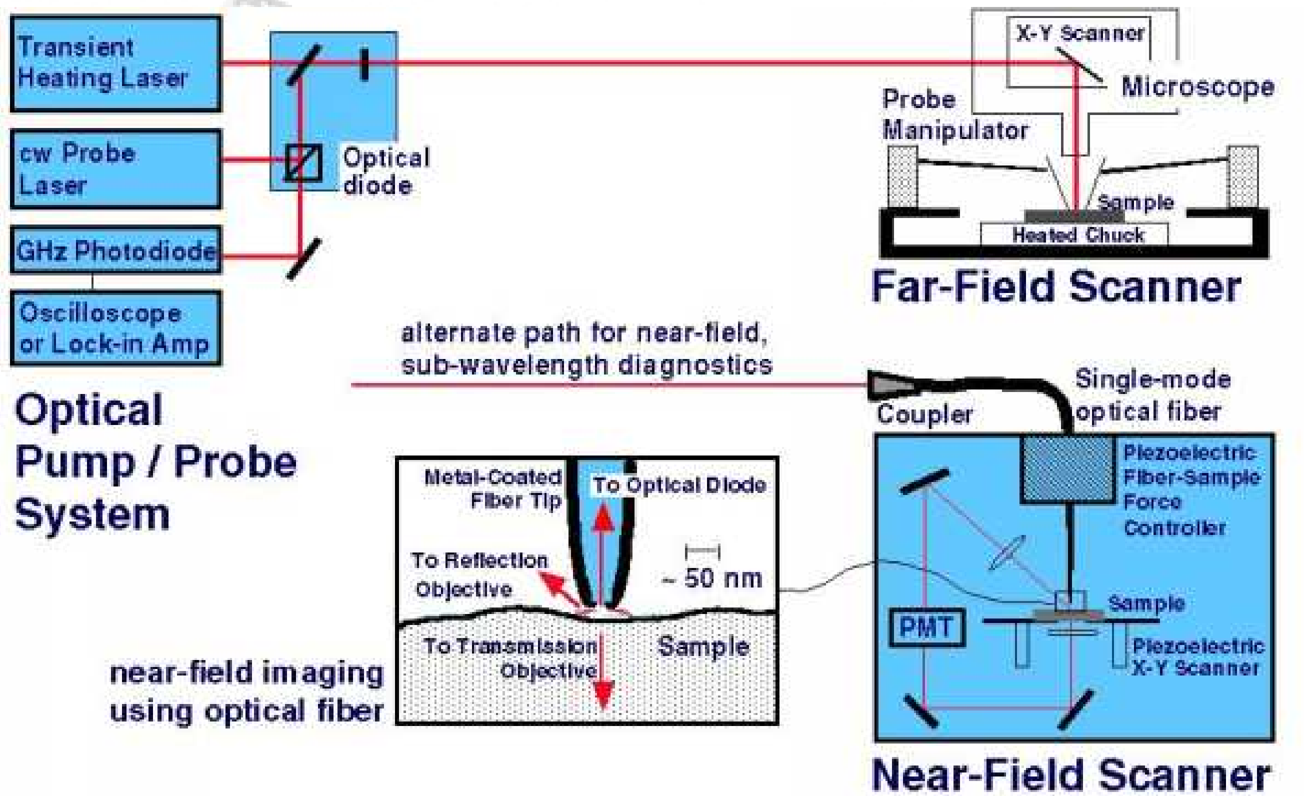

Picture from Goodson group at Stanford University

Ju et al., *IEEE Electron Device Lett.*, **18**, pp. 169-171, 1997.

Goodson and Asheghi, *Microscale Thermophysical Engineering*, **1**, pp. 225-235, 1997.

Summary and Conclusions

- Applications and processes involving laser irradiation of MEMS components include optical MEMS, optical actuators, laser processing, and optical characterization methods.
- A complete understanding of the absorption of laser energy, thermal transport, and mechanical response in microsystems is necessary to improve the design, operation, and reliability of MEMS devices exposed to laser heating.
- When the laser power incident on a MEMS component is increased, it will experience damage when the power handling capabilities are exceeded.
- For optically powered MEMS devices, target design has a significant impact on the likelihood for damage due to laser heating since it affects the distribution of energy within the target.
- Raman thermometry was used to make high spatial resolution temperature measurements on laser heated MEMS.
- The temperature dependence of the refractive index must be considered when modeling the performance of laser heated MEMS when optical interference is present.
- Optical methods are powerful diagnostic methods for MEMS.

Sandia National Laboratories

Thank You!

Questions?

Transient Imaging System

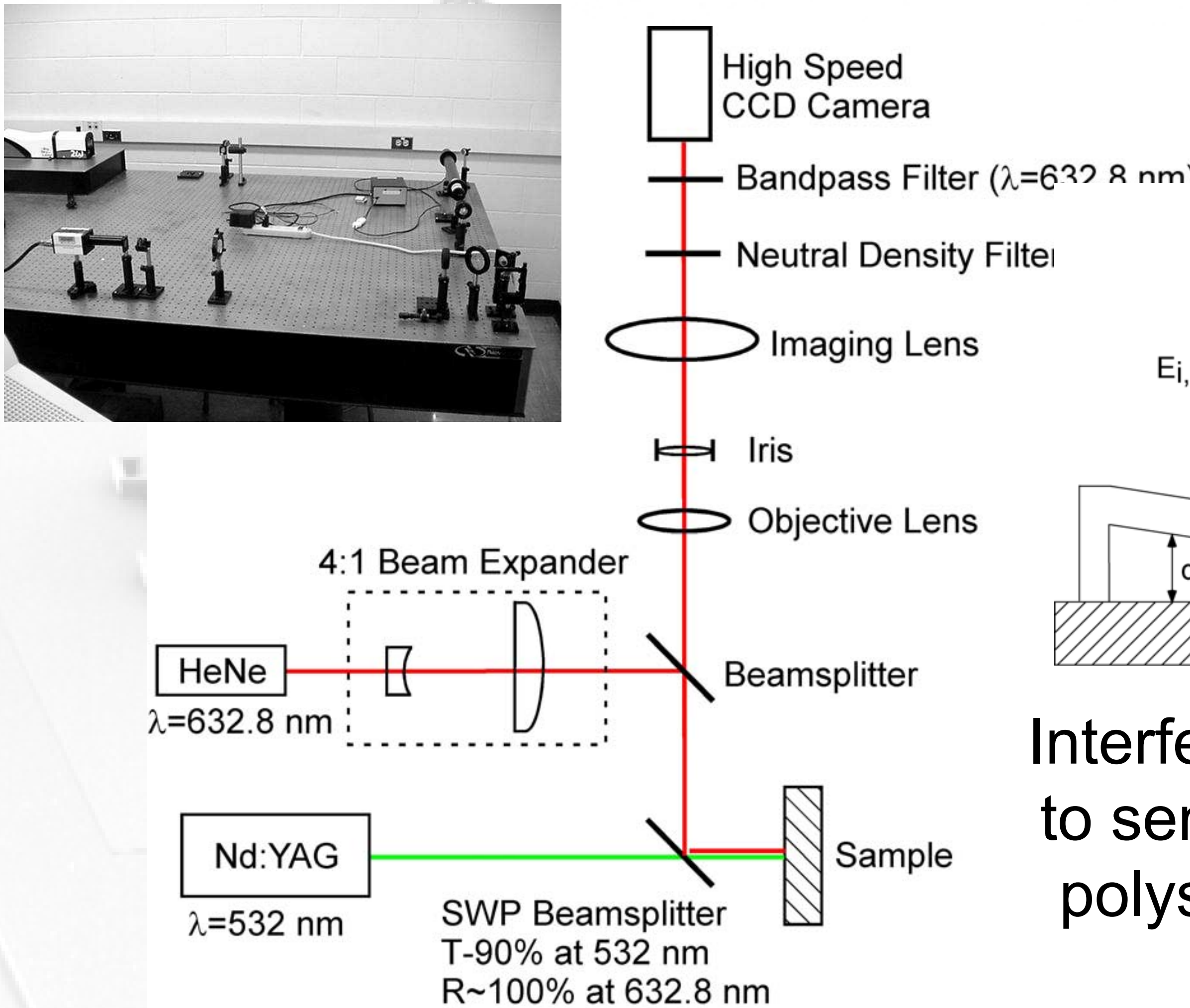

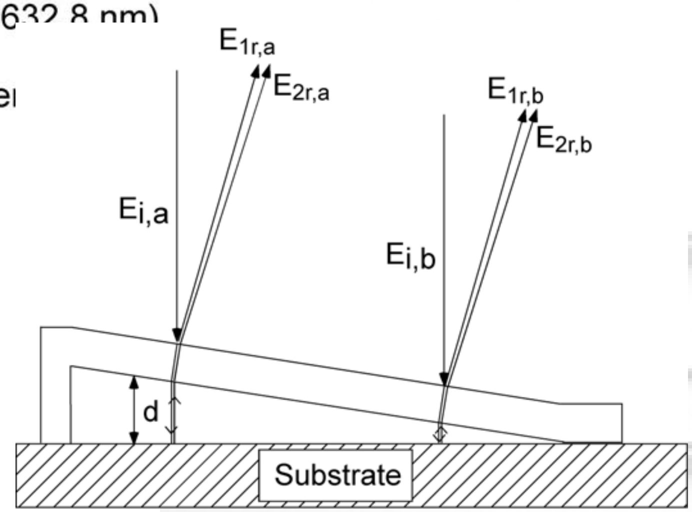

Interference created due to semi-transparence of polysilicon at 632.8 nm

Effect of Post Size

- Larger connecting posts:
  - Increase thermal mass
  - Improve heat transport out of irradiated zone
  - Less damage on target surface for same power levels
- Damage not prevented entirely, but greatly suppressed

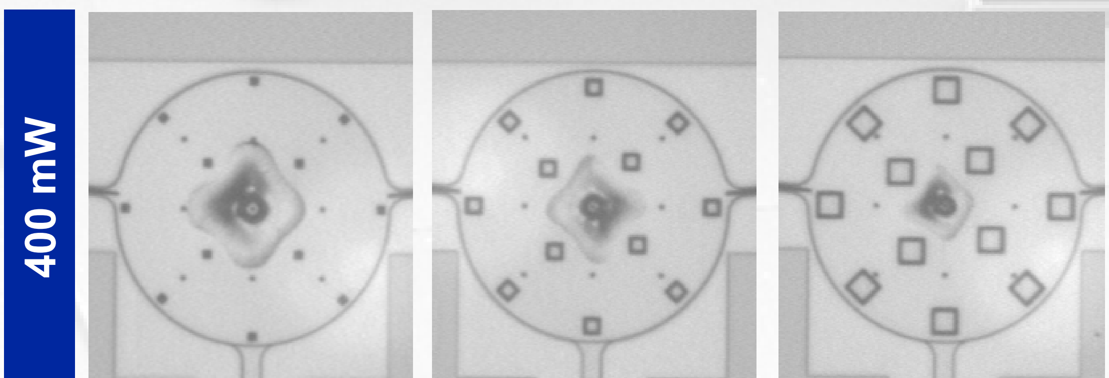

5 μm posts 10 μm posts 15 μm posts

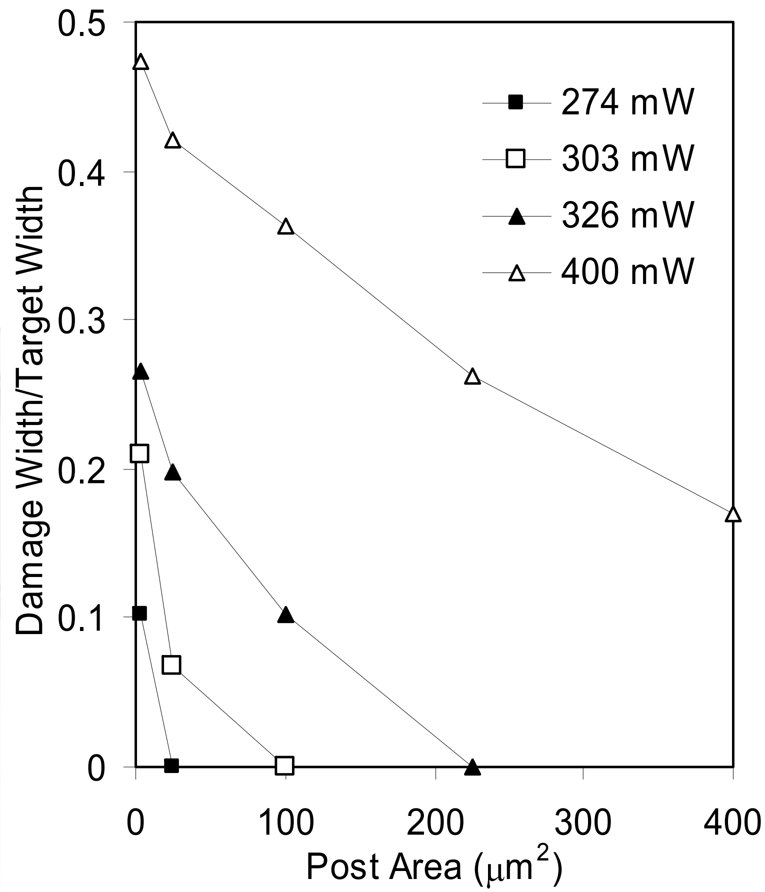

Sandia National Laboratories

Experimental Details

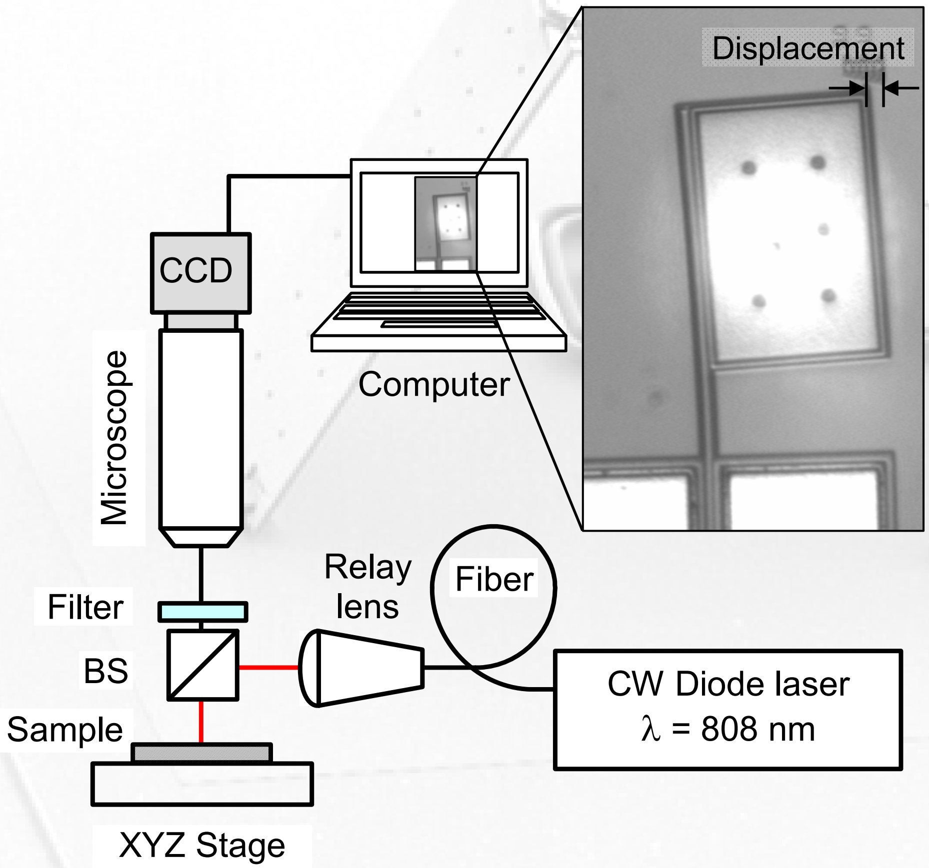

- Actuators irradiated with 808 nm, fiber-coupled, CW diode laser; 100 μm diameter spot
- Laser power varied from 100-650 mW
- Images of actuators captured before, during and after irradiation

Sandia National Laboratories

Experimental Details

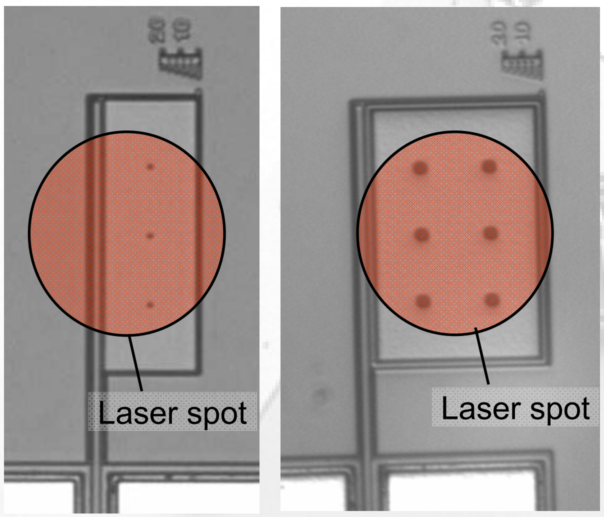

Laser spot centered on 100 μm wide leg; offset on 50 μm wide leg

- Displacement measured at the top-right corner of device; determined with image analysis
- Displacement determined to ± 1 pixel (0.65 μm)
- Irradiation schemes:
  - Power ramp: **laser power always incident on actuator, increased slowly; images captured at regular power intervals**
  - On/off irradiation: **images captured, laser power increased with each on/off cycle**
  - Prolonged exposure: **laser incident on actuator for extended period; images captured at regular time intervals**

Cantilever Plate Description

Cantilever plate (springboard)

- 500 µm long x 250 µm wide
- Single Poly4 layer (2.25 µm thick)
- 10.75 µm from the substrate
- Anchored to substrate at one end; opposite end is free
- Surface covered with 2 µm square etch-release holes spaced 25 µm apart

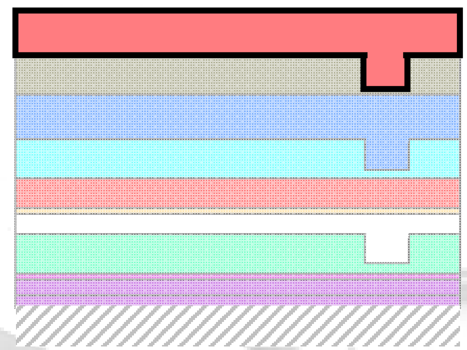

Serrano and Phinney, 2007, *Proc. InterPACK'07*, ASME, IPACK2007-33571, pp. 1-7.

Polysilicon Film on SiO_2/Si

- Laser power of **1.6 W** needed power to generate substantial heating due to large thermal mass
- Temperature measured along major and minor axes of elliptical laser spot at 20 µm intervals
- Along minor axis:
  - Peak temperature of 120°C
  - Strongest temperature gradient within beam spot
  - Uniform temperature outside immediate vicinity of laser spot

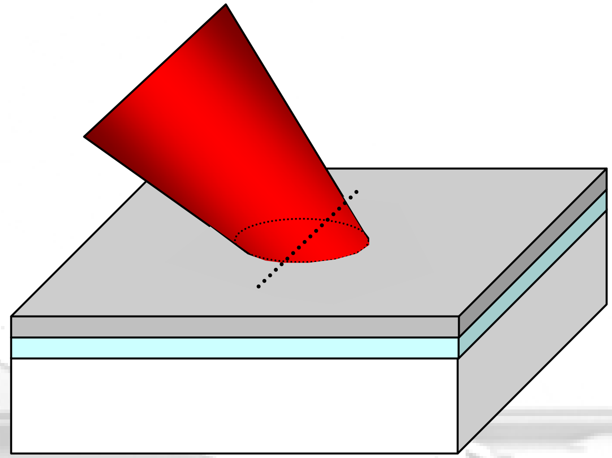

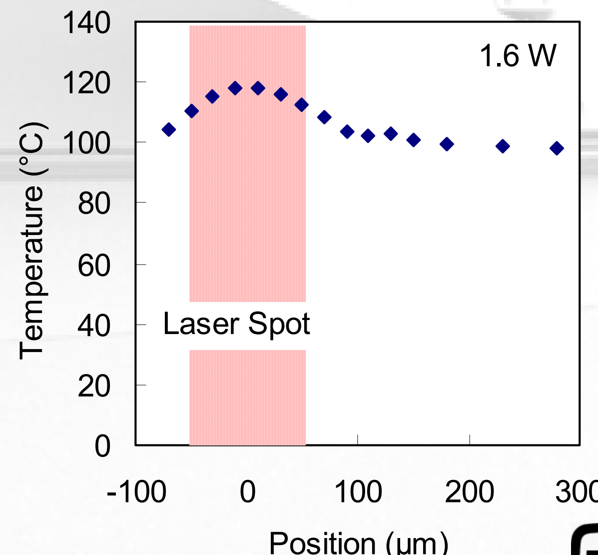

Polysilicon Film on SiO_2/Si

- Laser power of **1.6 W** needed power to generate substantial heating due to large thermal mass
- Temperature measured along major and minor axes of elliptical laser spot at 20 µm intervals
- Along minor axis:
  - Peak temperature of 120°C
  - Strongest temperature gradient within beam spot
  - Uniform temperature outside immediate vicinity of laser spot
- Along major axis
  - Weaker gradient within beam spot than along major axis
- Sample still at elevated temperature (85°C) three millimeters away from laser spot

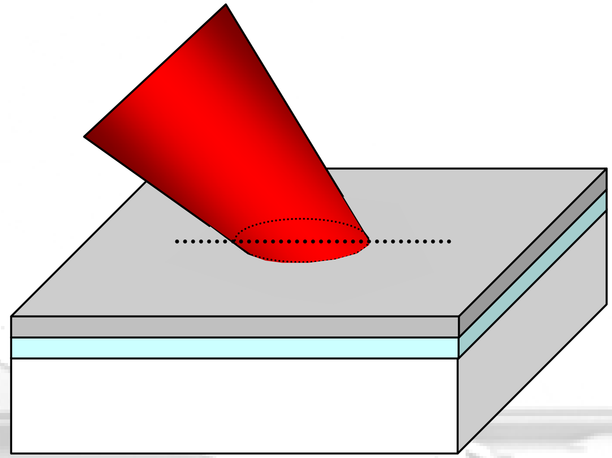

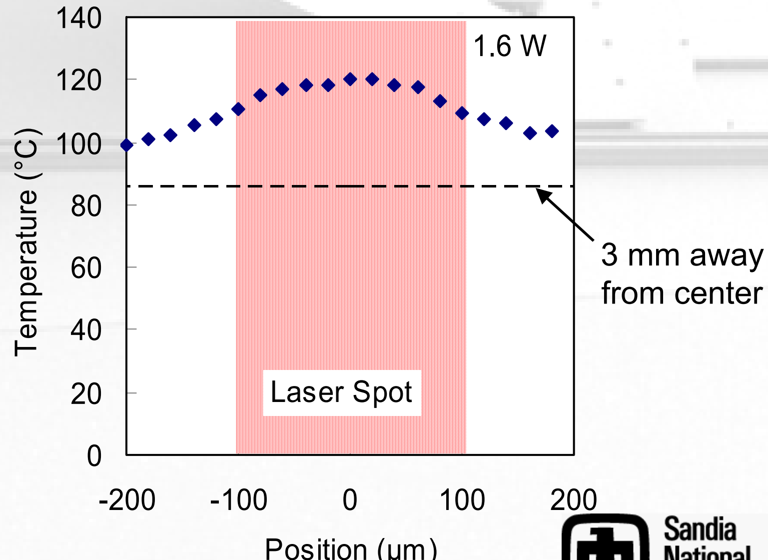

Sandia National Laboratories

Optical Energy Absorption in MEMS: P3-Air Gap-P4 Layers

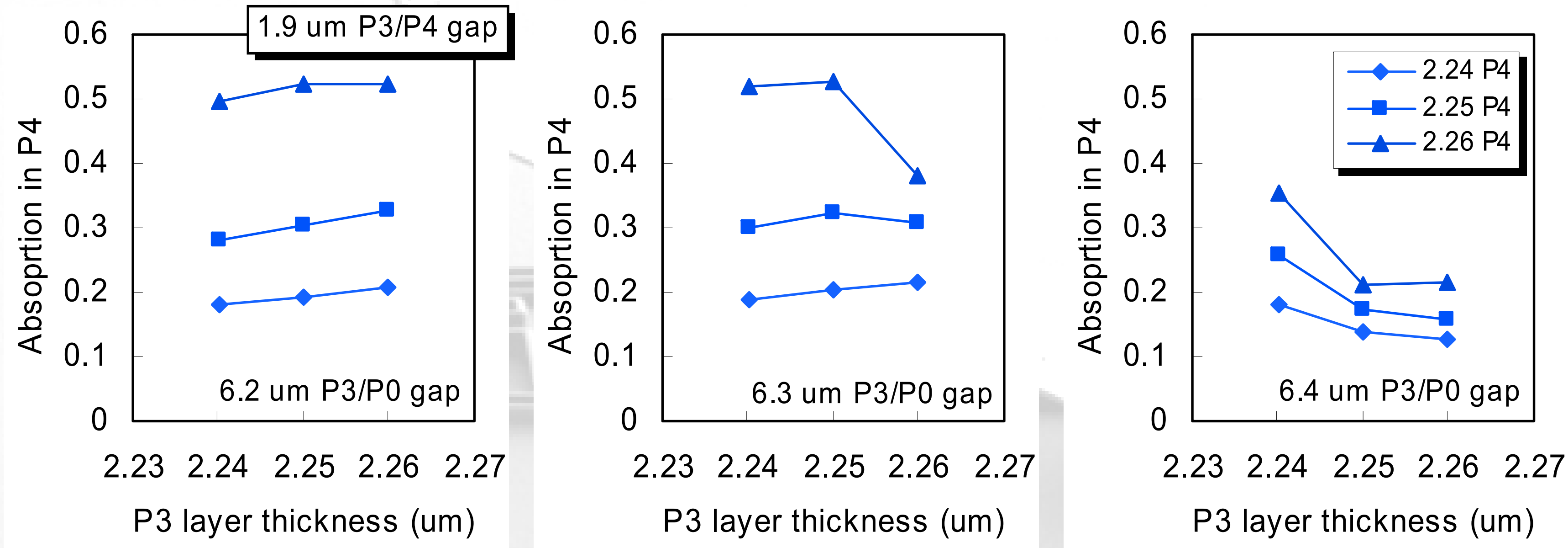

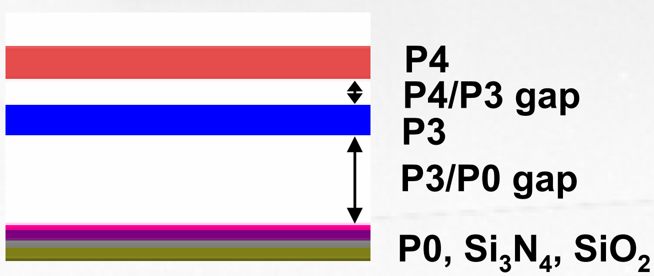

- Additional layers introduce more parameters that affect absorption
  - Multiple film thicknesses
  - Multiple gap distances